Dynamic system identification based on selective sensitivity

(Dynamische Systemidentifikation auf der Grundlage selektiver Sensitivität)

DISSERTATION

zur Erlangung des akademischen Grades

Doktor-Ingenieur

an der Fakultät Bauingenieurwesen
der
Bauhaus–Universität Weimar

vorgelegt von
M.-Eng. Pham Hoang Anh
aus Vietnam

Weimar, Dezember 2006

Gutachter: 1. Herr Prof. Dr. Christian Bucher
2. Herr Prof. Dr.-Ing. Armin Lenzen
3. Herr Prof. Dr. rer. nat. habil. Klaus Gürlebeck

Tag der Disputation: 14. März 2007

Acknowledgments

The research work in this dissertation was carried out in the period from October 2003 to December 2006 when I was a doctoral student at the Bauhaus-University Weimar.

During that time, I benefited from many discussions with my supervisor, Prof. Christian Bucher, and other colleagues at the Institute of Structural Mechanics (ISM). Prof. Bucher through his pleasant supervision has not only offered valuable suggestions but sometimes challenged me to clarify and re-think my approach. Dr. Volkmar Zabel gave helpful advices and assisted me in preparing as well as setting up the experiment. Dr. Thomas Most checked the spelling of the German text of the dissertation and gave detailed suggestions for its improvement. The staffs at ISM in their activities have created a friendly working atmosphere.

Prof. Christian Bucher, Prof. Armin Lenzen and Prof. Klaus Gürlebeck reviewed and evaluated the dissertation. To them I would like to express my gratitude and appreciation.

The German Academic Exchange Service (DAAD) has granted a full scholarship for my research and entire stay in Germany, which is gratefully acknowledged.

My parents, my sisters and my friends have constantly encouraged me over time. Without these supports the dissertation could not be possible.

Abstract

System identification is often associated with the evaluation of damage for existing structures. Usually, dynamic test data are utilized to estimate the parameter values for a given structural model. This requires the solution of an inverse problem. Unfortunately, inverse problems in general are ill-conditioned, particularly with a large number of parameter to be determined. This means that the accuracy of the estimated parameter values is not sufficiently high in order to enable a damage identification.

The goal of this study was to develop an experimental procedure which allows to identify the system parameters in substructures with high reliability. For this purpose, the method of selective sensitivity was employed to define special dynamic excitations, namely selectively sensitive excitation. Two different approaches have been introduced, which are the quasi-static approach and the iteratively experimental procedure. The former approach is appropriate for statically determinate structures and excitation frequencies below the structure's fundamental frequency. The latter method, which uses a-priori information about the parameters to be identified to set up an iterative experiment, can be applied to statically indeterminate structures. The viability of the proposed iterative procedure in detection of small changes of structure's stiffness was demonstrated by a simple laboratory experiment. The applicability of the strategy, however, depends largely on experimental capacity. It was also experienced that such a test is associate with expensive cost of equipments and time-consuming work.

Kurzfassung

Systemidentifikation wird oft als Werkzeug im Zusammenhang mit der Beurteilung von Schädigungen an Strukturen eingesetzt. Oftmals erfolgt eine Abschätzung der Parameter eines vorgegebenen Strukturmodells mittels der in dynamischen Versuchen gemessenen Daten. Dies erfordert die Lösung eines inversen Problems. Insbesondere bei einer großen Anzahl von zu bestimmenden Parametern sind inverse Probleme in der Regel schlecht konditioniert. Dies bedeutet, dass die Präzision der identifizierten Parameterwerte oft nicht ausreichend hoch ist, um die ursprünglich gestellte Frage nach einer Schädigungsidentifikation beantworten zu können.

Das Ziel dieser Arbeit war, eine experimentelles Verfahren zu entwickeln, das es erlaubt, die Systemparameter in Substrukturen mit hoher Verlässlichkeit zu identifizieren. Zu diesem Zweck wurde die Methode der selektiven Sensitivität eingesetzt, um spezielle dynamische Anregungen, nämlich selektiv sensitive Anregung zu bestimmen. Zwei verschiedene Ansätze wurden eingeführt, der quasistatische Ansatz und das iterativ experimentelle Verfahren. Der erste Ansatz ist für den Versuch einer statisch bestimmten Struktur mit Anregungsfrequenz unter der Grundfrequenz der Struktur geeignet. Der zweite Ansatz verwendet a-priori Information über die zu identifizierenden Parameter, um einen iterativen Versuch aufzubauen, und kann auch auf statisch unbestimmte Strukturen angewendet werden. Die Realisierbarkeit des vorgesclagten iterativen Verfahrens zur Detektion von kleinen lokalen Steifikeitsänderungen wurde durch einen einfachen Versuch im Labor demonstriert. Die Anwendbarkeit des Vorgehen hängt jedoch größtenteils von experimenteller Kapazität ab. Es wurde auch festgestellt, dass ein solcher Versuch mit einem erheblichen versuchstechnischen Mehraufwand und zeitraubender Arbeit verbunden ist.

Contents

List of Figures

List of Tables

Chapter 1

Introduction

1.1 Motivation

In recent years, there has been increasing focus on assessment of structural performance of existing structures. Often, it is desired to detect irregularities or changes of the structural system's properties that were caused by structural damages [1]. During the life-span of a structure this amounts to observing relatively small changes of system properties. In most cases, such evaluation is initially based on the results of visual inspections. For further and more detailed investigations, non-destructive tests (NDT) should be carried out. Due to their simplicity, measurements of dynamic responses are most suitable for permanent observations. These measurements are often followed by the estimation of parameter values for a given structural model [2].

Real structures generally exhibit random spatial fluctuations of their properties which are best described by random fields. It is well known, that the number of random variables required to represent a random field grows rapidly with decreasing correlation length of the field (e.g. [3]). Consequently, an appropriate procedure may require a large number of parameter values to be identified simultaneously. It has been shown in [4], that failure to consider spatial variability in system identification may lead to gross overestimation of structural safety.

Unfortunately, system identification often leads to rather ill-conditioned parameter estimation problem. The consequence of the ill-condition is that any small levels of measurement noise may lead to a large deviation in the identified parameters from their exact values. This tends to become more pronounced as the number of parameters increases. Another problem occurs when measurements are incomplete, so that the identification becomes under-determined and there are infinite solutions.

The treatment of ill-conditionedness is still a critical issue in system identification. Regularization methods which rely on minimum norm type solution may spread the identified damage over a large number of parameters. The process of subset selection [5, 6] requires the evaluation of many parameter subsets to derive the best set. It is desirable to have an efficient way to cope with the problem of ill-conditioning, so that parameter values can be estimated with sufficiently high accuracy in order to enable a damage identification.

The present study attempts to employ a different way to reduce ill-conditionedness, the method based on the concept of *Selective Sensitivity* [7, 8]. The idea of selective sensitivity is to transform the original (large) identification problem into a sequence of smaller ones by applying excitations which produces strong sensitivities to a subset of parameters while causing the sensitivities to other parameters to vanish. The aim is to adapt the load system so that the output is sensitive to the selected parameters and insensitive to others. Thus, only a small number of parameter values will be determined at a time.

The major disadvantage of selective sensitivity is the requirement of fairly good knowledge of all parameters to be tested in order to define the excitations. On the other hand, there are always physical difficulties associate to the realization of the required system of forces, which often relatively large and possibly complex. These drawbacks pose a serious problem to practical applications of selective sensitivity, especially to civil engineering structures.

1.2 Aims of the work

The goal of this work is the development of a procedure for system identification using dynamic experiments that allows to identify the system parameter values with high reliability. For this purpose the method of selective sensitivity is employed to define special dynamic forces. The applicability of selective sensitivity can be achieved by a careful test set-up with appropriate force configuration and suitable force control.

The objectives of the study are:

- Establishing efficient method to determine the selectively sensitive excitations,
- Setting up a procedure for estimating parameter values and their uncertainties,
- Finding suitable algorithm to control the applied forces,
- Aspects of realization of selectively sensitive load system for civil structures,
- and verification of the proposed methodology with a laboratory experiment.

In this study, only undamped linear structures are considered. The work focuses on the identification of stiffness only while the mass is assumed to be accurately known. Aspects of how the finite-element model should be parametrized will not be discussed since the central point is to deal with the ill-condition problem. It is also assume that a priori information about the parameter values is available. Moreover, only a simple verification experiment is carried out because of experiment capacity.

1.3 Outline of the dissertation

After the introduction, a brief review of system identification in the field of damage detection and location is presented in the second chapter. The ill-conditioned problem which is central to simultaneous identification of many parameters is emphasized.

In the third chapter, the basis concept of selective sensitivity as well as the existing approaches is given and discussed. Limitations of the conventional methods are highlighted.

A new approach for statically determinate structures, the *quasi-static* approach, which allows to attain selective sensitivity with no requirement of prior knowledge about the parameters is proposed in the fourth chapter.

For general case, an iteratively experimental procedure is developed in the fifth chapter. The basis formulation is expressed first and then incorporated with a Bayesian updating methodology. Several simulations are carried out to illustrate the effectiveness of the method.

In the sixth chapter, the realization of test is discussed and examined. First, discussions and recommendations are given. An algorithm for controlling the force is also proposed. After that, the main part of the chapter is placed on the laboratory experiment.

Finally, in the seventh chapter, summarization and assessment of the presented results as well as recommendations and directions for future research are shown.

Chapter 2

System Identification

System identification covers a large area of research. Usually, damage detection and location of existing structures are in the foreground. This condition assessment should be carried out by means of non-destructive investigations or NDT, in which often vibration measurements are utilized.

Although there are many researches on this topic, they can be categorised by the type of data that they use. The first category is based on identification using experimentally measured modal parameters. The basis of these techniques is detailed in [9]. In [10] this category is divided into two groups:

(i) Response-based approach: in which modal parameters of the undamaged structure and those of damaged one are compared, hereby damages can be identified from the changes in the natural frequencies, damping or vibration mode shapes. This approach is time efficient, and therefore is often employed in Structural Health Monitoring. However, it is still difficult to localize of the damage.

(ii) Model-based approach: in which a mathematic model is used and its parameter values will be determined through an optimal correlation between measured and analytical modal parameters. The damage can be qualified and localized from the obtained model's properties. Usually, model updating procedures are necessary (e.g [11], [12], [13]).

Other methods for assessment of the system matrices using measured modal data are presented in [10], [14] and [15]. A method using modal data for damage location is also introduced in [16] and [17], which was verified by simulation example as well as laboratory test. [18] uses the measured modal parameters for damage detection in beam structure.

Although there has been verification from laboratory experiments, the approach is still restricted in practice. This is due to, on one hand, the low sensitivity of the measured

data, especially mode shapes, to (small) damages or changes in the system, and on the other hand the strong sensitivity to changes of environmental conditions (temperature, wind, etc.), operation condition and structural uncertainties. This problem is studied in [19] and compensated through singular-value decomposition (SVD).

The second category evades the use of modal parameters. Mostly, the time series data is directly employed into identification. One technique is the application of the Wavelet-Analysis (e.g [20], [21], [22], [23], [24] and [25]). The practice application of the approach for damage detection has yet to be examined. A method based on measured flexibility is presented in the works of Bernal [26, 27], in which the localization of damage was verified only under laboratory conditions. Another possibility in damage detection is method that uses Frequency Response Functions (e.g [28]).

Indeed, a qualitative and quantitative damage detection is mostly possible with the use of a mathematical model, e.g. a finite-element-model (model-based approach). The focal issue is the estimation of the unknown parameter values for the model from experimental test data. This estimation usually requires the solution of an inverse problem, derived from the linear equation

$$\mathbf{A}\theta = \mathbf{b} \tag{2.1}$$

where θ is a vector of the N_p parameter changes to be determined, and $\mathbf{b}$ is a vector of N_o residual quantities derived from the measured data and the model. Normally, $\mathbf{b}$ is contaminated with noise. When $\mathbf{A}$ is close to being rank deficient, i.e rank($\mathbf{A}$) is smaller than N_p, then any small levels of measurement noise may lead to a large deviation in the identified parameters from their exact values. In this case, the inverse problem of Eq. 2.1 is said to be ill-conditioned and its solution is unstable. The problem becomes more pronounced with a large number of parameters to be identified.

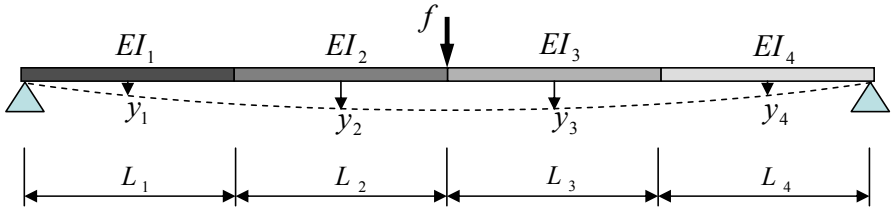

Figure 2.1: Simply supported beam under one-point excitation

As an illustration for the problem of ill-conditioning, a simple simulation example is carried out. The system under consideration is a simply supported beam, modelled as four-beam-element structure as shown in Fig. 2.1. The bending stiffnesses of the elements, $EI_j;\ j = 1 \ldots 4$, should be identified using harmonic excitation f. Simulated noisy measurements, y_j, are generated by adding random values chosen from zero-mean normal distribution

to the exact system output. The beam has element length $L_1 = L_2 = L_3 = L_4 = 1m$ and the mass per unit length $\rho A = 1kg/m$. The actual bending stiffnesses used to compute the output are given by $EI_1 = 0.8Nm^2$; $EI_2, EI_3 = 0.9Nm^2$; $EI_4 = 0.7Nm^2$. Using excitation with frequency of $1rad/s$ and with amplitude of $1N$, the results for EI_1 and EI_2 are shown in Fig. 2.2. These results are obtained from a Monte Carlo simulation using 100 samples

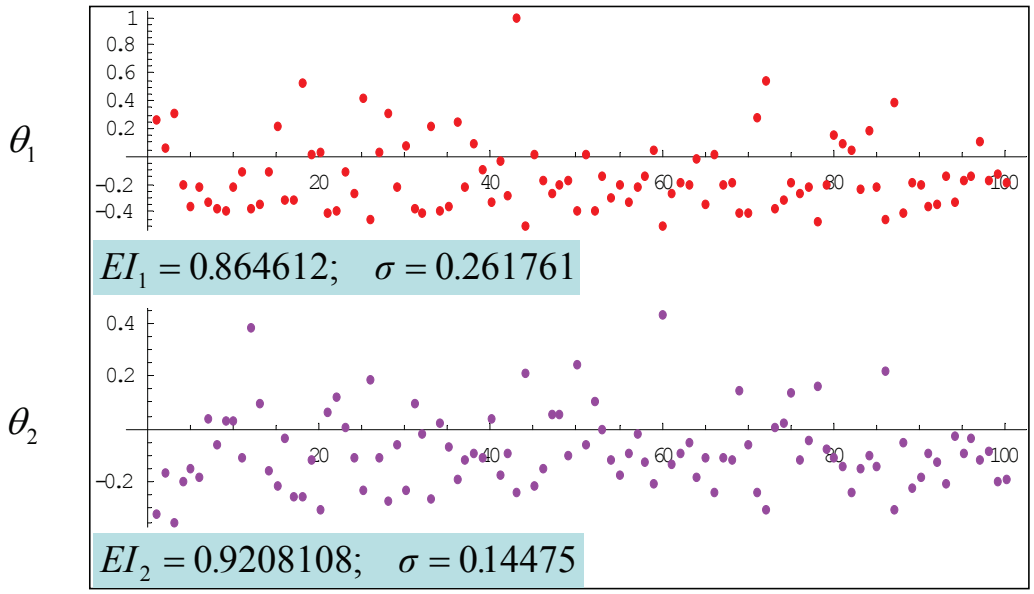

Figure 2.2: Identification of beam's bending stiffness: An illustration of ill-conditionedness

with assumed error in measurements of 2% coefficient of variation (COV). We obtain a COV of 30% for EI_1, and of 15% for EI_2, which clearly indicates the problem that generally arises from the simultaneous identification of many parameters.

Another problem occurs when $N_p > N_o$, so that Eq. 2.1 is under-determined and there are infinite solutions. The SVD can be applied in this case, and also in the case when rank($\mathbf{A}$) $< min(N_p, N_o)$, and provides the solution of minimum norm type. This form of regularization is widely applied to model updating. However, minimum norm solutions rarely result in physically meaningful updated parameters and damage location is still difficult as the identified damage tends to be spread over a large number of parameters. Some other useful regularization techniques applied to model updating are considered in [29].

In fact, the situation can be simply improved by choosing only a small number of parameter values for identifying simultaneously. Both subset selection [30] and statistical type approach [31] assume only a limited number of parameters are to be in error and examine all possible combinations. All the results are compared and the one that best correlates with the measured data is chosen. The problem is that to derive the best set of parameters many subsets of parameters have to be evaluated.

The method of *Selective Sensitivity* gives another way of reducing the number of parameters to be identified by means of excitations which produce strong sensitivities to a subset of parameters while insensitive to other parameters. This approach is the objective of the research and will be presented in the following chapters.

Chapter 3

Selective Sensitivity and Adaptive Excitation

The method of selective sensitivity was firstly introduced by Ben-Haim for adaptive diagnosis of an elastic structure with static loads [32] and then extended to dynamic excitations [7, 33]. By choosing an excitation which causes the response to be insensitive to most of the model parameters, the identification concentrates on a small number of specific parameters, thus allowing to reduce the ill-conditionedness.

In order to derive the excitation forces, this method requires the *true* values of the system properties, which are unknown. Often, an iterative solution is necessary (e.g the multi-hypothesis testing in [33]). The excitation forces in selective sensitivity method can be also obtained from the measured modal data of the tested structure [34]. However, the mass and stiffness matrices that are constructed on the basis of incompletely measured modes will be rank deficient. This has serious consequences for selective sensitivity and may lead to imprecise solution for the forces [11].

We recall that the method in general results in a relatively large and possibly complex system of excitation forces with extensive sensor and exciter requirements. The difficulty of realization of such system limits the applicability of selective sensitivity in practice. For instance, momental excitations are experimentally rather difficult to realize, or it is probably difficult to ensure that the actual forces on the tested structure will agree with the excitation signals based on the calculated force patterns. Oeljeklaus [35] studied this problem. Fritzen [36] proposed a smart system with distributed actuators on the structure, which by means of closed loop control only a certain region of the structure is vibrated while other parts remained almost undeformed. The application of this technique is still limited in laboratory and for small structural systems.

In the following part, the most important features of selective sensitivity which relate to the current research are given in details. Examples and discussions of the existing approach to selective sensitivity are also presented.

3.1 General concept

The equations of motion of an undamped multi-degree-of-freedom (MDOF) system in frequency domain is given in the following form

$$\mathbf{S}(\omega)\mathbf{x}(\omega) = \left(-\omega^2\mathbf{M} + \mathbf{K}\right)\mathbf{x}(\omega) = \mathbf{f}(\omega) \tag{3.1}$$

in which $\mathbf{M}$ denotes the mass matrix, $\mathbf{K}$ is the stiffness matrix, $\mathbf{f}$ is the external excitation, and $\mathbf{x}$ is the displacement response. Assume that the stiffness matrix can be written in the form

$$\mathbf{K} = \sum_{j=1}^{N_p} a_j \mathbf{K}_j \tag{3.2}$$

in which the unknown parameters $a_j;\ j = 1 \ldots N_p$ have to be determined from the identification procedure. Typically, $\mathbf{K}_j$ represent the given substructure matrices defining location and type of parameter uncertainties. Note that the rank of these matrices will generally be much smaller than their dimension. In order for the identification to be possible, the matrices $\mathbf{K}$ and $\mathbf{M}$ must guarantee that the system described by Eq. 3.1 is controllable and observable (see e.g. [37]). This will be satisfied, if both matrices are positive definite, thus restricting the range for the parameters a_j.

The purpose of selective sensitivity is to provide excitation vectors $\mathbf{f}_k$ in such a way, that the sensitivities of the system output to changes in the parameters a_j becomes (almost) zero for all $j \neq k$. The displacement response to this load shall be denoted by $\mathbf{x}_k$ and is given by

$$\mathbf{x}_k = \mathbf{S}^{-1}\mathbf{f}_k \tag{3.3}$$

Assume that a measurement R_k is obtained from the displacement response through a linear combination

$$R_k = \sum_{n=1}^{N} q_n x_n = \mathbf{q}^T\mathbf{x}_k \tag{3.4}$$

Its sensitivity S_{kj} with respect to a_j can be computed from

$$S_{kj} = \frac{\partial R_k}{\partial a_j} = \mathbf{q}^T\frac{\partial \mathbf{x}_k}{\partial a_j} = \mathbf{q}^T\frac{\partial \mathbf{S}^{-1}}{\partial a_j}\mathbf{f}_k \tag{3.5}$$

The derivative of the matrix $\mathbf{S}^{-1}$ is computed from

$$\frac{\partial \mathbf{S}^{-1}}{\partial a_j} = -\mathbf{S}^{-1}\frac{\partial \mathbf{S}}{\partial a_j}\mathbf{S}^{-1} = -\mathbf{S}^{-1}\mathbf{K}_j\mathbf{S}^{-1} \tag{3.6}$$

which leads to

$$S_{kj} = -\mathbf{q}^T\mathbf{S}^{-1}\mathbf{K}_j\mathbf{S}^{-1}\mathbf{f}_k \tag{3.7}$$

Ideally, these sensitivities should meet the condition

$$S_{kj} = \delta_{kj} \tag{3.8}$$

If this condition is to be met for arbitrary measurement vectors $\mathbf{q}$, then $\mathbf{f}_k$ must be chosen so that

$$\begin{aligned} \mathbf{S}^{-1}\mathbf{K}_j\mathbf{S}^{-1}\mathbf{f}_k &= \mathbf{0} \text{ for } j \neq k \\ \mathbf{S}^{-1}\mathbf{K}_j\mathbf{S}^{-1}\mathbf{f}_k &\neq \mathbf{0} \text{ for } j = k \end{aligned} \tag{3.9}$$

Since $\mathbf{S}^{-1}$ is non-singular, this can be achieved only if

$$\begin{aligned} \mathbf{K}_j\mathbf{x}_k &= \mathbf{0} \text{ for } j \neq k \\ \mathbf{K}_j\mathbf{x}_k &\neq \mathbf{0} \text{ for } j = k \end{aligned} \tag{3.10}$$

Eq. 3.10 is the necessary conditions for achieving selective sensitivity. Note that these conditions on the displacement vector $\mathbf{x}_k$ are independent of the actual parameter values a_j. Obviously, the vectors satisfying the first of Eq. 3.10 must be in the subspace spanned by the eigenvectors of $\mathbf{K}_j$ belonging to the zero eigenvalue. This means that the topology of the Finite-Element-discretization is sufficient to decide whether a selectively sensitive excitation exists. Actually, $\mathbf{x}_k$ can be determined by solving the following eigenvector problem

$$\sum_j \mathbf{K}_j\mathbf{x}_k = 0 \cdot \mathbf{x}_k \ ; \ j \neq k \tag{3.11}$$

Once the displacement vectors $\mathbf{x}_k$ have been determined, the corresponding force vectors $\mathbf{f}_k$ can be computed from Eq. 3.1. However, this step generally involves the knowledge of all parameters to be identified, thus possibly losing the advantages of selective sensitivity. Therefore, an experimental set-up is often suggested, which by an appropriate feed-back enforces the necessary conditions on $\mathbf{x}_k$, thus automatically rendering suitable excitations $\mathbf{f}_k$. This feed-back loop has to implement a solver for the system of linear equations

$$\mathbf{S}\mathbf{x}_k = \mathbf{f}_k \tag{3.12}$$

in which the matrix $\mathbf{S}$ is not explicitly known, but the inverse relation can be measured

$$\mathbf{S}^{-1}\mathbf{f}_k = \mathbf{x}_k \tag{3.13}$$

If the required set of displacement vectors $\mathbf{x}_k$ cannot be found, then it still may be possible to achieve selective sensitivity for special measurement vectors $\mathbf{q}$. This is always necessary if the number of unknown parameters is larger than the number of degrees of freedom of the FE-model, i.e. if $N_p > N$. In this case, it is convenient to determine vectors $\mathbf{y}_k$ defined as

$$\mathbf{y}_k = \mathbf{S}^{-1}\mathbf{q} \tag{3.14}$$

from the conditions

$$\mathbf{y}_k^T \mathbf{K}_j \mathbf{x}_k = \delta_{kj} \tag{3.15}$$

Again, this condition is independent of the actual parameter values. Of course, the final measurement vectors $\mathbf{q}$ have to be determined by using the relation given in Eq. 3.14 which requires the actual system parameters. However, the iteration as outlined above is not required if all N vectors $\mathbf{x}_j$ have already been determined. Since then any vector $\mathbf{y}_k$ can be written as a linear combination of the $\mathbf{x}_j$, i.e.

$$\mathbf{y}_k = \sum_{j=1}^{N_p} d_j \mathbf{x}_j \tag{3.16}$$

with readily determined coefficients d_j, it is easily seen that

$$\mathbf{q} = \mathbf{S}\mathbf{y}_k = \sum_{j=1}^{N_p} d_j \mathbf{S}\mathbf{x}_j = \sum_{j=1}^{N_p} d_j \mathbf{f}_j \tag{3.17}$$

so that the previously determined excitation vectors $\mathbf{f}_j$ can be used immediately.

It is important to note that in the above procedure measurements as well as excitations must be applied at all DOFs, which is however usually not possible to realize in practice or results in very high expense.

3.1.1 Application to a frame structure

Consider a simple four-degree-of-freedom shear beam system as sketched in Fig. 3.1. We assume that the mass M is known, and that the four inter-storey stiffnesses (springs) a_j; $j = 1 \ldots 4$ should be identified from dynamic experiments.

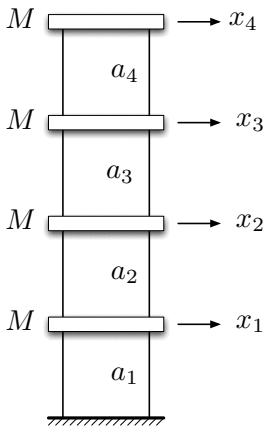

Figure 3.1: Four-degree-of-freedom shear beam system

The stiffness matrix is given by

$$\mathbf{K} = \begin{bmatrix} a_1 + a_2 & -a_2 & 0 & 0 \\ -a_2 & a_2 + a_3 & -a_3 & 0 \\ 0 & -a_3 & a_3 + a_4 & -a_4 \\ 0 & 0 & -a_4 & a_4 \end{bmatrix}.$$

This can easily be written in the form of Eq. 3.2

$$\mathbf{K} = a_1 \begin{bmatrix} 1 & 0 & 0 & 0 \\ 0 & 0 & 0 & 0 \\ 0 & 0 & 0 & 0 \\ 0 & 0 & 0 & 0 \end{bmatrix} + a_2 \begin{bmatrix} 1 & -1 & 0 & 0 \\ -1 & 1 & 0 & 0 \\ 0 & 0 & 0 & 0 \\ 0 & 0 & 0 & 0 \end{bmatrix} + a_3 \begin{bmatrix} 0 & 0 & 0 & 0 \\ 0 & 1 & -1 & 0 \\ 0 & -1 & 1 & 0 \\ 0 & 0 & 0 & 0 \end{bmatrix} + a_4 \begin{bmatrix} 0 & 0 & 0 & 0 \\ 0 & 0 & 0 & 0 \\ 0 & 0 & 1 & -1 \\ 0 & 0 & -1 & 1 \end{bmatrix}.$$

The analysis of the matrices $\mathbf{K}_j$ reveals that there is indeed a suitable set of displacement vectors $\mathbf{x}_k;\ k = 1 \ldots 4$ which is readily satisfies the condition in Eq. 3.10

$$\mathbf{x}_1 = C_1 \begin{Bmatrix} 1 \\ 1 \\ 1 \\ 1 \end{Bmatrix};\ \mathbf{x}_2 = C_2 \begin{Bmatrix} 0 \\ 1 \\ 1 \\ 1 \end{Bmatrix};\ \mathbf{x}_3 = C_3 \begin{Bmatrix} 0 \\ 0 \\ 1 \\ 1 \end{Bmatrix};\ \mathbf{x}_4 = C_4 \begin{Bmatrix} 0 \\ 0 \\ 0 \\ 1 \end{Bmatrix},$$

where C_i are arbitrary real numbers. It is interesting to note that these displacement vectors correspond physically to situations in which only the spring a_k has a non-zero stress. This means that selectively sensitive excitations produce stress only in the elements whose properties should be identified. The displacement patterns are shown in Fig. 3.2.

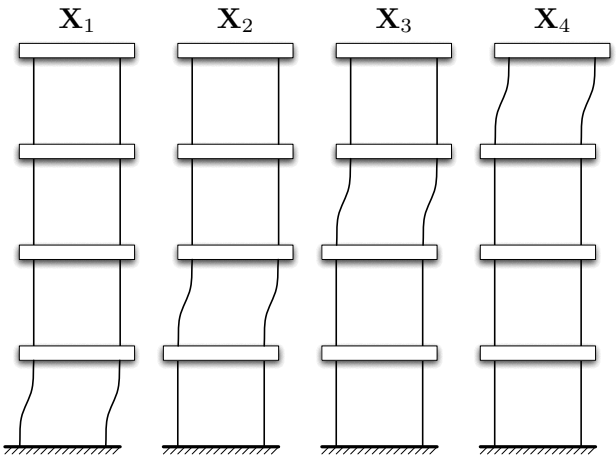

Figure 3.2: Sensitively selective displacement patterns for four-dof-system

3.1.2 Application to a simply supported beam

Consider a simply supported beam modeled by four beam elements (cf. Fig. 3.3). The elements have the length L_j and the bending stiffness $a_j = EI_j;\ j = 1 \dots 4$. We wish to make the response sensitive to each stiffness a_j. The substructure matrices are given by

$$\mathbf{K}_1 = \frac{\partial \mathbf{K}}{\partial a_1} = \begin{bmatrix} 4/L_1 & -6/L_1^2 & 2/L_1 & 0 & 0 & 0 & 0 & 0 \\ -6/L_1^2 & 12/L_1^3 & -6/L_1^2 & 0 & 0 & 0 & 0 & 0 \\ 2/L_1 & -6/L_1^2 & 4/L_1 & 0 & 0 & 0 & 0 & 0 \\ 0 & 0 & 0 & 0 & 0 & 0 & 0 & 0 \\ 0 & 0 & 0 & 0 & 0 & 0 & 0 & 0 \\ 0 & 0 & 0 & 0 & 0 & 0 & 0 & 0 \\ 0 & 0 & 0 & 0 & 0 & 0 & 0 & 0 \\ 0 & 0 & 0 & 0 & 0 & 0 & 0 & 0 \end{bmatrix}$$

$$\mathbf{K}_2 = \frac{\partial \mathbf{K}}{\partial a_2} = \begin{bmatrix} 0 & 0 & 0 & 0 & 0 & 0 & 0 & 0 \\ 0 & 12/L_2^3 & 6/L_2^2 & -12/L_2^3 & 6/L_2^2 & 0 & 0 & 0 \\ 0 & 6/L_2^2 & 4/L_2 & -6/L_2^2 & 2/L_2 & 0 & 0 & 0 \\ 0 & -12/L_2^3 & -6/L_2^2 & 12/L_2^3 & -6/L_2^2 & 0 & 0 & 0 \\ 0 & 6/L_2^2 & 2/L_2 & -6/L_2^2 & 4/L_2 & 0 & 0 & 0 \\ 0 & 0 & 0 & 0 & 0 & 0 & 0 & 0 \\ 0 & 0 & 0 & 0 & 0 & 0 & 0 & 0 \\ 0 & 0 & 0 & 0 & 0 & 0 & 0 & 0 \end{bmatrix}$$

$$\mathbf{K}_3 = \frac{\partial \mathbf{K}}{\partial a_3} = \begin{bmatrix} 0 & 0 & 0 & 0 & 0 & 0 & 0 & 0 \\ 0 & 0 & 0 & 0 & 0 & 0 & 0 & 0 \\ 0 & 0 & 0 & 0 & 0 & 0 & 0 & 0 \\ 0 & 0 & 0 & 12/L_3^3 & 6/L_3^2 & -12/L_3^3 & 6/L_3^2 & 0 \\ 0 & 0 & 0 & 6/L_3^2 & 4/L_3 & -6/L_3^2 & 2/L_3 & 0 \\ 0 & 0 & 0 & -12/L_3^3 & -6/L_3^2 & 12/L_3^3 & -6/L_3^2 & 0 \\ 0 & 0 & 0 & 6/L_3^2 & 2/L_3 & -6/L_3^2 & 4/L_3 & 0 \\ 0 & 0 & 0 & 0 & 0 & 0 & 0 & 0 \end{bmatrix}$$

$$\mathbf{K}_4 = \frac{\partial \mathbf{K}}{\partial a_4} = \begin{bmatrix} 0 & 0 & 0 & 0 & 0 & 0 & 0 & 0 \\ 0 & 0 & 0 & 0 & 0 & 0 & 0 & 0 \\ 0 & 0 & 0 & 0 & 0 & 0 & 0 & 0 \\ 0 & 0 & 0 & 0 & 0 & 0 & 0 & 0 \\ 0 & 0 & 0 & 0 & 0 & 0 & 0 & 0 \\ 0 & 0 & 0 & 0 & 0 & 12/L_4^3 & 6/L_4^2 & 6/L_4^2 \\ 0 & 0 & 0 & 0 & 0 & 6/L_4^2 & 4/L_4 & 2/L_4 \\ 0 & 0 & 0 & 0 & 0 & 6/L_4^2 & 2/L_4 & 4/L_4 \end{bmatrix}.$$

The selectively sensitive displacement patterns can be found quite easily. For the example, there are more degree-of-freedoms (DOFs) than parameters to be identified. Hence, more than one suitable displacement pattern exist for each parameter. Actually, two patterns were found for each parameter. They are given in Fig. 3.4 and 3.5 for a_1 and a_2, respectively.

Again, these displacement patterns have the property of inducing stresses only in those elements whose stiffness is to be identified. It can easily be seen that these displacements can be achieved only by having forces acting on both translational and rotational degrees of freedom. It is experimentally rather difficult to realize moment excitations, so this approach will not be very useful for structures in which bending plays a significant role.

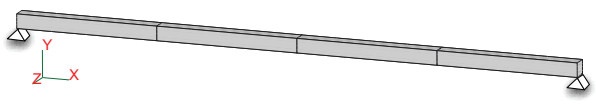

Figure 3.3: Simply supported beam

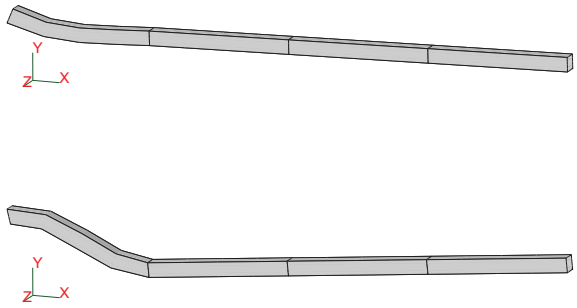

Figure 3.4: Sensitively selective displacement patterns for determining a_1

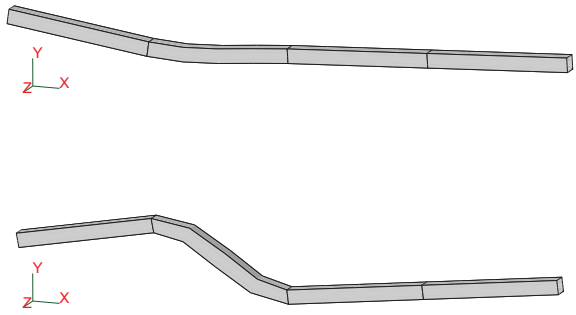

Figure 3.5: Sensitively selective displacement patterns for determining a_2

3.2 Weak selective sensitivity

It is found that selective sensitivity is often unattainable in practice, especially when measurements and excitations are limited. An alternative approach to handling this situation is to relax the definition of selective sensitivity.

3.2.1 Definition

Assume that the excitation is present as $\mathbf{Tf}(t)$ and the output is expressed in terms of the displacements $\mathbf{y}(t) = \mathbf{Gx}(t)$, where $\mathbf{T}$ is $N_d \times N_e$ matrix locating the loads and $\mathbf{G}$ is $N_o \times N_d$ matrix locating the outputs. The equation of motion becomes

$$\mathbf{S}(\omega)\mathbf{x}(\omega) = \left(-\omega^2\mathbf{M} + \mathbf{K}\right)\mathbf{x}(\omega) = \mathbf{Tf}(\omega) \tag{3.18}$$

and the output $\mathbf{y}$ is obtained from the displacement response through

$$\mathbf{y} = \mathbf{G} \cdot \mathbf{x} = \mathbf{G}\mathbf{S}^{-1}\mathbf{T}\mathbf{f} \tag{3.19}$$

Its sensitivity S_j with respect to a_j is defined as

$$S_j = \left(\frac{\partial \mathbf{y}}{\partial a_j}\right)^T \left(\frac{\partial \mathbf{y}}{\partial a_j}\right) = \mathbf{f}^T\mathbf{T}^T \left(\frac{\partial \mathbf{S}^{-1}}{\partial a_j}\right)^T \mathbf{G}^T\mathbf{G} \left(\frac{\partial \mathbf{S}^{-1}}{\partial a_j}\right) \mathbf{T}\mathbf{f} = \mathbf{f}^T\mathbf{D}_j\mathbf{f} \tag{3.20}$$

where

$$\mathbf{D}_j = \mathbf{T}^T \left(-\mathbf{S}^{-1}\mathbf{K}_j\mathbf{S}^{-1}\right)^T \mathbf{G}^T\mathbf{G} \left(-\mathbf{S}^{-1}\mathbf{K}_j\mathbf{S}^{-1}\right) \mathbf{T} \tag{3.21}$$

An excitation vector $\mathbf{f}_k$ will be said to be *weakly selectively sensitive* to parameters a_k if

$$\begin{aligned} \mathbf{f}_k^T\mathbf{D}_j\mathbf{f}_k &= small \text{ for } j \neq k \\ \mathbf{f}_k^T\mathbf{D}_j\mathbf{f}_k &= large \text{ for } j = k \end{aligned} \tag{3.22}$$

One possibility to obtain $\mathbf{f}_k$ is to minimize the sensitivities with respect to the parameters $a_j (j \neq k)$, while maintaining the sensitivities with respect to the parameters a_k as a constant, i.e $S_k = \alpha_k$. The objective function for this optimization problem therefore is defined as

$$J_k = \sum_j \mathbf{f}_k^T\mathbf{D}_j\mathbf{f}_k + \lambda \left(\mathbf{f}_k^T\mathbf{D}_k\mathbf{f}_k - \alpha_k\right) \tag{3.23}$$

where λ denotes a Lagrange multiplier. The condition to obtain optimum is $\frac{\partial J_k}{\partial \mathbf{f}_k} = 0$ which leads to the eigenproblem

$$\sum_j \mathbf{D}_j\mathbf{f}_k = -\lambda\mathbf{D}_k\mathbf{f}_k \tag{3.24}$$

in which $-\lambda$ is the eigenvalue and $\mathbf{f}_k$ is the corresponding eigenvector. The objective is to minimize J_k, thus the smallest eigenvalue and its corresponding eigenvector are selected. The displacement response $\mathbf{x}_k$ caused by $\mathbf{f}_k$, is then determined from

$$\mathbf{x}_k = \left(-\omega^2\mathbf{M} + \mathbf{K}\right)^{-1} \mathbf{T}\mathbf{f}_k \tag{3.25}$$

This displacement pattern will be used in order to evaluate the level of sensitivity of the obtained force.

In the following parts, we will examine weak selective sensitivity with two beam structures, one is statically determinate and the other is indeterminate. For simplicity, only static load case is considered.

3.2.2 Application to a simply supported beam

Consider the statically determinate simply supported beam with span length $L_1 = L_2 = L_3 = L_4 = L = 1m$ as shown in Fig. 3.6. We wish to determine the static load configurations $f_l;\ l = 1 \dots 4$ to identify the bending stiffness values $EI_j;\ j = 1 \dots 4$.

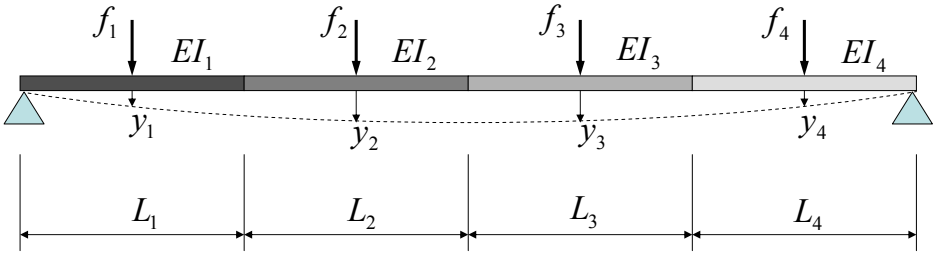

Figure 3.6: Simply supported beam under static loads

The system equation is given in the following form $\mathbf{Kx} = \mathbf{Tf}$ and the system output is obtained by $\mathbf{y} = \mathbf{Gx}$. For the considered beam structure, the matrices $\mathbf{T}$ and $\mathbf{G}$ are

$$\mathbf{T}^T = \mathbf{G} = \begin{bmatrix} N_2 & N_3 & N_4 & 0 & 0 & 0 & 0 & 0 \\ 0 & N_1 & N_2 & N_3 & N_4 & 0 & 0 & 0 \\ 0 & 0 & 0 & N_1 & N_2 & N_3 & N_4 & 0 \\ 0 & 0 & 0 & 0 & 0 & N_1 & N_2 & N_4 \end{bmatrix},$$

where $\mathbf{N}$ is the shape function of beam element [38], given by

$$\mathbf{N} = [N_1, N_2, N_3, N_4] = \left[\ 1 - \tfrac{3x^2}{L^2} + \tfrac{2x^3}{L^3},\ \ x - \tfrac{2x^2}{L} + \tfrac{x^3}{L^2},\ \ \tfrac{3x^2}{L^2} - \tfrac{2x^3}{L^3},\ \ -\tfrac{x^2}{L} + \tfrac{x^3}{L^2}\ \right]_{x=L/2},$$

thus

$$\mathbf{T}^T = \mathbf{G} = \begin{bmatrix} 0.125 & 0.5 & -0.125 & 0 & 0 & 0 & 0 & 0 \\ 0 & 0.5 & 0.125 & 0.5 & -0.125 & 0 & 0 & 0 \\ 0 & 0 & 0 & 0.5 & 0.125 & 0.5 & -0.125 & 0 \\ 0 & 0 & 0 & 0 & 0 & 0.5 & 0.125 & -0.125 \end{bmatrix}.$$

Giving $EI_1 = EI_2 = EI_3 = EI_4 = EI_0 = 1Nm^2$, the selectively sensitive force patterns for EI_1 and EI_2 obtained from Eq. 3.24 are respectively

$$\mathbf{f}_1 = \begin{Bmatrix} 1.0000000 \\ -0.425749 \\ 0.0707636 \\ -0.0157067 \end{Bmatrix}, \quad \mathbf{f}_2 = \begin{Bmatrix} -0.669849 \\ 1.0000000 \\ -0.592546 \\ 0.128168 \end{Bmatrix}.$$

Here, the expression for $\mathbf{D}_j$ in Eq. 3.24 applying to static identification is

$$\mathbf{D}_j = \mathbf{T}^T \left(-\mathbf{K}^{-1}\mathbf{K}_j\mathbf{K}^{-1}\right)^T \mathbf{G}^T\mathbf{G} \left(-\mathbf{K}^{-1}\mathbf{K}_j\mathbf{K}^{-1}\right) \mathbf{T} \tag{3.26}$$

and $\mathbf{K}_j$ are given in section 3.1.2. The corresponding displace patterns are illustrated in Fig. 3.7. These displacement patterns have property of including stresses (almost) only in those elements whose stiffness is to be identified.

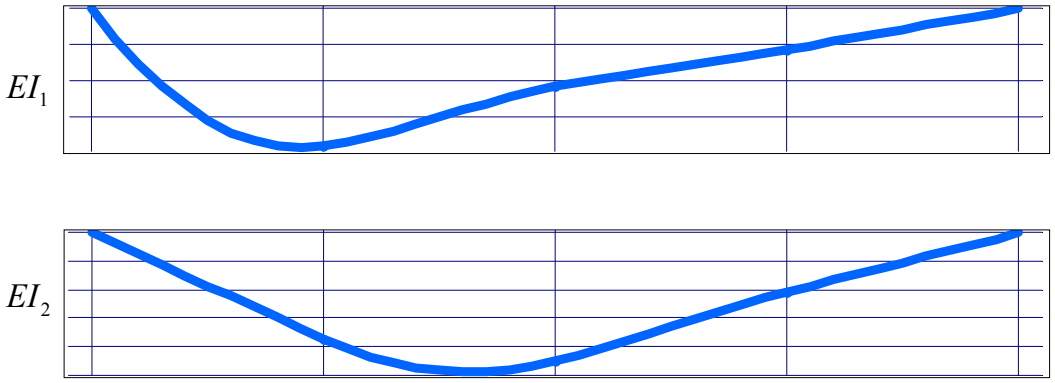

Figure 3.7: Simple beam: Weakly selectively sensitive displacement patterns

Now, the bending stiffness EI_j are randomly chosen from the range $[0.5, 2.0]$, i.e EI_j are assumed to be uniformly distributed in $[0.5, 2.0]$. Fig.3.8 shows the selectively sensitive force patterns for EI_1 and EI_2, respectively, corresponding to 10 model samples. In this case the force patterns remain almost unchanged for 10 different beam models. It implies that, for the determinate beam structure, the selectively sensitive force patterns determined from Eq. 3.24 are independent on the values of bending stiffness EI_j.

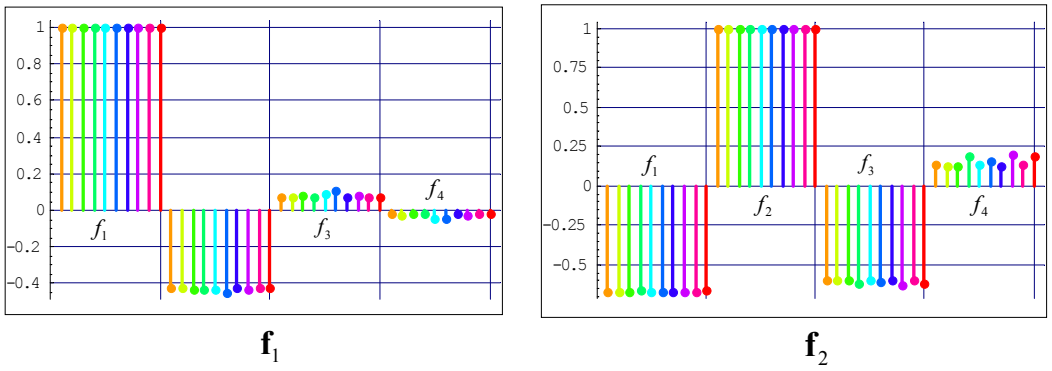

Figure 3.8: Weakly selectively sensitive force patterns for 10 simple beam's model samples

3.2.3 Application to a continuously supported beam

The weak selective sensitivity will now be demonstrated on a four-element beam structure shown in Fig. 3.9.

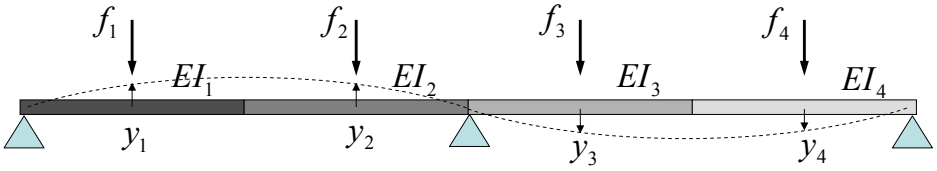

Figure 3.9: Continuously supported beam

The the stiffness matrix $\mathbf{K}$ is given by

$$\mathbf{K} = EI_1 \begin{bmatrix} 4 & -6 & 2 & 0 & 0 & 0 & 0 \\ -6 & 12 & -6 & 0 & 0 & 0 & 0 \\ 2 & -6 & 4 & 0 & 0 & 0 & 0 \\ 0 & 0 & 0 & 0 & 0 & 0 & 0 \\ 0 & 0 & 0 & 0 & 0 & 0 & 0 \\ 0 & 0 & 0 & 0 & 0 & 0 & 0 \\ 0 & 0 & 0 & 0 & 0 & 0 & 0 \end{bmatrix} + EI_2 \begin{bmatrix} 0 & 0 & 0 & 0 & 0 & 0 & 0 \\ 0 & 12 & 6 & 6 & 0 & 0 & 0 \\ 0 & 6 & 4 & 2 & 0 & 0 & 0 \\ 0 & 6 & 2 & 4 & 0 & 0 & 0 \\ 0 & 0 & 0 & 0 & 0 & 0 & 0 \\ 0 & 0 & 0 & 0 & 0 & 0 & 0 \\ 0 & 0 & 0 & 0 & 0 & 0 & 0 \end{bmatrix} +$$

$$EI_3 \begin{bmatrix} 0 & 0 & 0 & 0 & 0 & 0 & 0 \\ 0 & 0 & 0 & 0 & 0 & 0 & 0 \\ 0 & 0 & 0 & 0 & 0 & 0 & 0 \\ 0 & 0 & 0 & 4 & -6 & 2 & 0 \\ 0 & 0 & 0 & -6 & 12 & -6 & 0 \\ 0 & 0 & 0 & 2 & -6 & 4 & 0 \\ 0 & 0 & 0 & 0 & 0 & 0 & 0 \end{bmatrix} + EI_4 \begin{bmatrix} 0 & 0 & 0 & 0 & 0 & 0 & 0 \\ 0 & 0 & 0 & 0 & 0 & 0 & 0 \\ 0 & 0 & 0 & 0 & 0 & 0 & 0 \\ 0 & 0 & 0 & 0 & 0 & 0 & 0 \\ 0 & 0 & 0 & 0 & 12 & 6 & 6 \\ 0 & 0 & 0 & 0 & 6 & 4 & 2 \\ 0 & 0 & 0 & 0 & 6 & 2 & 4 \end{bmatrix}.$$

The input force matrix $\mathbf{T}$ and the output matrix $\mathbf{G}$ are given by

$$\mathbf{T}^T = \mathbf{G} = \begin{bmatrix} N_2 & N_3 & N_4 & 0 & 0 & 0 & 0 \\ 0 & N_1 & N_2 & N_4 & 0 & 0 & 0 \\ 0 & 0 & 0 & N_2 & N_3 & N_4 & 0 \\ 0 & 0 & 0 & 0 & N_1 & N_2 & N_4 \end{bmatrix}_{x=L/2} =$$

$$= \begin{bmatrix} 0.125 & 0.5 & -0.125 & 0 & 0 & 0 & 0 \\ 0 & 0.5 & 0.125 & -0.125 & 0 & 0 & 0 \\ 0 & 0 & 0 & 0.125 & 0.5 & -0.125 & 0 \\ 0 & 0 & 0 & 0 & 0.5 & 0.125 & -0.125 \end{bmatrix}.$$

For this indeterminate beam structure, it is impossible to obtain a force vector which produces a displacement response sensitive to only one stiffness parameter. Nevertheless, the displacement response sensitive to two parameters can be achieved. Therefore, the equation to generate the force in the form of Eq. 3.24 is rewritten as

$$\sum_j \mathbf{D}_j \mathbf{f}_k = -\lambda \sum_k \mathbf{D}_k \mathbf{f}_k \tag{3.27}$$

where k is the index of the bending stiffness to be identified. For the same values of bending stiffness as in previous example, the force pattern $\mathbf{f}_{1,4}$ for both EI_1 and EI_4, and $\mathbf{f}_{2,3}$ for both EI_2 and EI_3 obtained from Eq. 3.27 are

$$\mathbf{f}_{1,4} = \left\{ \begin{array}{c} -0.620444 \\ 0.33919 \\ -0.33919 \\ 0.620444 \end{array} \right\}, \quad \mathbf{f}_{2,3} = \left\{ \begin{array}{c} -0.324604 \\ 0.670188 \\ -0.592724 \\ 0.306852 \end{array} \right\}.$$

The corresponding displacement patterns are shown in Fig. 3.10. Clearly, there is no stress appears in the elements whose stiffness is not to be identified.

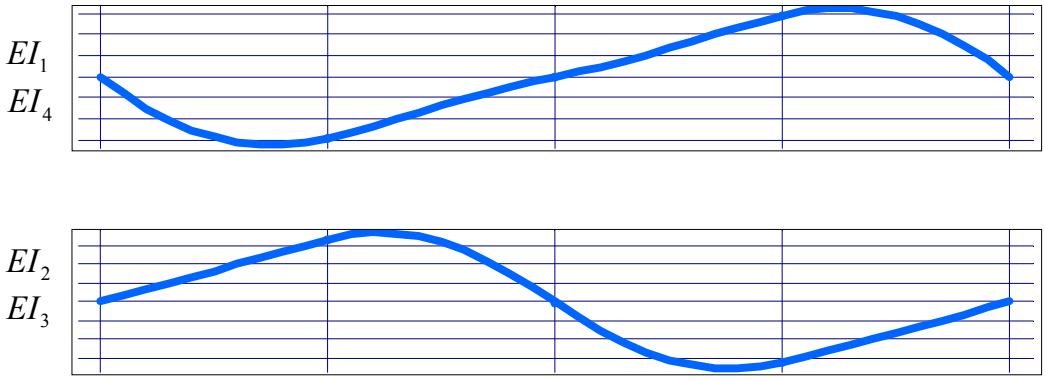

Figure 3.10: Continuous beam: Weakly selectively sensitive displacement patterns

Chapter 4

Quasi-static Approach

As discussed in the previous chapter, one of the major disadvantages of selective sensitivity is the requirement of precise knowledge about the parameters to be identified. A new approach which can evade the use of parameter values to attain nearly selective sensitivity, the *quasi-static* approach is presented in this chapter.

4.1 Theory

The selectively sensitive force $\mathbf{f}_k$ for static identification of the selected stiffness parameter a_k is computed by

$$\mathbf{f}_k = \mathbf{K}\mathbf{x}_k = \left(\sum_{j=1}^{N_p} a_j \mathbf{K}_j \right) \mathbf{x}_k \tag{4.1}$$

where $\mathbf{x}_k$ is the displacement response which satisfies the Eq. 3.10. Thus we have

$$\mathbf{f}_k = a_k \mathbf{K}_k \mathbf{x}_k \propto \mathbf{K}_k \mathbf{x}_k \tag{4.2}$$

Eq. 4.2 implies that, a force vector $\mathbf{f} = c \times \mathbf{K}_k \mathbf{x}_k$ with c is arbitrary constant will induce system displacement output proportional to $\mathbf{x}_k$, i.e. only sensitive to a_k. This force is independent of the actual value of the parameter a_j, so no prior information of the parameters is required.

The idea of *quasi-static* approach is to utilize the static force pattern for dynamic experiments as long as the frequency of the excitations stays below the fundamental frequency of the structure. It is expected that similar deformation behavior will be achieved, thus the sensitivities should remain in the same order of magnitude. The approach is illustrated by numerical examples in the next section.

4.2 Applications

4.2.1 Frame structure

Consider the same frame structure as in the previous chapter with the mass $M = 1kg$ and the springs $a_1 = a_2 = a_3 = a_4 = 1N/m$, giving the first natural frequency of the structure is $\omega_1 = 0.347296rad/s$. With $\mathbf{K}_k$ and $\mathbf{x}_k$ given in section 3.1.1, the static force patterns are easily computed by $\mathbf{f}_k = \mathbf{K}_k\mathbf{x}_k$. We obtain

$$\mathbf{f}_1 = C_1 \begin{Bmatrix} 1 \\ 0 \\ 0 \\ 0 \end{Bmatrix};\ \mathbf{f}_2 = C_2 \begin{Bmatrix} -1 \\ 1 \\ 0 \\ 0 \end{Bmatrix};\ \mathbf{f}_3 = C_3 \begin{Bmatrix} 0 \\ -1 \\ 1 \\ 0 \end{Bmatrix};\ \mathbf{f}_4 = C_4 \begin{Bmatrix} 0 \\ 0 \\ -1 \\ 1 \end{Bmatrix}$$

for $a_1,\ a_2,\ a_3$ and a_4, respectively.

Applying these force patterns ($C_i = 1$) with different frequencies ω in the range [0;0.25], the displacement patterns are obtained from the relation

$$\mathbf{x} = \left(\mathbf{K} - \omega^2\mathbf{M}\right)^{-1}\mathbf{f} \tag{4.3}$$

These displacement patterns are shown in Fig. 4.1. It is obviously that the displacement patterns under low frequency excitations (e.g for $\omega = 0.1$ and $\omega = 0.2$) are very similar to those for static forces ($\omega = 0$).

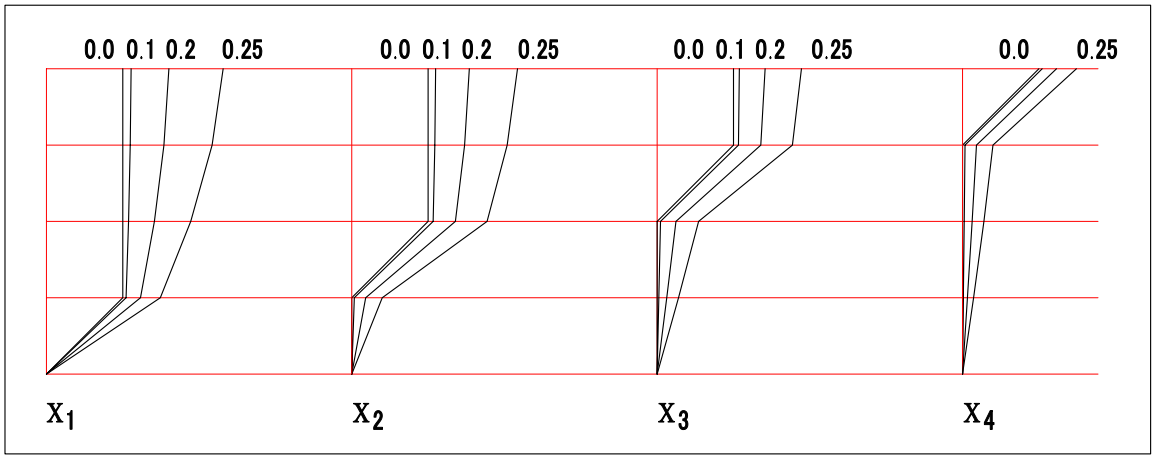

Figure 4.1: Quasi-static displacement patterns for frame structure with different excitation frequencies

4.2.2 Simply supported beam

Consider the statically determinate simply supported beam with span length L as shown in Fig. 4.2. We want to determine the bending stiffness values $EI_j;\ j = 1 \dots 4$ using selectively sensitive load configurations $f_l;\ l = 1 \dots 4$. For the beam structure, it is however difficult

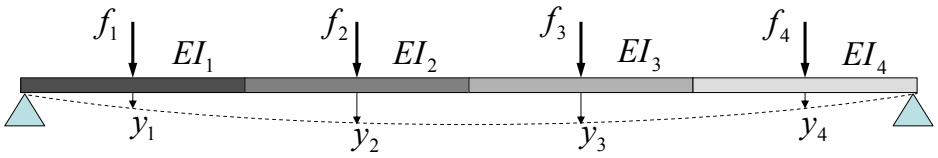

Figure 4.2: Simply supported beam under four-point excitation

to obtain selectively sensitive forces directly from displacement patterns. Therefore, it is desirable to develop an alternative approach (see in [44]).

Due to the fact that the structure is statically determinate, i.e. the distribution of the bending moments is independent of the actual bending stiffness values, it is possible to write the flexibility matrix $\mathbf{H}$ relating the forces f_l to the displacements y_k by means of $\boldsymbol{y} = \mathbf{H}\mathbf{f}$ in the following form

$$\mathbf{H} = \sum_{j=1}^{4} \mathbf{H}_j \frac{1}{EI_j} \tag{4.4}$$

so that

$$y_k = \sum_{l,j=1}^{4} H_{klj} f_l \frac{1}{EI_j} \tag{4.5}$$

where the flexibility contributions of each element $\mathbf{H}_m$ are given by

$$\mathbf{H}_1 = \begin{bmatrix} 0.001790 & 0.001831 & 0.001099 & 0.000366 \\ 0.001831 & 0.002034 & 0.001221 & 0.000407 \\ 0.001099 & 0.001221 & 0.000732 & 0.000244 \\ 0.000366 & 0.000407 & 0.000244 & 0.000081 \end{bmatrix} \cdot L^3$$

$$\mathbf{H}_2 = \begin{bmatrix} 0.001546 & 0.003947 & 0.002685 & 0.000895 \\ 0.003947 & 0.010416 & 0.007202 & 0.002401 \\ 0.002685 & 0.007202 & 0.005127 & 0.001709 \\ 0.000895 & 0.002401 & 0.001709 & 0.000570 \end{bmatrix} \cdot L^3$$

$$\mathbf{H}_3 = \begin{bmatrix} 0.000570 & 0.001709 & 0.002401 & 0.000895 \\ 0.001709 & 0.005127 & 0.007202 & 0.002685 \\ 0.002401 & 0.007202 & 0.010416 & 0.003947 \\ 0.000895 & 0.002685 & 0.003947 & 0.001546 \end{bmatrix} \cdot L^3$$

$$\mathbf{H}_4 = \begin{bmatrix} 0.000081 & 0.000244 & 0.000407 & 0.000366 \\ 0.000244 & 0.000732 & 0.001221 & 0.001099 \\ 0.000407 & 0.001221 & 0.002034 & 0.001831 \\ 0.000366 & 0.001099 & 0.001831 & 0.001790 \end{bmatrix} \cdot L^3$$

It is now possible to choose the elements of a force vector $\mathbf{f}_k$ in such a way, that one specific displacement y_k depends only on the stiffness EI_k but not on any other stiffness. This can be achieved by assembling the k-th rows of the matrices $\mathbf{H}_m$ into a matrix $\mathbf{B}_k$ and solve the system of equations

$$\mathbf{B}_k\mathbf{f}_k = \mathbf{u}_k \tag{4.6}$$

in which $\mathbf{u}_k$ is a vector with only one arbitrary, non-zero entry at the k-th position. For $k = 1$, we have

$$\mathbf{B}_1 = \begin{bmatrix} 0.001790 & 0.001831 & 0.001099 & 0.000366 \\ 0.001546 & 0.003947 & 0.002685 & 0.000895 \\ 0.000570 & 0.001709 & 0.002401 & 0.000895 \\ 0.000081 & 0.000244 & 0.000407 & 0.000366 \end{bmatrix}; \quad \mathbf{u}_1 = \begin{Bmatrix} 1 \\ 0 \\ 0 \\ 0 \end{Bmatrix},$$

which leads to a force vector

$$\mathbf{f}_1 = \begin{Bmatrix} 1.00000 \\ -0.44751 \\ 0.08960 \\ -0.02260 \end{Bmatrix} \cdot F_0$$

Here the k-th element of $\mathbf{f}_1$ has been set to a reference value of F_0, since the scaling is arbitrary. Applying this load vector to the structure, it is seen that the displacement y_1 becomes

$$y_1 = 0.0010609\frac{F_0L^3}{EI_1}$$

from which the bending stiffness EI_1 is readily computed. In the same manner, force vectors and displacement relations involving the remaining bending stiffnesses can be obtained as

$$\mathbf{f}_2 = \begin{Bmatrix} -0.75079 \\ 1.00000 \\ -0.59320 \\ 0.15969 \end{Bmatrix} \cdot F_0; \quad y_2 = 0.0035631\frac{F_0L^3}{EI_2}.$$

The remaining equations for EI_3 and EI_4 are easily obtained by symmetry considerations. These relations clearly show that the outputs depend only on those bending stiffness should be identified.

It is interesting to notice that, these forces are consistent with the results obtained in the example in section 3.2.2. This implies that for the statically determinate beam structure, the weak selective sensitivity can also utilized to compute the force pattern, regardless of the parameter values.

Now, the computed force patterns are applied for dynamic experiments. For simplicity, it will be assumed that the mass matrix can be sufficiently well approximated by a diagonal matrix (lumped mass matrix, see Fig. 4.3). In this case, the relationship between applied

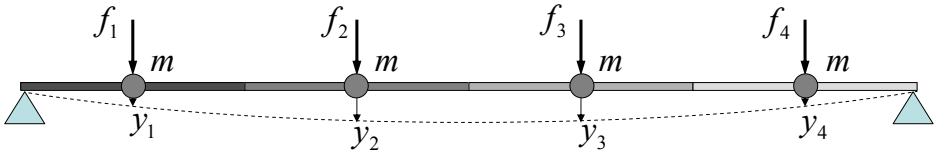

Figure 4.3: Simply supported beam with point masses

force $\mathbf{f}$ and output displacement $\mathbf{y}$ in the frequency domain becomes (cf. Eq. 3.1)

$$\left(\mathbf{K} - \omega^2\mathbf{M}\right)^{-1}\mathbf{f} = \mathbf{y} \tag{4.7}$$

The inverse of stiffness matrix $\mathbf{K}$ is given by Eq. 4.4. Thus, Eq. 4.7 spells out as

$$\left[\left(\sum_{j=1}^{4}\frac{1}{EI_j}\mathbf{H}_j\right)^{-1} - \omega^2\mathbf{M}\right]^{-1}\mathbf{f} = \mathbf{y} \tag{4.8}$$

Given the measured values of force and displacement, this system of equations can be solved for the bending stiffnesses.

A numerical example is carried out using values of the lump mass $m = 1$ and $EI_j = 1$. For this case, the first natural circular frequency of the system is $\omega_1 = 2.14 rad/s$. An excitation frequency of $\omega = 1$ is used. Carrying out the identification with a uniform load pattern (all loads equal to 1), and assuming a COV of 2% for the measurements, we obtain a COV of 24% for EI_1, and of 15% for EI_2. These results were obtained from a Monte Carlo simulation using 400 samples. In contrast, the application of the (statically) selectively sensitive force pattern $\mathbf{f}_1$ yields a COV of 2% for EI_1. This clearly indicates that the selectivity carries over to the dynamic case.

It is shown from these examples that the static force patterns can efficiently applied for dynamic excitations. An explanation for the relatively good performance of the approach is that the influence of mass becomes small when the excitation frequency is low. As we can see, $-\omega^2\mathbf{M}$ becomes small and consequently the the required dynamic force patterns are very similar to the static ones, since $\mathbf{f}_k = \left(\mathbf{K} - \omega^2\mathbf{M}\right)\mathbf{x}_k$.

It can be also deduced from the above results that selectively sensitive forces allow to significantly reduce the propagation and amplification of measurement errors to the identified parameter values.

Chapter 5

Iteratively Experimental Procedure

Generally, in order to determine selectively sensitive excitations we must know the exact values of the parameters to be identified, which is not practical. Therefore, an iterative solution is sought, which by an appropriate feed-back enforces the necessary conditions on $\mathbf{x}_k$, thus automatically rendering suitable excitations $\mathbf{f}_k$. The present study attempts to develop an experimental procedure which allows to efficiently updating the parameter values and the input. The proposed method is presented in the following.

5.1 General description

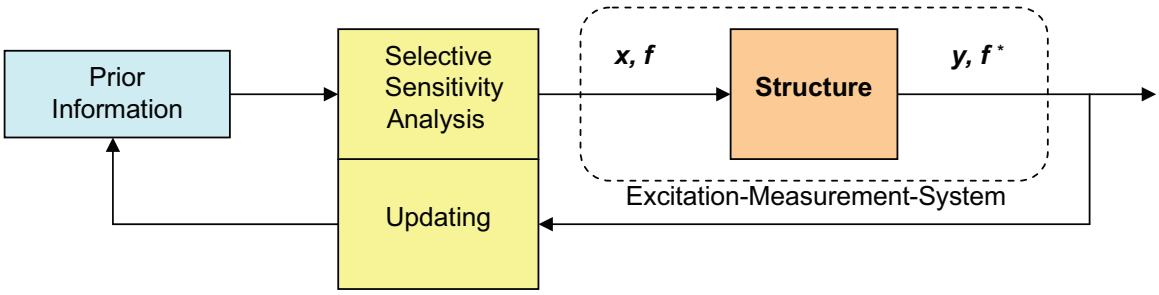

Figure 5.1: Schematic representation of the experimental procedure

The procedure is sketched in Fig. 5.1. The first step is to determine the displacement and force patterns with respect to the selected parameter(s). These values are obtained by introducing the prior information of the system parameters into selective sensitivity analysis (see Chapter 3). In a second step the force pattern is used to derive dynamic loads on the tested structure and measurements are carried out. In a third step, measured outputs are employed to update the prior information. The strategy is to minimize the difference

between a predicted displacement response, formulated as function of the unknown selected parameters and the measured displacements, and the selectively sensitive displacement calculated in the first step. With the updated values of the parameters a re-analysis of selective sensitivity is performed and the experiment is repeated until the displacement responses of model and actual structure are conformed.

5.2 Basis formulation

Consider a general case of testing a linear system whose equation of motion is described by Eq. 3.18 and the displacement output is given by Eq. 3.19. For iterative identification, it is convenient to parameterize the stiffness matrix in the form

$$\mathbf{K} = \mathbf{K}_0 + \sum_{j=1}^{N_p} \theta_j \mathbf{K}_j = \mathbf{K}_0 + \Delta\mathbf{K} \tag{5.1}$$

where $\mathbf{K}_0$ is a nominal stiffness matrix which could be built based on the prior information about the structural system; θ_j are the stiffness parameters which must be determined iteratively. The initial values for θ_j are usually set equal to zero to reflect that the nominal structural model is the most probable model in the absence of any data.

Assume that a force vector $\mathbf{f}_k$ can be found from the relation

$$\mathbf{T}\mathbf{f}_k = \left(-\omega^2\mathbf{M} + \mathbf{K}_0 + \sum_{j=1}^{N_p} \theta_j \mathbf{K}_j \right) \mathbf{x}_k \tag{5.2}$$

where the displacement response $\mathbf{x}_k$ satisfies Eq. 3.10, thus giving

$$\mathbf{T}\mathbf{f}_k = \left(-\omega^2\mathbf{M} + \mathbf{K}_0 \right) \mathbf{x}_k + \theta_k \mathbf{K}_k \mathbf{x}_k \tag{5.3}$$

In Eq. 5.3, θ_k is the selected parameter and the term $(-\omega^2\mathbf{M} + \mathbf{K}_0)$ represents the nominal structural model. The Eq. 5.3 implies that a selectively sensitive force depends only on the parameter to be identified and the current model of the structure. Let $\mathbf{f}_k = \mathbf{f}_k^{(0)} + \triangle\mathbf{f}_k$, where $\mathbf{f}_k^{(0)}$ is the selectively sensitive force vector obtained from the nominal model and $\triangle\mathbf{f}_k$ must be determined, we can write

$$\mathbf{T}\mathbf{f}_k^{(0)} = \left(-\omega^2\mathbf{M} + \mathbf{K}_0 \right) \mathbf{x}_k; \;\; \mathbf{T}\triangle\mathbf{f}_k = \theta_k \mathbf{K}_k \mathbf{x}_k \tag{5.4}$$

The system displacement output due to $\mathbf{f}_k$ will become

$$\mathbf{y}_k = \mathbf{G}\mathbf{x}_k = \mathbf{G}\left(-\omega^2\mathbf{M} + \mathbf{K}_0 + \theta_k\mathbf{K}_k\right)^{-1}\left(\mathbf{T}\mathbf{f}_k^{(0)} + \mathbf{T}\triangle\mathbf{f}_k\right) \tag{5.5}$$

Since the actual value of θ_k is unknown, the force can be derived only in iterative manner. The condition for rendering the necessary force is that the system output must be conformed to the selectively sensitive displacement $\mathbf{y}_k$. For this purpose, the concept of predictive control (c.f [39], [40]) is applied. The main idea of predictive control is to provide a suitable control force that minimizes the error between a predicted displacement response and a reference trajectory.

It is supposed that a sequence of N_t tests is performed until a closed match between measured output and model output is attained. The excitation force and the unknown parameter will be updated in this iterative procedure:

$$\triangle\mathbf{f}_k = \sum_{i=1}^{N_t}\triangle\mathbf{f}_k^{(i)} = \sum_{i=1}^{t}\triangle\mathbf{f}_k^{(i)} + \sum_{i=t+1}^{N_t}\triangle\mathbf{f}_k^{(i)} \tag{5.6}$$

$$\theta_k = \sum_{i=1}^{N_t}\theta_k^{(i)} = \sum_{i=1}^{t}\theta_k^{(i)} + \sum_{i=t+1}^{N_t}\theta_k^{(i)} \tag{5.7}$$

where $\triangle\mathbf{f}_k^{(i)}$ and $\theta_k^{(i)}$ are, respectively, the updated amount of force and displacement in the i-th test. The above formula describes the parameter θ_k in terms of known information, $\sum_{i=1}^{t}\theta_k^{(i)}$ obtained after t tests, and unknown information $\sum_{i=t+1}^{N_t}\theta_k^{(i)}$. Let $\mathbf{f}_k^{(t)}$ is the force applied on the structure in the current test, t-th, the required force vector for the following test, $t+1$-th, is written as

$$\mathbf{f}_k^{(t+1)} = \mathbf{f}_k^{(t)} + \triangle\mathbf{f}_k^{(t+1)} \tag{5.8}$$

where $\triangle\mathbf{f}_k^{(t+1)}$ is the control force we want to determine. Here, this force must be determined, so that it minimize an error term P, given by

$$P = \parallel \boldsymbol{e} \parallel^2 = \parallel \mathbf{y}_k^{(t+1)} - \mathbf{y}_k \parallel^2 \tag{5.9}$$

Here, $\boldsymbol{e} \in R^{N_o}$, called prediction error, is a vector representing the difference between a predicted displacement response $\mathbf{y}_k^{(t+1)}$ and the displacement output $\mathbf{y}_k = \mathbf{G}\mathbf{x}_k$,

$$\boldsymbol{e} = \mathbf{y}_k^{(t+1)} - \mathbf{G}\mathbf{x}_k \tag{5.10}$$

We now formulate the predicted displacement response $\mathbf{y}_k^{(t+1)}$ for our optimization problem. Substituting Eq. 5.6 and Eq. 5.7 into Eq. 5.5 yields

$$\begin{aligned}\mathbf{y}_k &= \mathbf{G}\left(-\omega^2\mathbf{M}+\mathbf{K}^{(t)}+\sum_{i=t+1}^{N_t}\theta_k^{(i)}\mathbf{K}_k\right)^{-1}\left(\mathbf{T}\mathbf{f}_k^{(t)}+\mathbf{T}\sum_{i=t+1}^{N_t}\triangle\mathbf{f}_k^{(i)}\right)\\ &= \mathbf{y}_k^{(t)}+\mathbf{G}\left(-\omega^2\mathbf{M}+\mathbf{K}^{(t)}+\sum_{i=t+1}^{N_t}\theta_k^{(i)}\mathbf{K}_k\right)^{-1}\mathbf{T}\sum_{i=t+1}^{N_t}\triangle\mathbf{f}_k^{(i)}\end{aligned} \tag{5.11}$$

with the currently updated stiffness matrix

$$\mathbf{K}^{(t)} = \mathbf{K}_0+\sum_{i=1}^{t}\theta_k^{(i)}\mathbf{K}_k \tag{5.12}$$

and

$$\mathbf{y}_k^{(t)} = \mathbf{G}\left(-\omega^2\mathbf{M}+\mathbf{K}^{(t)}+\sum_{i=t+1}^{N_t}\theta_k^{(i)}\mathbf{K}_k\right)^{-1}\mathbf{T}\mathbf{f}_k^{(t)} \tag{5.13}$$

It is noted that $\mathbf{y}_k^{(t)}$ will approach the actual system output when t increases. Base on Eq. 5.11, the response prediction is formulated as

$$\mathbf{y}_k^{(t+1)} = \widehat{\mathbf{y}}^{(t)}+\mathbf{G}\left(-\omega^2\mathbf{M}+\mathbf{K}^{(t)}+\theta_k^{(t+1)}\mathbf{K}_k\right)^{-1}\mathbf{T}\triangle\mathbf{f}_k^{(t+1)} \tag{5.14}$$

where $\widehat{\mathbf{y}}^{(t)}$ is the measured output at the current test under the excitation force $\mathbf{f}_k^{(t)}$. By noticing Eq. 5.4 we can write $\mathbf{T}\triangle\mathbf{f}_k^{(t+1)} = \theta_k^{(t+1)}\mathbf{K}_k\mathbf{x}_k$. Thus, the predicted displacement response finally becomes

$$\mathbf{y}^{(t+1)} = \widehat{\mathbf{y}}^{(t)}+\mathbf{G}\left(-\omega^2\mathbf{M}+\mathbf{K}^{(t)}+\theta_k^{(t+1)}\mathbf{K}_k\right)^{-1}\theta_k^{(t+1)}\mathbf{K}_k\mathbf{x}_k \tag{5.15}$$

These prediction is a function of the unknowns $\theta_k^{(t+1)}$ and the current state of the system. By introducing Eq. 5.15 into Eq. 5.9 and solving the optimization problem, the value of $\theta_k^{(t+1)}$ can be obtained, from which updating the force is straightforward.

In the case of weak selective sensitivity, where the force vector $\mathbf{f}_k$ is determined by Eq. 3.24 and the corresponding displacement $\mathbf{x}_k$ is calculated from Eq. 3.25, the condition of Eq. 5.3 may not be fully met, rather $\mathbf{T}\mathbf{f}_k \approx \left(-\omega^2\mathbf{M}+\mathbf{K}_0\right)\mathbf{x}_k+\theta_k\mathbf{K}_k\mathbf{x}_k$. Nevertheless, by choosing appropriate parameters and suitable force configuration, selective sensitivity still can be achieved (see section 3.2) and the above formulation (Eq. 5.15) can be also applied.

The effectiveness of the iterative method is demonstrated in the following by two simulation examples.

5.2.1 Example 5.1: Frame structure

The frame structure in Fig. 3.1 is considered with the actual stiffnesses $a_1 = 0.6$; $a_2 = 0.4$; $a_3 = 0.5$; $a_4 = 0.3N/m$ and the mass $M = 1kg$, giving the first natural circular frequency $\omega_1 = 0.239628rad/s$. This example presents the case where selectively sensitive forces are determined directly from the corresponding displacements. Noting both matrices $\mathbf{T}$ and $\mathbf{G}$ equal to identity, the force patterns $\mathbf{f}_k$ can be easily obtained for a selected stiffness a_k; $\mathbf{f}_k = (-\omega^2\mathbf{M} + a_k\mathbf{K}_k)\,\mathbf{x}_k$; $k = 1 \dots 4$. With the selectively sensitive displacements

$$\mathbf{x}_1 = \begin{Bmatrix} 1 \\ 1 \\ 1 \\ 1 \end{Bmatrix};\ \mathbf{x}_2 = \begin{Bmatrix} 0 \\ 1 \\ 1 \\ 1 \end{Bmatrix};\ \mathbf{x}_3 = \begin{Bmatrix} 0 \\ 0 \\ 1 \\ 1 \end{Bmatrix};\ \mathbf{x}_4 = \begin{Bmatrix} 0 \\ 0 \\ 0 \\ 1 \end{Bmatrix},$$

the forces are determined by

$$\mathbf{f}_1 = \begin{Bmatrix} a_1 - \omega^2 M \\ -\omega^2 M \\ -\omega^2 M \\ -\omega^2 M \end{Bmatrix}; \mathbf{f}_2 = \begin{Bmatrix} -a_2 \\ a_2 - \omega^2 M \\ -\omega^2 M \\ -\omega^2 M \end{Bmatrix}; \mathbf{f}_3 = \begin{Bmatrix} 0 \\ -a_3 \\ a_3 - \omega^2 M \\ -\omega^2 M \end{Bmatrix}; \mathbf{f}_4 = \begin{Bmatrix} 0 \\ 0 \\ -a_4 \\ a_4 - \omega^2 M \end{Bmatrix}$$

Let the nominal inter-storey stiffness for all four storeys is $a_0 = 1N/m$, which differs quite far from the actual values. The actual stiffness a_k are given by $a_k = a_0 + \theta_k$, where θ_k are determined from the above iterative procedure. With excitation frequency of $0.1rad/s$, the above force patterns are in turn applied to determine each selected parameter. The results are listed in Table 5.1. We can see all parameters are well updated after four iterations. For the case using excitation with frequency higher than ω_1, the convergence of the parameter and the force is slower (see Table 5.2). In Table 5.2, together with the force, displacement error (in percentage) for θ_1 are also displayed, which show that system output is gradually conformed to the required displacement (selectively sensitive displacement).

t	θ_1	θ_2	θ_3	θ_4
0	0	0	0	0
1	-0.414224	-0.611336	-0.516441	-0.708483
2	-0.399084	-0.5994	-0.498812	-0.699627
3	-0.400057	-0.600031	-0.500082	-0.700016
4	-0.399996	-0.599998	-0.499994	-0.699999
5	-0.4	-0.6	-0.5	-0.7

Table 5.1: Example 5.1: Updated stiffness parameter values with excitation frequency $0.1rad/s$

t	θ_1	$\mathbf{f}_1$	$\frac{\|\widehat{\mathbf{y}}^{(t)}-\mathbf{G}\mathbf{x}_1\|}{\|\widehat{\mathbf{y}}^{(t)}\|}\times 100$
0	0	1.0, -0.253918, -0.253918, -0.253918	46.883
1	-0.224432	1.0, -0.353361, -0.353361, -0.353361	21.8609
2	-0.322557	1.0, -0.426367, -0.426367, -0.426367	9.67744
3	-0.365766	1.0, -0.469039, -0.469039, -0.469039	4.26441
4	-0.384852	1.0, -0.490733, -0.490733, -0.490733	1.88255
5	-0.393295	1.0, -0.500983, -0.500983, -0.500983	0.83234

Table 5.2: Example 5.1: Updated values of θ_1 and $\mathbf{f}_1$ with excitation frequency $0.45 rad/s$

5.2.2 Example 5.2: Continuously supported beam

Consider the continuously supported beam in Fig. 3.9. The mass of the beam is assumed to be precisely known with mass per unit length $\rho A = 1 kg/m$. The mass matrix $\mathbf{M}$ is constructed based on the average mass model of each element

$$\mathbf{m}_a = \frac{\rho A L}{420}\begin{bmatrix} 183 & & & sym \\ 11L & 2.5L^2 & & \\ 27 & 6.5L & 183 & \\ -6.5L & -1.5L^2 & -11L & 2.5L^2 \end{bmatrix}$$

Given are the nominal bending stiffness $EI_{0,1}, EI_{0,2}, EI_{0,3}, EI_{0,4} = 1.0 Nm^2$, the initial model parameter $\theta_1 = \theta_2 = \theta_3 = \theta_4 = 0$. The actual bending stiffness $EI_1 = 0.8 Nm^2; EI_2, EI_3 = 0.9 Nm^2; EI_4 = 0.7 Nm^2$, thus the actual values of the parameters $\theta = \{-0.2, -0.1, -0.1, -0.3\}^T$. For this indeterminate beam structure, it is possible to obtain a force vector which produces a displacement response sensitive to two selected parameters only, e.g θ_1 *and* θ_4 or θ_2 *and* θ_3. The force patterns are determined from Eq. 3.27 and the corresponding displacements are computed by Eq. 3.25.

Using harmonic excitation with frequency $\omega = 1 rad/s$, the updated values of θ_1 and θ_4 as well as the corresponding force patterns are listed in Table 5.3. With the updated values

t	θ_1	θ_4	$\mathbf{f}_{1,4}$	$\frac{\|\widehat{\mathbf{y}}^{(t)}-\mathbf{G}\mathbf{x}_{1,4}\|}{\|\widehat{\mathbf{y}}^{(t)}\|}\times 100$
0	0	0	0.604673, -0.366566, 0.366566, -0.604673	29.6348
1	-0.20179	-0.30298	0.628108, -0.398342, 0.348971, -0.570108	0.27954
2	-0.200605	-0.301226	0.627886, -0.398083, 0.349129, -0.570437	0.13181
3	-0.200612	-0.301243	0.627889, -0.398086, 0.349127, -0.570433	0.131803

Table 5.3: Example 5.2: Updated values of θ_1 and θ_4 and excitation patterns

of θ_1 and θ_4, the selectively sensitive excitation vector with respect to the parameters θ_2 and θ_3 is computed. The results of updating θ_2 and θ_3 are given in Table 5.4. Table 5.3 and Table 5.4 also list the errors between actual outputs and model outputs. The displacement

t	θ_2	θ_3	$\mathbf{f}_{2,3}$	$\frac{\|\hat{\mathbf{y}}^{(t)}-\mathbf{G}\mathbf{x}_{2,3}\|}{\|\hat{\mathbf{y}}^{(t)}\|} \times 100$
0	0	0	-0.380841, 0.912711, 0.0983024, 0.110702	11.7062
1	-0.099959	-0.100017	-0.383638, 0.911227, 0.100738, 0.111082	0.00
2	-0.099984	-0.099988	-0.383621, 0.911229, 0.100824, 0.111049	0.00
3	-0.099984	-0.099988	-0.383621, 0.911229, 0.100824, 0.111049	0.00

Table 5.4: Example 5.2: Updated values of θ_2 and θ_3 and excitation patterns

patterns corresponding to initial and updated states are shown in Fig. 5.2 as well.

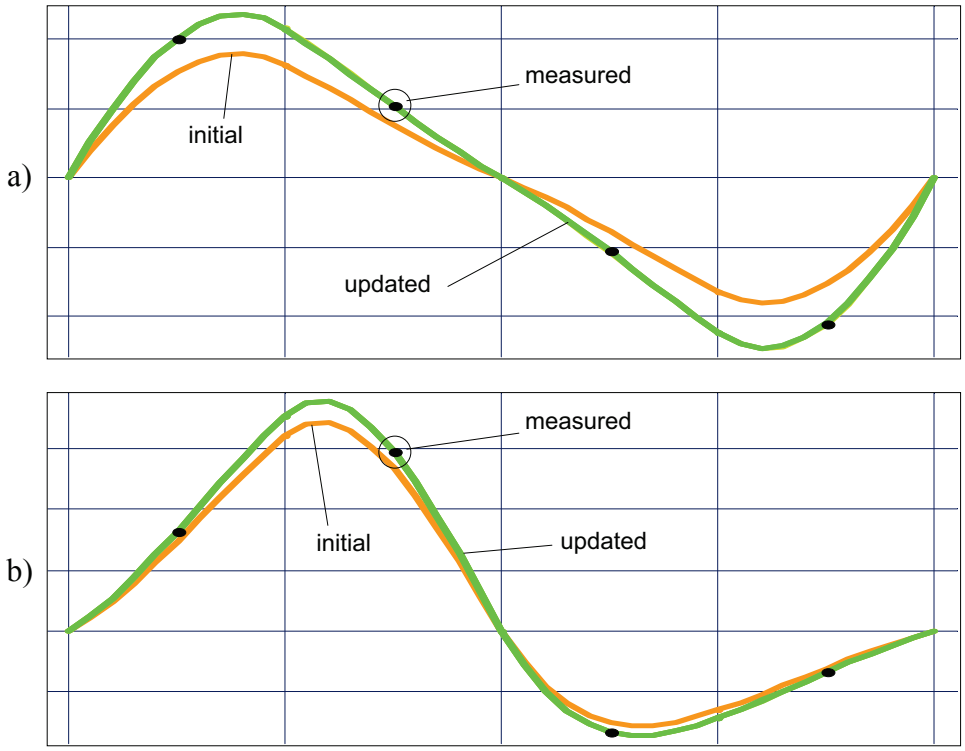

Figure 5.2: Example 5.2: Displacement patterns with respect to: a) θ_1 *and* θ_4; b) θ_2 *and* θ_3

It can be seen from these results that the selected parameter values and the corresponding excitation forces can be well estimated after two iterations. In addition the displacement patterns show no bending deformation in the elements whose stiffness is not to be identified.

5.3 Bayesian updating

In practice, the Eq. 3.1 does not describe the actual system behaviour, i.e. there always exists model error and there are no "true" values of the model parameters. Furthermore, the dynamic test data are contaminated by measurement noise. Because of these errors, updating procedure is best tackled as a statistical inference problem. A general statistical frame work for system identification is detailed in [41], which was originally established for

the case using measured dynamic responses in time domain. In this section, this methodology is extended to frequency-domain data and combined with the above iterative procedure.

5.3.1 Prediction error

The prediction error $\boldsymbol{e}$ can be re-write by substituting Eq. 5.15 into Eq. 5.10

$$\boldsymbol{e} = \widehat{\mathbf{y}}^{(t)} + \mathbf{G}\left[\left(-\omega^2\mathbf{M} + \mathbf{K}^{(t)} + \theta_k^{(t+1)}\mathbf{K}_k\right)^{-1}\theta_k^{(t+1)}\mathbf{K}_k - \mathbf{I}\right]\mathbf{x}_k \tag{5.16}$$

In the above equation $\mathbf{I}$ is the identity matrix of size N_d. Defining a model output

$$\mathbf{y}(\theta_k^{(t+1)}) = \mathbf{G}\left[\mathbf{I} - \left(-\omega^2\mathbf{M} + \mathbf{K}^{(t)} + \theta_k^{(t+1)}\mathbf{K}_k\right)^{-1}\theta_k^{(t+1)}\mathbf{K}_k\right]\mathbf{x}_k \tag{5.17}$$

and suppressing the step-index in the notation, the prediction error is written in a simple form,

$$\boldsymbol{e} = \widehat{\mathbf{y}} - \mathbf{y}(\theta_k) \tag{5.18}$$

which now represents the difference between the model output $\mathbf{y}(\theta_k)$ and the measured system output $\widehat{\mathbf{y}}$.

This prediction error $\boldsymbol{e}$ is a combined effect of modelling error, measurement error and measurement noise, and error due to noisy input filtered through the system. To describe the uncertainty in the prediction error, a class of probability models is chosen, which prescribes a probability density function (PDF) of the prediction error. Rather than present a general case, the probability model is chosen so that $\boldsymbol{e}$ is statistically independent and normally distributed with zero mean and covariance matrix Σ equal to a diagonal matrix with the diagonal elements represented by a vector of unknown variances $\boldsymbol{v} = \left\{v_1^2, \ldots, v_{N_o}^2\right\}^T$.

5.3.2 Parameter estimation

The model parameter vector to be identified using the measured data, denoted by $\boldsymbol{a}$, includes θ_k and the elements of $\boldsymbol{v}$, i.e $\boldsymbol{a} = \{\theta_k, v_1, \ldots, v_{N_o}\}^T$. It is assumed that a set of displacement responses $\widehat{\mathbf{y}}(\omega_f) \in \mathbf{R}^{N_o}$ measured at N_f frequencies $\omega_f; f = 1 \ldots N_f$ is available. This data set for the m–th observation is referred to by $\widehat{\mathbf{O}}_m = \{\widehat{\mathbf{y}}_m(\omega_1), \ldots, \widehat{\mathbf{y}}_m(\omega_{N_f})\}$. A grouping of data sets from N_m different observations is denoted by $\boldsymbol{D} = \{\widehat{\mathbf{O}}_1, \ldots, \widehat{\mathbf{O}}_{N_m}\}$.

From the Bayes' theorem, the updated (posterior) probabilistic distribution function

(PDF) of the model parameter $\boldsymbol{a}$ given the data $\boldsymbol{D}$ is

$$p(\boldsymbol{a}|\boldsymbol{D}) = c \times p(\boldsymbol{a})p(\boldsymbol{D}|\boldsymbol{a}) \tag{5.19}$$

where c is a normalizing constant; $p(\boldsymbol{a})$ is the prior PDF of the model parameter $\boldsymbol{a}$; and $p(\boldsymbol{D}|\boldsymbol{a})$ is the PDF of the data given the parameters $\boldsymbol{a}$. Assume that all measurements are statistically independent. Thus, we have

$$p(\boldsymbol{a}|\boldsymbol{D}) = c \times p(\boldsymbol{a}) \prod_{m=1}^{N_m} p(\widehat{\mathbf{O}}_m|\boldsymbol{a}) = c \times p(\boldsymbol{a}) \prod_{m=1}^{N_m} \prod_{f=1}^{N_f} p(\widehat{\mathbf{y}}_m(\omega_f)|\boldsymbol{a}) \tag{5.20}$$

where the PDF of the observation m-th at frequency ω_f, $p(\widehat{\mathbf{y}}_m(\omega_f)|\boldsymbol{a})$, also the *likelihood* can be derived for our particular selection of probability model of the prediction error

$$p(\widehat{\mathbf{y}}_m(\omega_f)|\boldsymbol{a}) = \frac{1}{(\sqrt{2\pi})^{N_o}|\Sigma|^{1/2}} \exp\left[-\frac{1}{2}\left(\widehat{\mathbf{y}}_m(\omega_f) - \mathbf{y}(\theta_k)\right)^T \Sigma^{-1} \left(\widehat{\mathbf{y}}_m(\omega_f) - \mathbf{y}(\theta_k)\right)\right] \tag{5.21}$$

The choice for $p(\boldsymbol{a})$ depends on engineering and modelling judgment. It can be chosen as a normal distribution with zero mean and covariance matrix $\mathbf{C}$.

$$p(\boldsymbol{a}) = \frac{1}{(\sqrt{2\pi})^{N_o+1}|\mathbf{C}|^{1/2}} \exp\left[-\frac{1}{2}\boldsymbol{a}^T\mathbf{C}^{-1}\boldsymbol{a}\right] \tag{5.22}$$

The individual parameters is also assumed to be independent, so that $\mathbf{C}$ becomes a diagonal matrix of variances σ_i^2. For mathematical convenience, σ_i are chosen to make $p(\boldsymbol{a})$ a smooth, slowly varying function. The posterior PDF of $\boldsymbol{a}$ finally becomes

$$p(\boldsymbol{a}|\boldsymbol{D}) = c_1 \times \frac{1}{|\Sigma|^{N_f N_m/2}} \exp\left[-J(\boldsymbol{a})\right] \tag{5.23}$$

where

$$J(\boldsymbol{a}) = \frac{1}{2}\left[\boldsymbol{a}^T\mathbf{C}^{-1}\boldsymbol{a} + \sum_{f=1}^{N_f}\sum_{m=1}^{N_m} \left(\widehat{\mathbf{y}}_m(\omega_f) - \mathbf{y}(\theta_k)\right)^T \Sigma^{-1} \left(\widehat{\mathbf{y}}_m(\omega_f) - \mathbf{y}(\theta_k)\right)\right] \tag{5.24}$$

The most probable model parameters, $\widehat{\boldsymbol{a}} = \left\{\widehat{\theta}_k, \widehat{v}_1, \ldots, \widehat{v}_{N_o}\right\}^T$ are the values that maximize $p(\boldsymbol{a}|\boldsymbol{D})$ and can be obtained by minimizing a function $g(\boldsymbol{a}) = -\ln[p(\boldsymbol{a}|\boldsymbol{D})]$. From Eq. 5.23, it can be easily obtained

$$g(\boldsymbol{a}) = J(\boldsymbol{a}) - \ln\frac{1}{|\Sigma|^{N_f N_m/2}} + constant \tag{5.25}$$

Here, $g(\boldsymbol{a})$ is a multi-variable function. For searching the optimal solution of the numerical examples and the laboratory experiment in this study, the first algorithm of Differential Evolution (DE), "DE/rand/1" [42] is utilized. A short description of the applied algorithm is given in Appendix A. The updated PDF of $\boldsymbol{a}$ can be well approximated by a multi-dimensional Gaussian distribution $N[\widehat{\boldsymbol{a}}, \mathbf{H}^{-1}(\widehat{\boldsymbol{a}})]$ with mean $\widehat{\boldsymbol{a}}$ and covariance matrix $\mathbf{H}^{-1}(\widehat{\boldsymbol{a}})$, where $\mathbf{H}(\widehat{\boldsymbol{a}})$ is the Hessian matrix of $g(\boldsymbol{a})$ calculated at $\boldsymbol{a} = \widehat{\boldsymbol{a}}$ (see [41, 43]). The derivation of $\mathbf{H}(\widehat{\boldsymbol{a}})$ is given in Appendix B.

After each test, the optimal stiffness parameter values will be updated according to Eq. 5.7. These updated values then will be used to computed the sensitive force and sensitive displacement vectors for the next test.

5.4 Illustration examples

5.4.1 Example 5.3: Frame structure

The Bayesian updating will now be demonstrated on the same frame structure as in the previous section. In this example, the excitation is assumed to be harmonic with frequency ω and the output will be measured at steady state of vibration and at the frequency of excitation, i.e $N_f = 1$. It is further assumed that the variances of prediction error at all DOFs are equal, i.e the standard deviations $v_1 = v_2 = v_3 = v_4 = v$. The Eq. 5.22 and Eq. 5.21 can be rewritten respectively as

$$p(\theta_k, v) = \frac{1}{(\sqrt{2\pi})^{1+1}\sigma_{\theta_k}\sigma_v} \exp\left[-\frac{1}{2}\left(\frac{\theta_k^2}{\sigma_{\theta_k}^2} + \frac{v^2}{\sigma_v^2}\right)\right] \tag{5.26}$$

$$p(\widehat{\mathbf{y}}_m|\theta_k, v) = \frac{1}{(\sqrt{2\pi}v)^4} \exp\left[-\frac{1}{2v^2}\left(\widehat{\mathbf{y}}_m - \mathbf{y}(\theta_k)\right)^T\left(\widehat{\mathbf{y}}_m - \mathbf{y}(\theta_k)\right)\right] \tag{5.27}$$

and the posterior PDF of the model parameters becomes

$$p(\theta_k, v|\boldsymbol{D}) = c \times \frac{1}{(\sqrt{2\pi})^{1+1}\sigma_{\theta_k}\sigma_v(\sqrt{2\pi}v)^{4N_m}} \exp\left[-J(\theta_k, v)\right] \tag{5.28}$$

where

$$J(\theta_k, v) = \frac{1}{2}\left(\frac{\theta_k^2}{\sigma_{\theta_k}^2} + \frac{v^2}{\sigma_v^2}\right) + \frac{1}{2v^2}\sum_{m=1}^{N_m}\left(\widehat{\mathbf{y}}_m - \mathbf{y}(\theta_k)\right)^T\left(\widehat{\mathbf{y}}_m - \mathbf{y}(\theta_k)\right) \tag{5.29}$$

A simulation is carried out for parameter θ_1 with excitation frequency $\omega = 0.1rad/s$ and displacement error of 2% coefficient of variation (COV), generated by adding random values

chosen from zero-mean normal distribution to the exact system output. Fig. 5.3 shows the prior PDFs and posterior PDFs of the model parameters using $N_m = 10$ observations. It can be seen that, after just first step ($t = 1$), the uncertainty of the model parameters is significantly reduced. As the test being continued, the optimal value $\widehat{\theta}_1^{(t)}$ approaches zero.

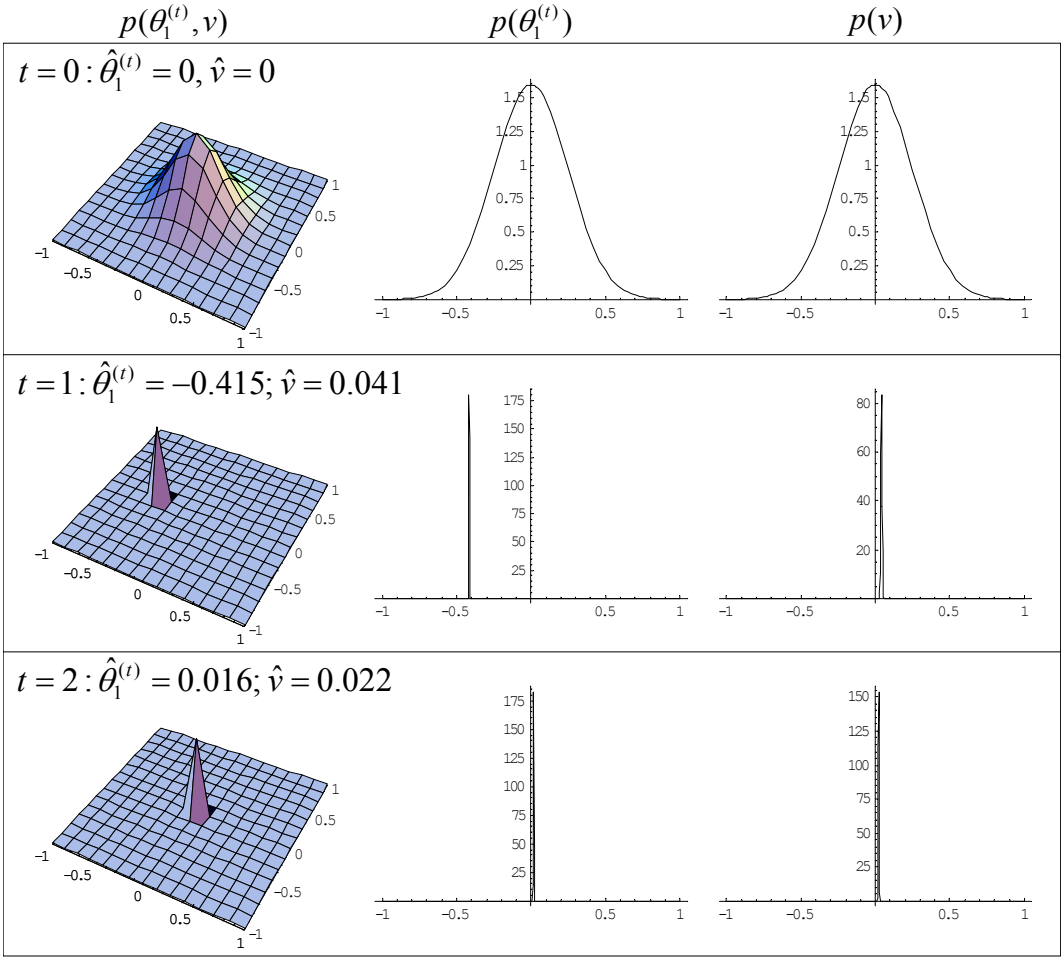

Figure 5.3: Example 5.3: Prior PDFs and updated PDFs corresponding to θ_1

Applying the updating procedure to the other parameters give the results listed in Table 5.5. The optimal values of the stiffness parameters and the approximate variances, σ^2, are shown. Clearly, it takes only some few steps to get close to the true values of the selected parameters. Moreover, the parameter uncertainty is also efficiently reduced.

t	$\widehat{\theta}_1$; σ^2	$\widehat{\theta}_2$; σ^2	$\widehat{\theta}_3$; σ^2	$\widehat{\theta}_4$; σ^2
0	0.0; 0.25^2	0.0; 0.25^2	0.0; 0.25^2	0.0; 0.25^2
1	-0.415041; 0.0022^2	-0.612095; 0.0014^2	-0.51699; 0.0020^2	-0.707374; 0.0016^2
2	-0.398973; 0.0019^2	-0.598255; 0.0010^2	-0.502443; 0.0013^2	-0.699334; 0.0012^2

Table 5.5: Example 5.3: Updated values of the stiffness parameters and variances

5.4.2 Example 5.4: Continuously supported beam

Consider the continuously supported beam in Example 5.2 (c.f. Fig. 3.9). With the same assumptions as in Example 5.3, all the equations 5.26 to 5.29 can be applied for the updating.

Random noise with COV of 2% is now added to the simulated output (with excitation frequency $\omega = 1rad/s$). Using $N_m = 10$ observations, the updated optimal values are shown for stiffness parameter θ_1 and θ_4 in Table 5.6 and for θ_2 and θ_3 in Table 5.7. It is seen that parameters values are well estimated in some iterations and the deviations, σ, which represent the parameter uncertainty are significant reduced. The updating also allows to estimate the uncertainty of the prediction error, given by the values $\widehat{v}$ in the tables. For this case, the prediction error consists of only measurement noise.

t	$\widehat{\theta}_1$	$\widehat{\theta}_4$	$\widehat{v}$
0	0; σ=0.25	0; σ=0.25	0; σ=0.25
1	-0.200927	-0.310206	0.000412664
2	-0.192855	-0.304421	0.000531383
3	-0.205000; $\sigma \approx$0.0018884	-0.302839; $\sigma \approx$0.001507	0.000619725; $\sigma \approx$0.000021251

Table 5.6: Example 5.4: Updated optimal values $\widehat{\theta}_1$ and $\widehat{\theta}_4$ under noisy output

t	$\widehat{\theta}_2$	$\widehat{\theta}_3$	$\widehat{v}$
0	0; σ=0.25	0; σ=0.25	0; σ=0.25
1	-0.103503	-0.092881	0.000359761
2	-0.105204	-0.104144	0.000364731
3	-0.096783; $\sigma \approx$0.005038	-0.099589; $\sigma \approx$0.009427	0.000380559; $\sigma \approx$0.000023756

Table 5.7: Example 5.4: Updated optimal values $\widehat{\theta}_2$ and $\widehat{\theta}_3$ under noisy output

In the following, discretisation error is included in the simulation by generating the simulated measurements using a finer finite element model. The results are obtained from simulated data of a 8-beam-element model without noise and shown in Table 5.8. Obviously, the identified stiffness parameters do not match the values used to generate measurements. It implies that, with the presence of modelling error, there is no *true* parameters values. This can also be seen in Fig. 5.4, that there is still difference between model output and measured output. Nevertheless, with Bayesian updating, these differences can be assessed (see the values of $\widehat{v}$ in Table 5.8).

t	$\widehat{\theta}_1$	$\widehat{\theta}_2$	$\widehat{\theta}_3$	$\widehat{\theta}_4$	$\widehat{v}$
0	0	0	0	0	0
1	-0.230322			-0.334816	0.000770214
2	-0.236805			-0.336167	0.000390582
3	-0.236907			-0.336184	0.00293185
4	-0.236908			-0.336185	0.00293188
5	-0.236909			-0.336185	0.00293187
6		-0.15433	-0.0886148		0.0027858
7		-0.157627	-0.117306		0.00275765
8		-0.151134	-0.131675		0.00275834
9		-0.14649	-0.138619		0.00276225
10		-0.143936	-0.141849		0.00276523
11	-0.235234			-0.334688	0.00287019
12	-0.235172			-0.334671	0.00287029
13	-0.235171			-0.33467	0.00287028
14		-0.142713	-0.143344		0.00276767
15		-0.142113	-0.144018		0.00276853
$\sigma \approx$	0.030557	0.098885	0.180355	0.025188	0.00069202

Table 5.8: Example 5.4: Updated optimal parameter values under discretisation error

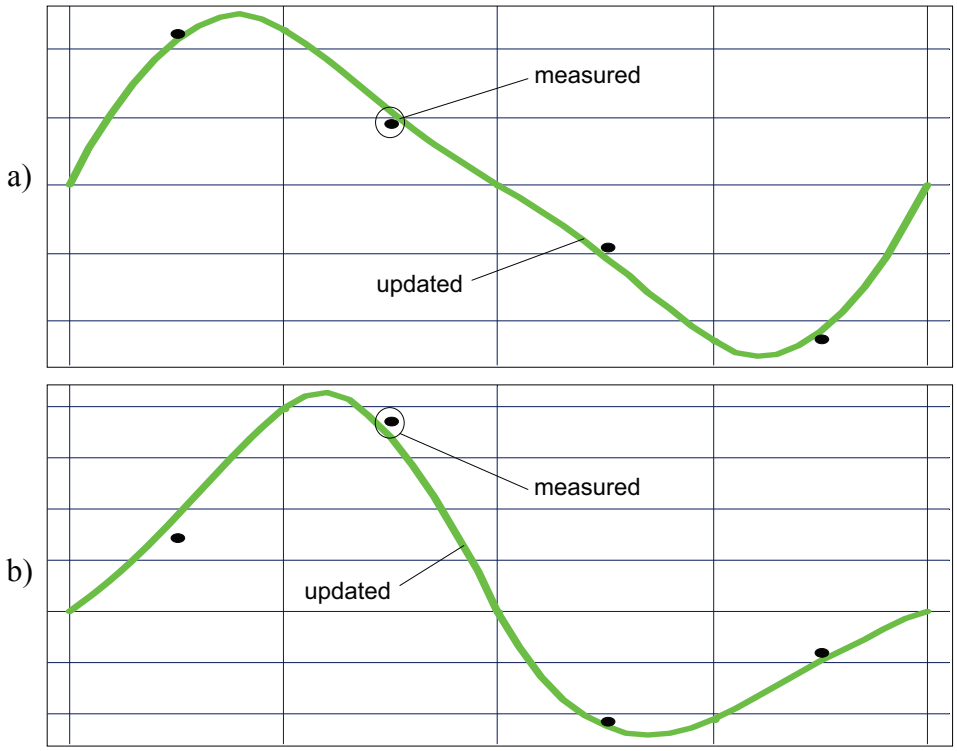

Figure 5.4: Example 5.4: Displacement patterns with respect to: a) θ_1 *and* θ_4; b) θ_2 *and* θ_3

Chapter 6

Realization of Test

6.1 Test planning

Practice applications of selective sensitivity in general require a relatively large and complex excitation-measurement-system, and often leads to a high expense of extensive number of sensors and exciters. A careful test planning can bring considerable advantage in terms of the cost of testing and the effectiveness of each test. The test planning has to consider which parameter(s) will be selected and how the test should be conducted for maximum effectiveness under certain experimental capacity. For this purpose, computer simulations as a rehearsal of each test are carried out before any actual testing. By using such "Virtual Testing", much more effective testing can be achieved, with a considerable reduction in the total time and cost of each test and a increase in the reliability of the test results. The major aspects in which virtual testing can have significant influence on the progress and prosecution of a selectively sensitive test are (i) suitable parameter selection and test sequence, (ii) optimisation of the test set-up by choosing the best set of excitation and response measurement DOFs and (iii) appropriate frequencies to excite the tested structure. Furthermore, in simulation, more damage cases may be used and the effect of errors can be investigated.

6.1.1 Parameter selection and testing sequence

It is desirable that the number of parameters selected for each test is small. In general, the decision for how many parameter values can be efficiently identified depends largely on experimental capacity. For statically determinate structures, the useful condition for parameter selection is

$$n = N_e - N_p \tag{6.1}$$

where N_e is the number of DOFs can be excited and N_p is the total unknown parameters need to be identified. For instance, if $n \geq 0$ a single parameter can be chosen to be determined at a time. Otherwise, a group of small number of parameters may be selected as an alternative. To decide whether the parameter(s) selected is appropriate, selectively sensitive analysis must be performed and the obtained displacement pattern will be evaluated. The displacement pattern should have the property of inducing stress only in the element(s) whose stiffness should be identified.

The sequence for testing the selected subsets of parameters should result in a quick convergence of the parameter values. It is obviously that the test should start with the most uncertain parameter(s). In many cases, different trials are useful to find the optimal sequence. Here, we can see the important role of simulation in reduction of time and cost for an actual test.

6.1.2 Excitation and measurement locations

The second consideration will be to the location of the best points to excite the structure so as to minimise the sensitivity of the system to the undesired parameters. The choice for excitation location must also ensure that the region of interest (selected element(s) or substructure(s)) can be excited. It is essential that the magnitude of the force stays in a reasonable level, so that the structure follows the linearity and the force can be realized. Thus, the excitation points should allow maximum effectiveness for a given force level. For example, if a beam structure is being tested and we want to determine the bending stiffness of one of the beam elements, then it is expected that the excitation will be applied at the middle of each element.

The third of these primary test planning considerations is to the selection of those DOFs at which the response is to be measured. There are two major considerations: which points should be measured so as to present a visually informative display of the resulting displacement patterns? and which DOFs are necessary in order to ensure an unambiguous correlation between test and analysis models? The former consideration essentially calls for a fairly uniform distribution of points with a sufficiently fine mesh that the essential feature of displacement patterns can be seen. The latter consideration is the more critical in many cases for the reason that the desired parameter(s) must be identifiable in the context of selective sensitivity. The essential requirement is to specify which are the necessary DOFs to be measured in order to obtain a reliable result, i.e an unique solution with minimum effect

of measurement noise.

Given the analytical model, several selections of DOFs for excitation and response measurement can be examined to check which one is the "best". On the other hand, a proposed set of DOFs have to be based on the actual experimental condition, i.e. these DOFs are excitable and measurable.

6.1.3 Excitation frequency

In general, there will be a range of frequencies at which selective sensitivity can be achieved. The consideration concerns with determining which are the better frequencies from the point of view of selective insensitivity of the unwanted parameters. Basically, frequencies below the fundamental frequency of the structure will provide great advantage. However, it does not always ensure in practice that the wanted substructure can be effectively excited under a low frequency vibration. The reason is that the low frequency modes of vibration can become dominant and their spatial wavelengths are large, and typically far larger than the extent of the chosen substructure. Higher frequency excitation can excite each substructure with the desired insensitivity to the complementary substructure. Nevertheless, care must be given to practical aspects, such as (fundamental) frequency of noise, natural frequencies of slave systems attached on the tested structure, allowable frequency range of available devices. Often, decision can be made only after some trials of real test.

6.2 Test system

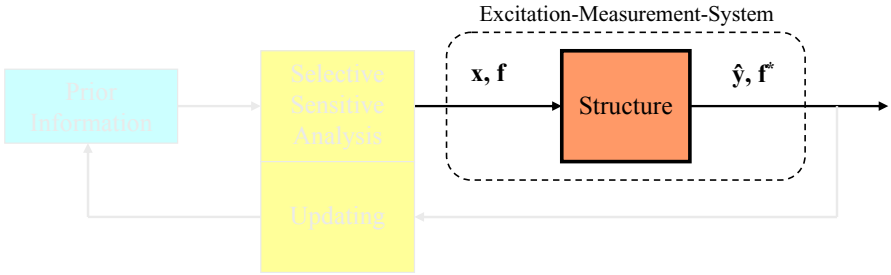

Figure 6.1: Excitation-measurement-system in the experimental procedure

Fig. 6.1 highlights the excitation-measurement-system in the iterative procedure. Since this system is used here in order to measure data in frequency domain, it has a similar set-up as a Frequency Response Function measurement system in Modal Testing [9] and consists of four major items:

- an excitation mechanism, to excite the test structure;

- a transduction system, to measure the various parameters of interest;

- an analyzer, to extract the desired information; and

- a controller, to ensure the required (selectively sensitive) forces.

A typical layout for the excitation-measurement-system is shown in Fig. 6.2.

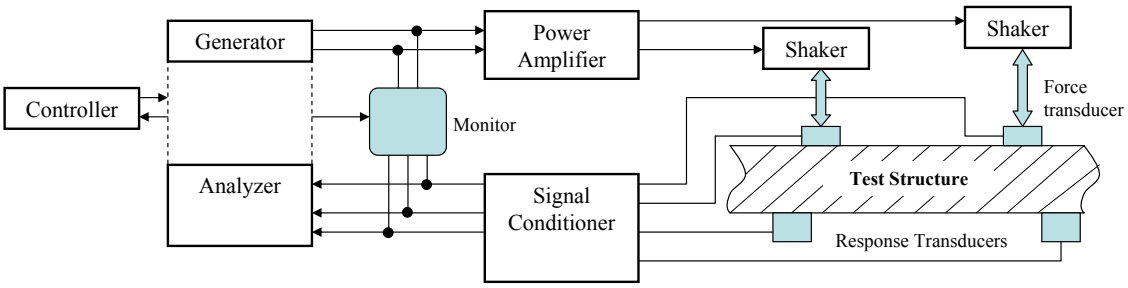

Figure 6.2: General layout of Excitation-Measurement-System

6.2.1 Excitation system

The excitation system consists of the following elements:

- A generator, which is capable of producing sinusoidal signals with specific frequency content(s), since harmonic excitation is found suitable for selectively sensitive testing.

- Power amplifier, which is necessary in order to drive the actual devices used to vibrate the structure and will be chosen to match the excitation devices.

- Exciters, which are shakers attached on the structure. Two major considerations for the selection of shakers are the frequency range and the magnitude of force, which are essential to ensure the desired selective insensitivity. Other aspects such as flexibility for control, weight (relative to the weight of the test structure) are also important. Among various types of vibrators, the most common type which can be useful is electrodynamic shaker whose frequency and amplitude of excitation can be controlled independently of each other, giving more operational flexibility. However, the disadvantage of using this type of shaker is that it is not usually possible to deduce the excitation force from the voltage applied to the shaker, because the electrical impedance of these devices varies with the amplitude of motion of the moving coil which is attached to the drive part of the device. Therefore, adjustment in the input signals is necessary in order to derive the required force.

6.2.2 Transduction system

Two parts of the transduction system are:

- Transducers. The most commonly used are piezoelectric transducers which are convenient for both excitation and response measurement. There are many aspects of the selection of appropriate force transducers, in which magnitude of the excitation force and the frequency range should be highly considered. For multi-point response measurement, accelerometers are most popular although in order to obtain displacement components it requires double integrals, which may induce systematic errors.

- Conditioner(s) to amplify the (usually) small signals produced by the transducers. The choice depends largely on the type of transducer used, and in fact is often provided as part of it.

6.2.3 Analyzer

The function of this item is to measure the various signals generated by the transducers in order to ascertain the magnitudes of the excitation forces and responses. Classically, this is a Spectrum Analyzer provided by its manufacturer as one unit. Now a day, with the development of computer technology, this element is preferably divided into two parts: (i) a hardware (often seen as Data Acquisition (DAQ) device), which can be a unit or just a small card connected to a computer, and (ii) a user's computer software, which can be developed by the experimenter or an expert. This set-up builds up a Virtual Instrument, and although it is not an "instant lunch", it provides great advantage of cost and flexibility for the user in different kinds of testing.

The task of the spectrum analyzer is to transform the acquired signals (accelerometer or force transducer outputs) from time domain into frequency domain. The process is done by a Discrete Fourier Transform (DFT) analysis, which is well-known in modal testing. The theory of DFT and discussion on important aspects concerning to this digital signal processing are detailed in [9]. Powerful computer tools for programming are available in some software packages or programming environments (e.g. MATLAB, LabVIEW,...).

6.2.4 Controller

The controller, which is a software package with various functions, has an important role is to adjust the input signals so as to produce the necessary forces successfully. Besides the disagreement between the input voltages and the actual forces, the need for force controlling

arises because our excitation system is multi-point excitation and under vibration each shaker influences the others, resulting in unexpected forces applied to the structure. The controlling can be performed 'manually' by the user him- or her self. On the other hand, in most cases with complex system of forces, an algorithm which allows automatic force control is desired.

In the following section, an control scheme based on the concept of predictive control is proposed to ensure selectively sensitive excitation.

6.3 Force control

To excite the structure into vibration, signals are generated and transferred to the shakers attached on the structure. These signals in the form of voltage will be amplified in order to drive the actual devices. For selectively sensitive forces, it is reasonable to use excitation signals which are sinusoidal. Thus, a vector of signal amplitudes (vector of input voltages) will be sufficient for generating. This vector is supposed to be proportional to the required forces, but it is commonly not. Moreover, the phases of the actual forces may be far from expectation.

For example, suppose that the force pattern required to attain sensitive displacement is given by $\mathbf{f} = \{0.316395, -0.948628\}^T$. The time series of the exciting forces at $33Hz$ are expected as in Fig. 6.3a. However, using a vector of input voltages proportional to $\mathbf{f}$ to generate excitations on a simple beam structure may results in actual forces as in Fig. 6.3b. Therefore, in order to obtain the necessary forces voltage signals must be changed. In this case, predictive control will be used.

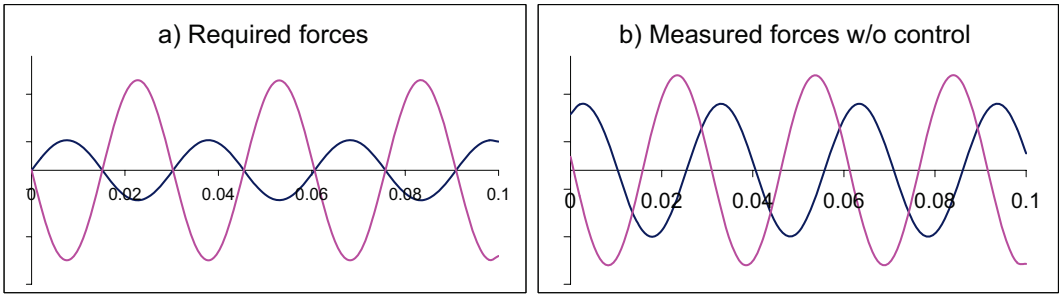

Figure 6.3: Required excitation forces vs actual forces w/o control

Let $\mathbf{v}_t$ is the vector of input voltage and $\mathbf{p}_t$ is the vector of input phase at time t. Our task is to adjust these values so that the required excitation forces can be achieved, i.e.

$$\mathbf{v}_{t+1} = \mathbf{v}_t + \triangle\mathbf{v}_{t+1};\ \mathbf{p}_{t+1} = \mathbf{p}_t + \triangle\mathbf{p}_{t+1}; \tag{6.2}$$

where $\triangle \mathbf{v}_{t+1}$ and $\triangle \mathbf{p}_{t+1}$ are, respectively, the control values of voltage and phase and will be determined by minimizing the error between the predicted and the required values of force and phase.

Given the predictions of force and phase respectively as $(\mathbf{f}^* + \mathbf{A}\triangle \mathbf{v}_{t+1})$ and $(\mathbf{p}^* + \mathbf{B}\triangle \mathbf{p}_{t+1})$ the formulation of this error is provided by

$$error = \parallel (\mathbf{f}^* + \mathbf{A}\triangle \mathbf{v}_{t+1}) - \mathbf{f}_k \parallel^2 + \parallel (\mathbf{p}^* + \mathbf{B}\triangle \mathbf{p}_{t+1}) - \mathbf{p}_k \parallel^2 + w_v \parallel \triangle \mathbf{v}_{t+1} \parallel^2 + w_p \parallel \triangle \mathbf{p}_{t+1} \parallel^2 \tag{6.3}$$

where $\mathbf{f}^*$ and $\mathbf{p}^*$ are, respectively, vectors of measured forces and measured phases corresponding to the initial inputs ($\mathbf{v}_t$, $\mathbf{p}_t$); $\mathbf{A}$ and $\mathbf{B}$ are constant matrices referred to as *internal model* of the controller; w_v and w_p are the weights put on the changes in force and phase inputs. The reason for introducing the two terms $w_v \parallel \triangle \mathbf{v}_{t+1} \parallel^2$ and $w_p \parallel \triangle \mathbf{p}_{t+1} \parallel^2$ is that the changes in the input signals are unwanted.

The control process (Fig. 6.4) will be performed until measured values meet the requirement. Obviously, this process depends on the choice of the matrices $\mathbf{A}$ and $\mathbf{B}$ and the weights w_v and w_p. Fig. 6.5 shows an example of controlling the force amplitude and phase for two shakers exciting on a steel beam with $\mathbf{A}$ and $\mathbf{B}$ set equal to the identity matrix. For optimal control, a *trial and error* procedure prior to actual tests is suggested.

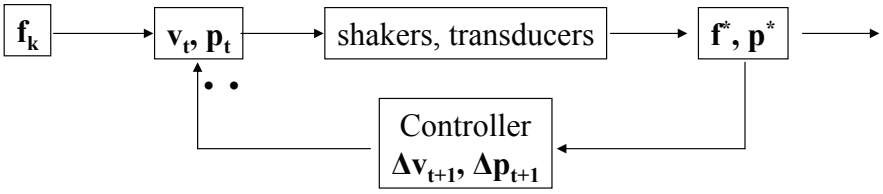

Figure 6.4: Force control procedure

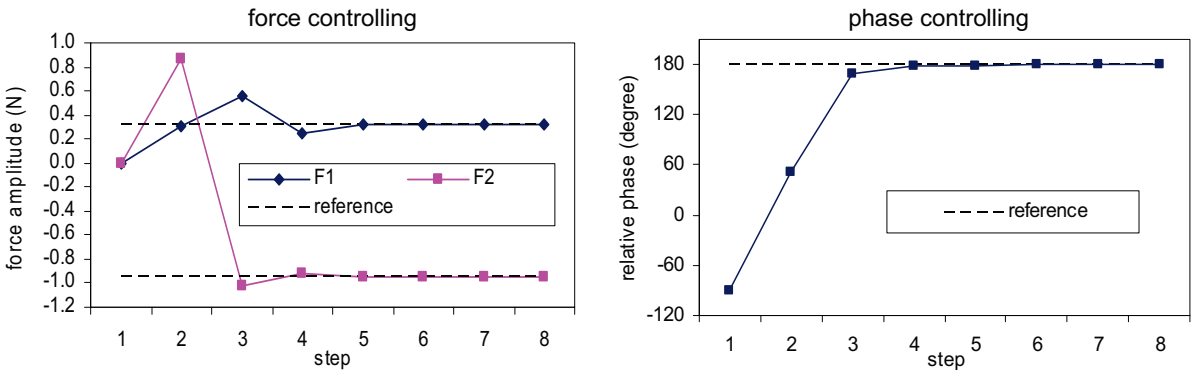

Figure 6.5: Example of force controlling for two shakers in a laboratory experiment

6.4 Laboratory experiment

A laboratory experiment was carried out in the laboratory of the Institute of Structural Mechanics (ISM) at the Bauhaus-University Weimar. The objective for the dynamic testing exercise was to demonstrate the capability of the proposed methodology. It also serves as an experience of realization of selective sensitivity for an actual situation.

The system under investigation was a simply supported beam modelled as four-beam-element structure with a span of $3.2m$ (Fig. 6.6). The elements' bending stiffnesses were identified for three variations of the beam, induced by changing local stiffness which imitates different damage states. The beam was excited through harmonic loads by using controllable shakers attached on the beam. The available measurement system could handle eight analog input channels and simultaneously, generate two analog output signals. Vertical acceleration was measured with four accelerometers fixed at the middle of the elements.

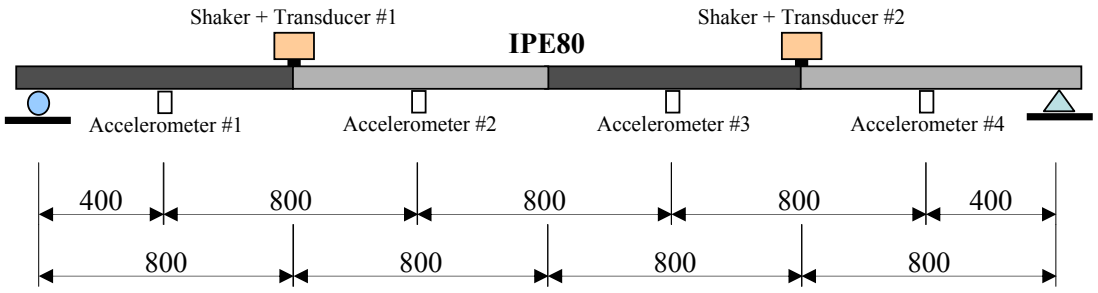

Figure 6.6: Layout of the experiment model

6.4.1 Experiment design

The beam was made from a standard steel profile IPE80. Thirty one additional steel plates were regularly screwed at the lower flange. By removing a plate to the web at the same position, local bending stiffness can be modified while the mass is kept unchanged. The sketch of the beam's design can be seen in Fig. 6.7. With this design several variations of the beam stiffness can be examined and the beam can be reused for future identification purpose.

The equipments used in the experiment are listed in Table 6.1. The reason for using only two shakers, i.e. two excitation points, is that the PCI-6024E card has only two analog output channels for generating excitation signals. To excite the structure, say, with four shakers requires other hardware (DAQ Card) together with a multi-channel amplifier, which could not be afforded due to financial reason.

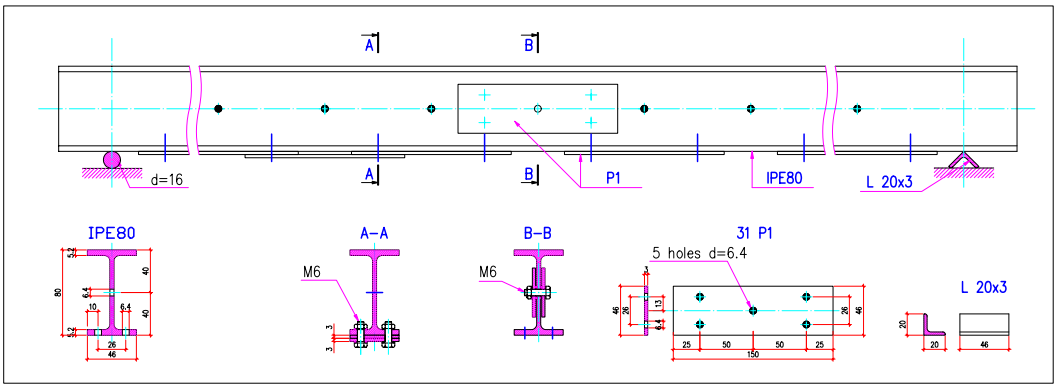

Figure 6.7: Design of the steel beam for local change of bending stiffness

Shaking devices	2 low-bass shakers 1 150W Sony stereo amplifier cables
Measurement devices	2 force transducers (M) 201B01 plus 1 signal conditioner 4 accelerometers KB12V plus 1 signal conditioner
Hardware	PC Pentium 4 PCI-6024E Data Acquisition Card BNC-2120 Connector
Software	Windows XP Controlling program developed in LabVIEW

Table 6.1: List of experiment equipments

In the test, Body-Shakers (also known as Bass-Shaker, Bass-Pump) were used to generate vibration. This type of shaker which is belong to the 'electrodynamic' shaker family has great advantage of price over other sophisticated ones, however, limitations on accuracy, magnitude of force and range of frequency. The properties of one typical body shaker used are given in Table 6.2. A numerical calculation shows the natural frequencies of the

Effective frequency range	28 $\sim$ 55 Hz
Resonance frequency	ca. 40 Hz
Power	100 W
Dimensions	120 $\times$ 30 mm
Weight	ca. 690 gr

Table 6.2: Technical data of the body shaker

beam structure including shakers and measurement devices (see Table 6.3). The results are shown for two cases, without ("original") and with ("modified") screwed plates. It can be seen that, the effective frequency range of the shakers lies between the first and the second natural frequencies.

	Natural frequencies $[Hz]$	
	original beam	modified beam
1	21.0843	23.573
2	80.0362	89.4832
3	187.398	209.518
4	500.046	559.069
5	667.358	746.129
6	1006.15	1124.91
7	1519.49	1698.84
8	1853.85	2072.66

Table 6.3: Natural frequencies of the tested beam including measurement devices

In order to excite the structure the shakers were tightly attached on the beam's upper flange by using bolts. Details of the attachment design is depicted in Fig. 6.8. Vibration generated by shakers was transmitted to the beam through a support plate (**P2**). Two essentials in designing the plate **P2** were: it must ensure only vertical transmission of excitation force to the beam; and it should has sufficient stiffness so as to avoid unwanted local low-frequency vibrations. Here, the plate has the first natural frequency of $256.28Hz$, which is much higher than those frequencies used to excite the structure. Fig. 6.9 shows the pictures of the shakers attached on the tested beam in laboratory.

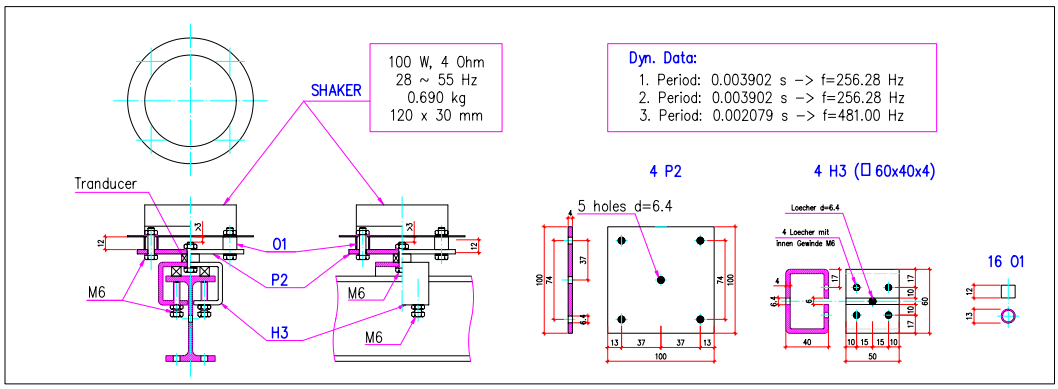

Figure 6.8: Design of shaker attachment

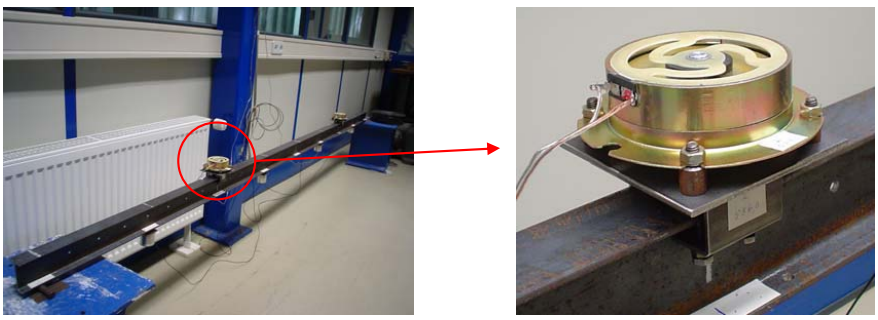

Figure 6.9: Attachment of shaker on the beam in the laboratory

One important point was to ensure the contact of the beam and the supports during vibration. The supports at the two ends of the beam can be seen in Fig. 6.10, which were simply designed. Nevertheless, the above requirement was ensured because the weight of the beam was much larger than the maximum exciting force, which was actually less than $2N$.

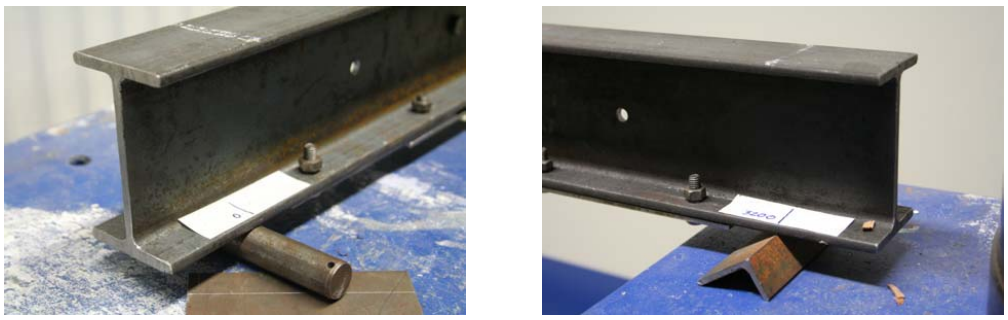

Figure 6.10: Supports at two ends of the tested beam

6.4.2 Test control program

The control of the testing process basically consist of the following tasks:

- Analyzing: to determine force and displacement patterns with respect to the selected parameters.
- Exciting & measuring: to generate excitation signals, to acquire output signals, to analyse the data, and to control the forces.
- Updating: to estimate parameter values as well as their uncertainties and to update the elements' bending stiffnesses.

The control program was realized in the programing environment LabVIEW 7.1 (LabVIEW, National Instruments, $http://ni.com/labview/$). The main program interface is shown in Fig. 6.11. Fig. 6.12 shows the dialog of the subprogram for controlling force and acquiring data.

The choice of using LabVIEW instead of other environments is that LabVIEW contains a comprehensive set of tools for acquiring, analyzing, displaying, and storing data, as well as other powerful mathematical tools. Thus, all the above tasks can be combined into one unique software, allowing 'on-line' testing to be done. In addition, differing from conventional text-based languages, LabVIEW provides graphical-based programing environment giving an user-convenient interface. In fact, LabVIEW programs has been used as virtual instruments in diversified applications for testing, controlling, producing, manufacturing.

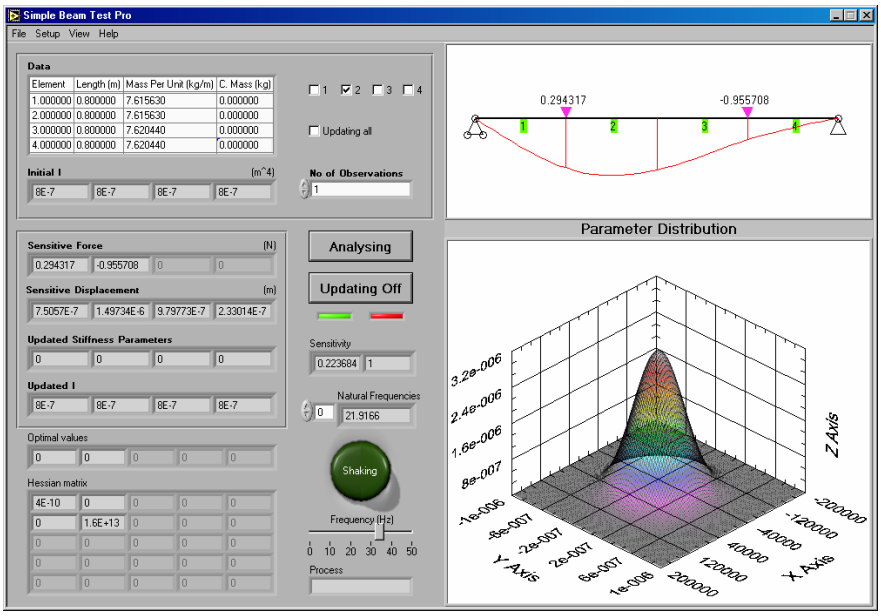

Figure 6.11: Test program dialog

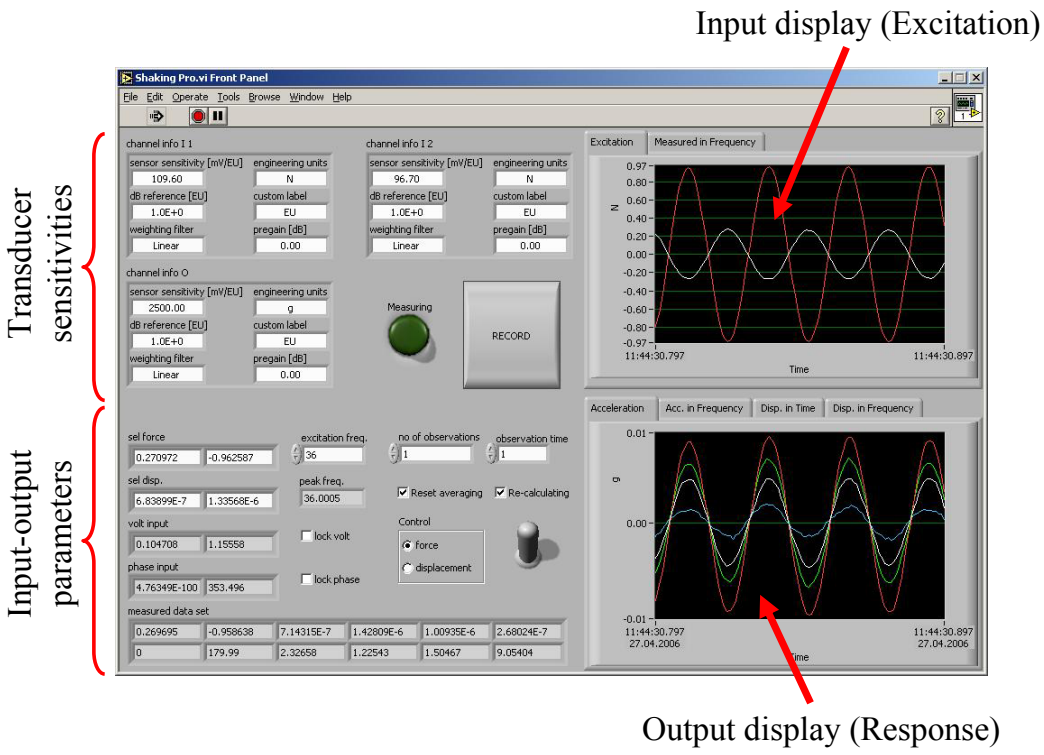

Figure 6.12: Controlling dialog

6.4.3 Vibration measurements

The test was conducted in the laboratory during the working time. Noise was found from different sources, such as laboratory works, air-conditioners. In oder to reduce errors and the influence of noise in the results, window of Hanning type and averaging (over 50 samples) were employed into the Fourier transform. All force and displacement signals were recorded at the rate $1024 samples/s$. Displacements were obtained by integrating measured accelerations. Fast-Fourier-transform (FFT) was utilized to transform time series data in to frequency domain. The values required for force controlling and parameter updating were extracted at the frequency of excitation from frequency-domain data in steady state of vibration.

6.4.4 Force controlling

Adjustment in input signals is required in order to ensure the desired values of excitation force applied on the tested structure. The problem of disagreement between input voltages and the measured force amplitudes was found during testing. An example is illustrated in Fig. 6.13. In this pre-testing, although sinusoidal voltage signals were applied only to Shaker No.1, non-zero forces were measured at Shaker No.2 (f_2), which actually also sinusoidal. Moreover, non-linear relationship between the input voltage and forces was found (Fig. 6.13a). Nevertheless, the dependence of the force f_2 on the other, f_1, was found linear as shown in Fig. 6.13b.

For our test, the algorithm in section 6.3 was employed for automatically controlling the forces. The matrix $\mathbf{A}$ and $\mathbf{B}$ were simply set equally to identify matrix, $\mathbf{A} = \mathbf{B} = \text{dia}[1,1]$, with the fact that this choice worked quite well when the amplifier was set at appropriate level (see also Fig. 6.5).

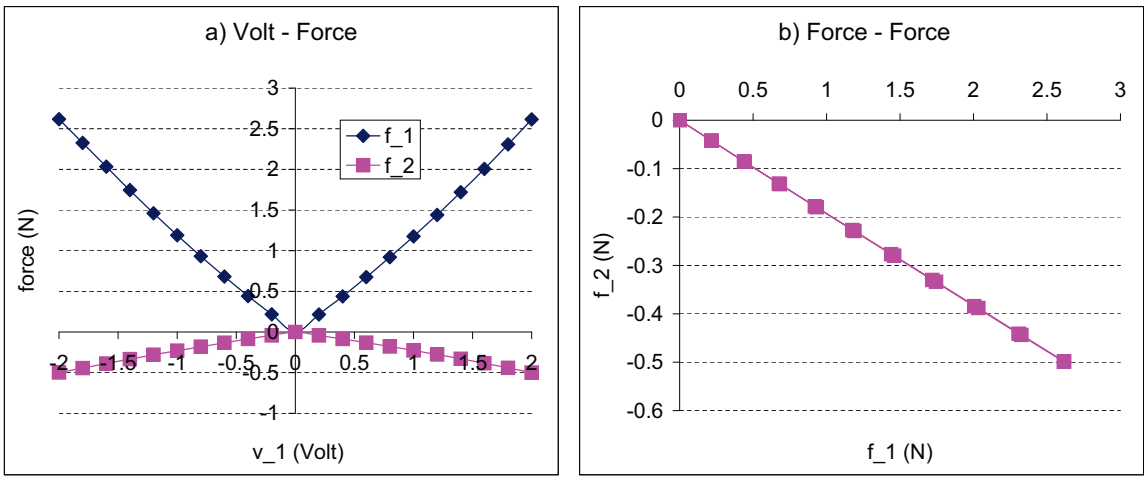

Figure 6.13: Disagreement between input voltage and measured forces

6.4.5 Excitation frequency selection

For our test harmonic forces were used to excite the beam. It is important to know which frequencies are applicable and effective for the test set-up. For this purpose different frequencies in the allowable range (of the shaker) were examined. It was found that selectively sensitive excitation could hardly be obtained with frequencies below $30Hz$. As it can be seen in Fig. 6.14, with frequencies $15Hz$, $20Hz$ and $25Hz$, there appear other frequency components in the excitation forces. Fig. 6.15 shows the phases of the forces and two measured displacements. Again, the phases were unstable when excitation frequencies were lower than $30Hz$. On the other hand, a good agreement between the phases of force and displacement was found with higher-frequency vibrations. Base on these pre-testings, selection for suitable excitation frequencies could be made, which was in the range from $30Hz$ to $40Hz$ for this particular experiment.

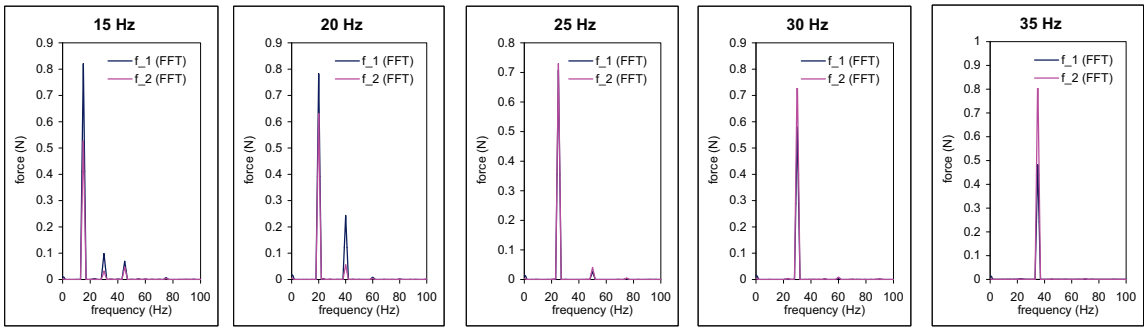

Figure 6.14: Fourier transformations of applied excitations at different frequencies

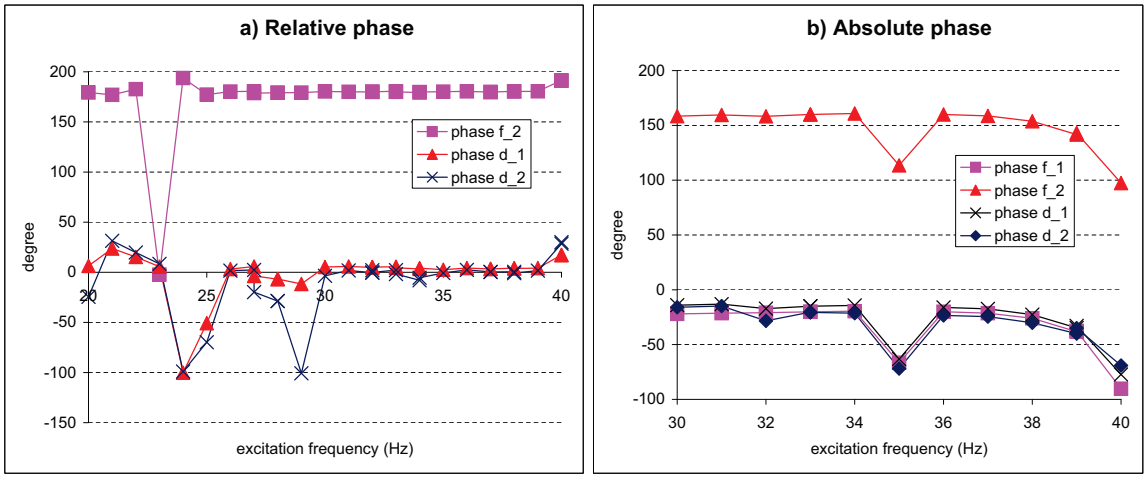

Figure 6.15: Measured phases of force and displacement under changes in frequency

6.4.6 Structural model and parameter selection

The mass matrix was constructed that included the mass of the original beam, the mass of plates constantly distributed along the span of each element, the mass of the accelerometers and additional mass of the shaker's attachments below the force transducers. All masses were measured with sufficient accuracy (see Appendix C). The bending stiffnesses, $EI_j;\ j = 1 \ldots 4$, were assumed to be constant along the length of each element. The stiffness matrix was therefore computed from

$$\mathbf{K} = \sum_{j=1}^{4} EI_j \mathbf{K}_j$$

with $\mathbf{K}_j$ are given in section 3.1.2 and the element's lengths $L_j = 0.8m$. The input matrix is given by

$$\mathbf{T} = \begin{bmatrix} 0 & 1 & 0 & 0 & 0 & 0 & 0 & 0 \\ 0 & 0 & 0 & 0 & 0 & 1 & 0 & 0 \end{bmatrix}^T$$

and the output matrix is

$$\mathbf{G} = \begin{bmatrix} 0.125 & 0.5 & -0.125 & 0 & 0 & 0 & 0 & 0 \\ 0 & 0.5 & 0.125 & 0.5 & -0.125 & 0 & 0 & 0 \\ 0 & 0 & 0 & 0.5 & 0.125 & 0.5 & -0.125 & 0 \\ 0 & 0 & 0 & 0 & 0 & 0.5 & 0.125 & -0.125 \end{bmatrix}.$$

According to the condition of Eq. 6.1, $n = 2 - 4 = -2 < 0$, the smallest number of parameters can be efficiently identified is two parameters. Analysis of the finite-element model showed that the most suitable parameter sets were $\{EI_1, EI_2\}$ and $\{EI_3, EI_4\}$. As can be seen from Fig. 6.16, the displacement patterns with respect to the parameter pair $\{EI_1, EI_2\}$ show almost no deformation in the unselected elements. The same results were found for $\{EI_3, EI_4\}$.

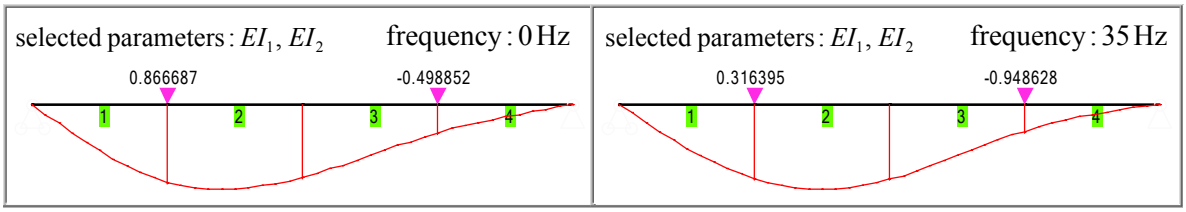

Figure 6.16: Experiment: Displacement patterns with respect to parameter pair $\{EI_1, EI_2\}$

Fig. 6.17 depicts the response sensitivity in frequency range $[0, 500Hz]$. Setting the response sensitivity with respect to the selected parameters to be unit, the sensitivity to the unwanted parameters always stays below this value. Also from Fig. 6.17, better selective

insensitivity can be attained with lower frequencies in the range $[0, 50Hz]$.

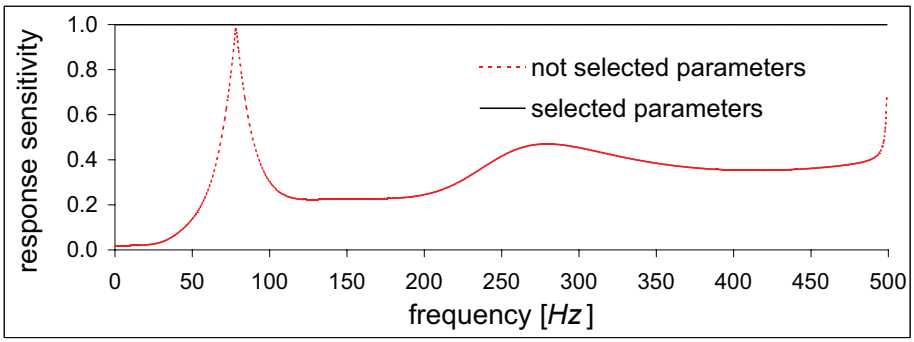

Figure 6.17: Response sensitivity in frequency

6.4.7 Vibration testing and results

Due to the noisy environment, testing was performed several times to get a good results. Sometimes, the test had to be delayed or cancelled since the measured data were severely contaminated with noise, which were mainly induced from laboratory works and/or the operating of the air-conditioner. It was found that the air-conditioner at the laboratory had a frequency of about $20Hz$ which was quite closed to the first natural frequency of the tested structure, and during its operating the test control was quite difficult. The results presented here were obtained in quite a long-time of testing.

Some trial and error was used to establish the optimum operation, and also to choose the best excitation frequency in the range $[30, 40Hz]$. It was discovered that frequency of $33Hz$ was most suitable for the test.

Three variations of the original steel beam, namely Beam I, II and III were examined. For each modification, different scheme were employed for the identification of the elements' stiffnesses. All parameters were identified based on one observation.

Beam I

In this first modification, thirty one designed steel plates were tightly screwed along the lower flange of the beam (Fig. 6.18). Using sinusoidal excitations with frequency of $33Hz$, the results obtained from the tests are given in Table 6.4. The first column shows the indexes of the selected stiffnesses, whose updated optimal values appear in the table. The calculated force vectors and the actual (measured) forces after control are also presented. It was found difficult to attain to the required force values. Nevertheless, the differences were inconsiderable (see Table 6.4). In addition, the errors (in percentage) between the model and

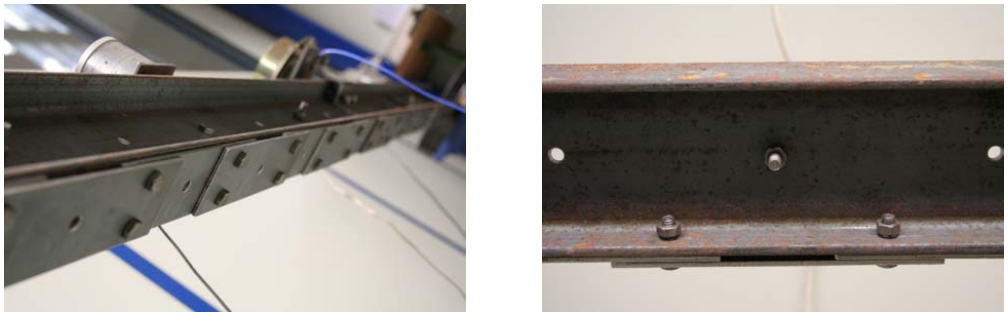

Figure 6.18: Tightly screwed plates at the bottom of the beam

measured displacements are viewed for each test, which show that a close match between model outputs and measured outputs can be achieved after some few tests (see Table 6.4).

For a different testing sequence, the results can be seen in Table 6.5. Herein, only the final values after a number of tests are presented (the number of the tests is put between brackets in the first column). As can be seen from Table 6.5, the displacement errors were also well reduced after some tests. However, there were differences in the identified parameters values between the two test sequences (see also Table 6.4).

$33Hz$ test	Force $[N]$		Stiffness $\times EI_0$				Disp. error [%]
	calculated	measured	EI_1	EI_2	EI_3	EI_4	
0			8.0	8.0	8.0	8.0	
3-4	0.91628; -0.400538	0.916447; -0.400645			9.59	8.65	12.16
3-4	0.870703; -0.491809	0.870634; -0.491817			9.18	9.08	1.89
3-4	0.876303; -0.48176	0.876387; -0.481847			9.24	9.02	0.69
1-2	0.397878; -0.917438	0.397813; -0.917337	8.63	9.35			11.97
1-2	0.478171; -0.878267	0.478019; -0.878297	8.61	9.39			0.78
1-2	0.479639; -0.877466	0.479598; -0.877455	8.63	9.39			0.72
3-4	0.880162; -0.474673	0.880161; -0.474835			9.11	9.09	1.04
3-4	0.882899; -0.469563	0.882885; -0.469519			9.09	9.21	0.51
1-2	0.482727; -0.875771	0.482741; -0.875796	8.63	9.36			0.78
$\sigma \approx$	-	-	0.281	0.135	0.082	0.210	

Table 6.4: Beam I - Test results with the 1st testing sequence

$33Hz$ test	Force $[N]$		Stiffness $\times EI_0$				Disp. error [%]
	calculated	measured	EI_1	EI_2	EI_3	EI_4	
0			8.0	8.0	8.0	8.0	
1-2(3)	0.475137; -0.879912	0.475062; -0.879964	8.84	9.16			0.72
3-4(3)	0.872437; -0.488727	0.87238; -0.488713			9.52	8.88	0.76
1-2(3)	0.466188 -0.884686	0.466243 -0.884754	8.69	9.17			0.43
3-4(2)	0.875942; -0.482416	0.875893; -0.482382			9.43	8.85	0.54
1-2(1)	0.467849; -0.883808	0.467832; -0.883748	8.75	9.12			0.41
$\sigma \approx$	-	-	0.138	0.060	0.100	0.218	

Table 6.5: Beam I - Test results with the 2nd testing sequence

In the above tables, the stiffness values should be multiplied by EI_0, where E is Young's modulus and I_0 is a nominal values of inertial moment, $I_0 = 10^4 Nm^2$. The initial value of the standard deviation of stiffness parameters was assumed to be $2.5 \times EI_0$. Table 6.4 and 6.5 show the updated standard deviation of the identified stiffnesses, which decreased more than ten times.

Beam II

For Beam II, three plates in the span of the element 2 were removed to the web of the beam (Fig. 6.19). This modification, as shown in Fig. 6.20, did not change the mass but the bending stiffness of the beam (expectably only stiffness of the modified elements).

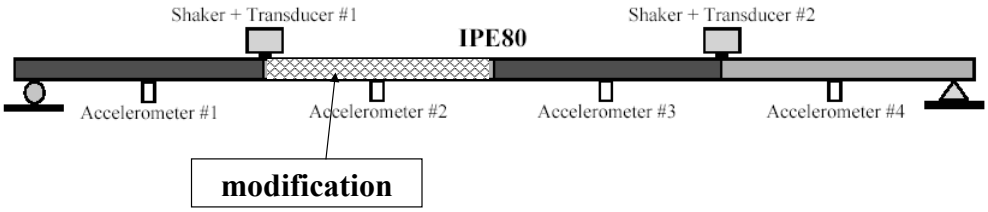

Figure 6.19: Modification location for Beam II

Figure 6.20: A plate removed from the flange to the web of the beam

Two different sequences were examined with the start value for all the parameter equal $8.0 \times EI_0$. In addition, a test using uniform force pattern ($f_1 = f_2 = 1N$) was also carried out, i.e without selectively sensitive force (w/o sel-force). The results obtained from the tests are listed in Table 6.6. Clearly, there appeared a decrease in the stiffness of the element 2, which could estimated in some iterations. The identified stiffnesses of the other elements remained almost the same as those for Beam I.

Moreover, for each parameter selection both sequences gave a considerable reduction of displacement error after the first update, which can be seen in Fig. 6.21. Further tests could bring only small amounts of improvement.

$33Hz$ test	Force $[N]$		Stiffness $\times EI_0$				Disp. error [%]
	calculated	measured	EI_1	EI_2	EI_3	EI_4	
0			8.0	8.0	8.0	8.0	
1-2(3)	0.438521; -0.898721	0.438552; -0.898756	8.71	8.43			0.58
3-4(3)	0.872887; -0.487923	0.872977; -0.487976			9.32	9.04	0.69
$\sigma \approx$	-	-	0.249	0.097	0.119	0.272	
0			8.0	8.0	8.0	8.0	
3-4(3)	0.876477; -0.481444	0.876274; -0.481332			9.21	9.00	0.56
1-2(3)	0.445557; -0.895253	0.445647; -0.895277	8.77	8.34			2.00
3-4(2)	0.882644; -0.470042	0.882607; -0.470035			9.05	9.12	0.70
1-2	0.449244; -0.893409	0.44933; -0.893275	8.70	8.41			1.96
$\sigma \approx$	-	-	0.724	0.318	0.116	0.289	
1-2-3-4	1; 1	0.99988; 0.99898	9.94	7.81	9.58	9.29	7.47

Table 6.6: Beam II - Test results with two different testing sequence

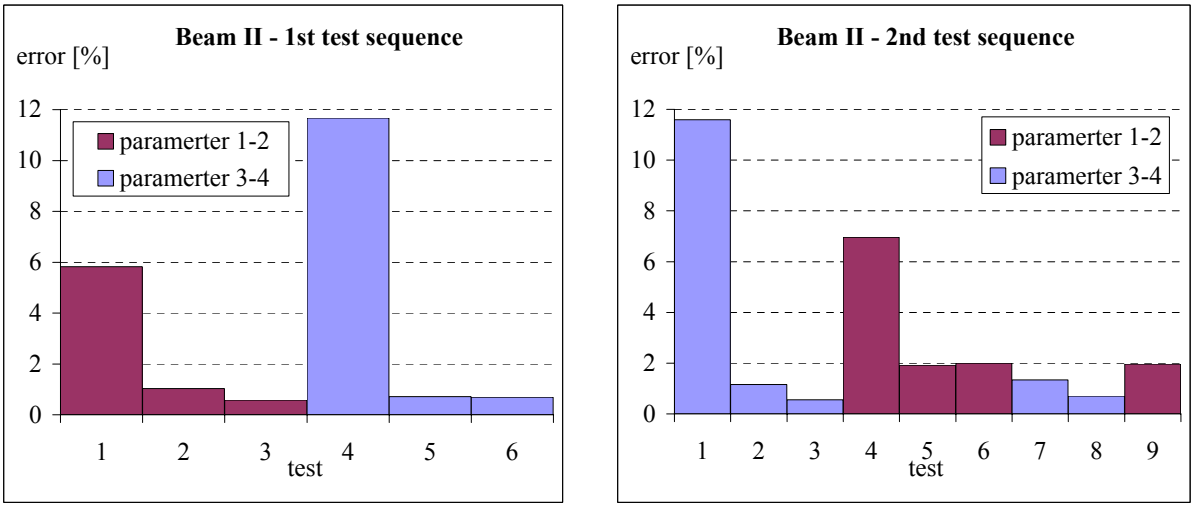

Figure 6.21: Displacement errors for two different sequences in testing Beam II

Beam III

An additional change to Beam II was made with the element 4 to form the Beam III (Fig. 6.22). Beam III was tested with only one sequence. However, all parameter values were set to $10.0 \times EI_0$ in the first identification scheme, whilst in the second one the parameters were initiated with value of $8.0 \times EI_0$. The obtained results are given in Table 6.7. It was found for these two cases that relatively equal amounts of displacement error were obtained after some certain tests (see Table 6.7 and Fig. 6.23).

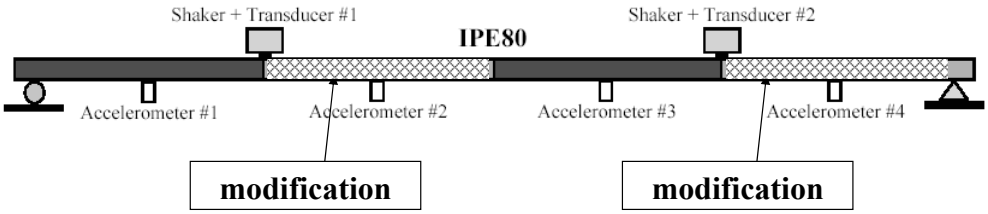

Figure 6.22: Modification location for Beam III

$33Hz$ test	Force $[N]$		Stiffness $\times EI_0$				Disp. error [%]
	calculated	measured	EI_1	EI_2	EI_3	EI_4	
0			10.0	10.0	10.0	10.0	
3-4(3)	0.880833; -0.473426	0.880985; -0.473396			9.70	7.63	1.85
1-2(3)	0.400047; -0.916495	0.400056; -0.916549	8.77	8.37			1.49
3-4(2)	0.881876; -0.471482	0.881856; -0.471484			9.35	8.02	0.80
1-2(2)	0.418149; -0.908378	0.418231; -0.908379	8.66	8.47			1.88
$\sigma \approx$	-	-	0.788	0.310	0.150	0.265	
0			8.0	8.0	8.0	8.0	
3-4(3)	0.885325; -0.464973	0.885506; -0.464933			9.10	8.36	0.90
1-2(3)	0.434794; -0.90053	0.434749; -0.900656	8.62	8.57			2.30
3-4(2)	0.886024; -0.46364	0.885977; -0.463666			9.14	8.27	0.86
1-2(2)	0.42944; -0.903095	0.429407; -0.903088	8.69	8.49			2.10
$\sigma \approx$	-	-	0.861	0.332	0.149	0.297	
1-2-3-4	1; 1	0.999637; 0.999012	13.0	7.37	9.93	8.61	0.06

Table 6.7: Beam III - Test results with different selections of start values

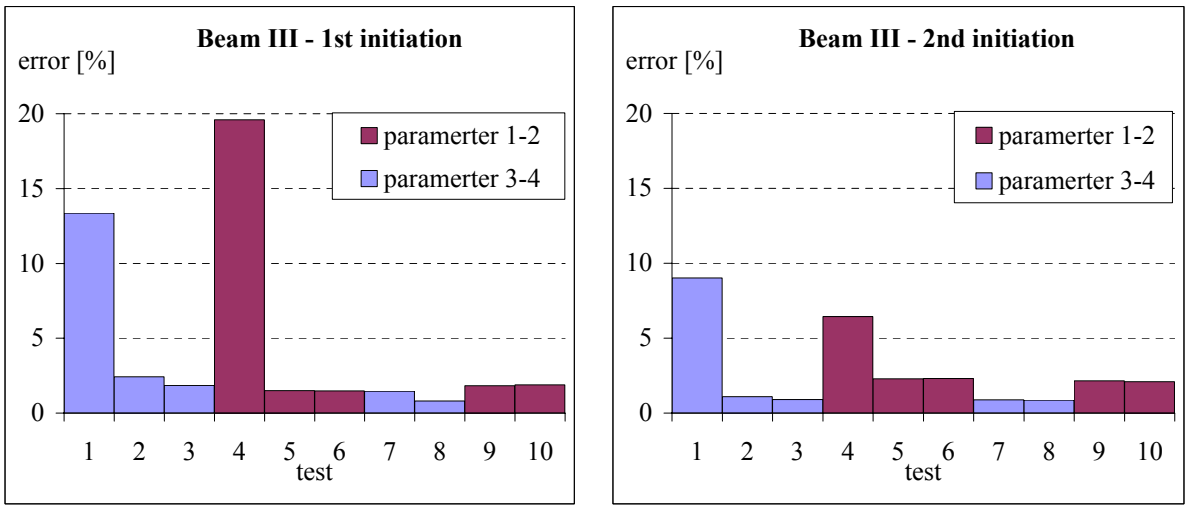

Figure 6.23: Displacement errors for different selections of start values in testing Beam III

By comparing the stiffness values with those obtained for Beam II, again, an amount of stiffness decrease was observed in the element 4 (see Table 6.7). This is also illustrated in Fig. 6.24. Here, the optimal parameter values identified for Beam I, II and III are are viewed together. Clearly stiffness reductions were detected for the elements that correspond to the change positions in the tested beam. It is also important to notice that, the optimal stiffness values of the same element estimated for different beam variations were not identical (see also Table 6.4 to 6.7). However, the difference was relatively small in comparison with the changes induced by stiffness modification. In contrast, the simultaneous identification of all four stiffness values using uniform force pattern gave unstable results, even beyond realistic parameters (see Table 6.6, 6.7 and Fig. 6.24).

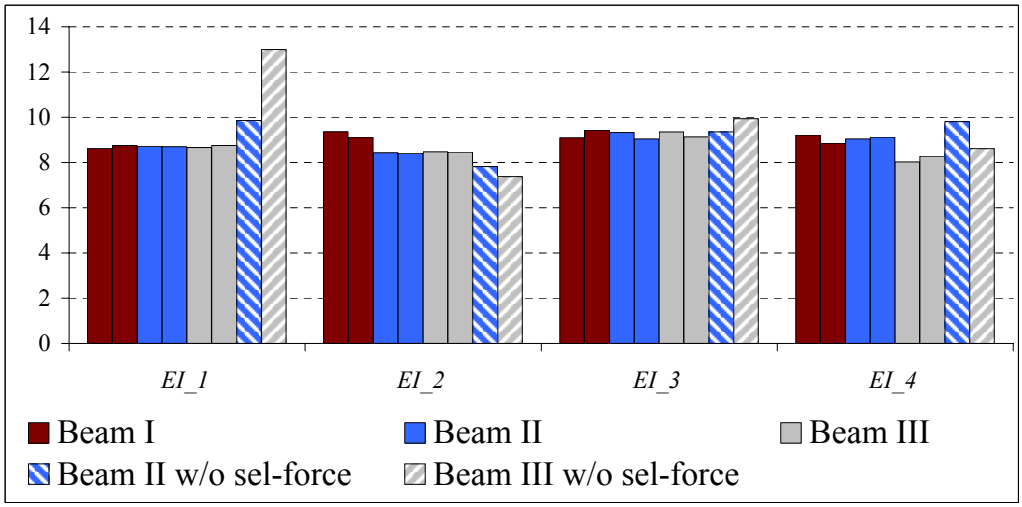

Figure 6.24: Optimal parameters values identified from three beam's modifications

A comparison between the average natural frequencies of first four bending modes of the Beam III's estimated model and those detected from measured free vibration due to a vertical hammer impact can be seen in Table 6.8. The differences between the model's and measured frequencies are quite small for the first three modes, however, relatively large for the fourth mode (see Table 6.8). In fact, it was discovered that the fourth measured frequency corresponded to the fundamental vibration frequency of the ground support, which was assumed to be fixed in the finite element modelling.

$f_{n,model}[Hz]$	$f_{n,meas}[Hz]$	error [%]
22.0593	21.9	0.727
83.06825	83.775	0.844
194.653	194.8	0.075
519.451	315.267	64.765

Table 6.8: Average natural frequencies of Beam III's estimated model and those detected from measured free vibration

Chapter 7

Conclusion

7.1 Discussions

Efficient procedure for dynamic system identification can be established by using special excitation forces which produce the system response sensitive to only a small substructure, whilst insensitive to other part of the system. However, the application of these special forces is not without problems. Firstly, it requires relatively precise knowledge of the system parameters. Secondly, it is the experimental difficulty associated with the realization of the desired excitations. Different approaches have been presented in this study to overcome these difficulties, including the quasi-static approach and the experimentally iterative procedure.

The quasi-static approach allows to attain nearly selective sensitivity by using force patterns from static identification. The advantage of this approach is that no prior knowledge of the parameters is required. However, this occurs only when selective sensitivity can be obtained for one single parameter. Therefore, this approach is appropriate for statically determinate structures. Moreover, for successful utilization of the obtained static force patterns in dynamic experiments the excitation frequency must be below the fundamental frequency of the tested structure. It may be difficult in practice to ensure that the selected small substructure will be effectively excited under low frequency vibrations (see Chapter 6).

For more general case, a procedure by means of iterative experiment has been proposed. From simulated examples, it is shown to be efficient for estimating the stiffness parameters and reducing the parameter uncertainties. With an appropriate excitation frequency, this method can produce a relatively fast convergence. An explanation for the good performance of the method is that, it takes advantage of the property of selectively sensitive displacements to directly formulate the required force for each iteration in terms of those parameters to be identified. The rate of convergence, however, depends on the frequency used and better

convergence was obtained with lower frequencies. As found in the examples, parameter values were well updated after just few steps under low frequencies. It is explained that the influence of the mass becomes small when the excitation frequency is low. Since the prior information of the parameters is used to determine the forces which will be applied on the tested structure, its quality may have also significant effect on convergence rate. On the other hand, different results were obtained with different testing sequence. Besides noise and measurement error, it may be because of the reason that the updated values were used to computed the forces for the following testing, thus resulting biased estimation.

In order to ensure the accuracy of the excitation forces, force control is required. This control is necessary because of the fact that the actual forces applied on the tested structure differ from the input voltage signals which are generated based on the computed force patterns. The control has to adjust the input signals so as to produce the necessary forces successfully, and in general automatically. The proposed algorithm which is based on predictive control was found efficient for this task.

A laboratory test has been conducted. Basically, the test system has components that are similar to those in a modal test. The difference is that much more sensors and actuators will be used, resulting in high expense. In fact, only a simple experiment could be realized due to the experimental capacity. It can be deduced from this example that the proposed experimental procedure allows to efficiently obtain selectively sensitive excitation for the identification of a finite-element model that represents a tested structure. Local stiffness changes could be identified with a suitable frequency. However, the effective range of frequency was found to be limited. This may be improved by using precise electrodynamic shakers. It was also found on the other hand that much more efforts (in terms of setting-up, programing, testing time) were needed for this strategy than others, e.g modal test.

7.2 Conclusions

The experimental procedure produced in this study could estimate the stiffness parameter values for a finite-element model of an undamped structure with relatively high accuracy. Simultaneous convergence of the required inputs and the parameters to be identified was efficiently achieved through iterative experiment. Further more, the uncertainty of the estimated parameter values could be assessed by means of Bayesian updating. The precision of the applied forces was assured by a predictive force control algorithm. The application of the procedure to a relatively simple test in laboratory showed clearly the potential for such a procedure to identify and locate damage.

Nevertheless, there are still shortcoming of the method. Firstly, when applied with high frequencies which are often necessary to effectively excite a small substructure the convergence rate becomes very low, i.e. more time and efforts. Besides that, high frequency means that the effect of the model mass is also large and error in mass measurement may lead to large error in the estimation of stiffness. Secondly, the convergence rate depends on the quality of the prior knowledge about the stiffness parameter values. Thirdly, if only few iterative tests are the conducted, the testing sequence will biases the estimated values. Fourthly, since the structure is assumed to be linear, tests must be performed under low-amplitude vibration. Thus, the identification may become problematic if the measured data is erroneous and largely contaminated by noise. The errors may become larger through integrals of noisy measured accelerations, which leads to the unavailability of accurate results of the identified stiffness. Finally, this methodology involves high expenditure and much work.

It is recommended to use simulation before testing. Careful test planning and virtual testing can produce considerable advantage in terms of not only the cost of testing but also the effectiveness of each test. The essentials which should be determined from virtual testing are: (i) suitable parameter selection and test sequence, (ii) optimisation of the test set-up by choosing the best set of excitation and response measurement DOFs and (iii) appropriate frequencies to excite the tested structure, although some aspects will be fully decided with actual tests. It is suggested that the frequency should be kept as low as possible. Also, prior information about the structure based on expert's judgement, previous tests (e.g modal test) should be utilized thoroughly. Although more tests means more time spent, which implies higher cost, sufficient repetitions of testing should be made.

The practice application of the proposed procedure depends largely on the experimental capacity and condition. In oder to isolate and excite a small substructure effectively, lots of actuators and sensors may be required. Therefore, the number of actuators which can be simultaneously operated play significant role. A very noisy environment may cause the force control to be difficult. The effectiveness of such a test is also restricted by the maximum force which the shakers can produce. It is seen that, this method is beneficial for relative small structures or structural components.

The presented method is based on a mathematical model where damping is neglected. Consequently, it cannot be applied to damped system, which can be found in various situations in practice. Further development of the method is necessary. In addition, it is essential to verify the procedure on more complex structures, e.g identification of local stiffness change for plate or slap structures. Also, for complex excitation systems, the force control may be much more complicated and it should be a focus for future work.

References

[1] V. Zabel. *Application of wavelet Analysis in system identification*. PhD thesis, Bauhaus-University Weimar, 2003.

[2] M. Macke and C. Bucher. Reliability-based condition assessment of existing structures utilizing dynamic measurements. In H. Grundmann and G.I. Schuëller, editors, *Structural Dynamics - EURODYN 2002*, pages 287–292, Lisse, 2002. Swets & Zeitlinger.

[3] H. G. Matthies and C. Bucher. Finite elements for stochastic media problems. *Com. Methods Appl. Mech. Engng*, 168:3–17, 1999.

[4] C. Bucher, O. Huth, and M. Macke. Accuracy of system identification in the presence of random fields. In S. Madanat A. DerKiureghian and J. M. Pestana, editors, *Applications of Statistics and Probability in Civil Engineering*, pages 427–433, Rotterdam, 2003. Millpress.

[5] M. I. Friswell, S. D. Garvey, and J. E. T. Penny. Parameter subset selection in model updating and damage location. In *6th International Conference on Recent Advances in Structural Dynamics*, Southamton, UK, July 1997.

[6] M. I. Friswell, J. E. Mottershead, and H. Ahmadian. Combining subset selection and parameter constraints in model updating. *J. Vib. Acoust.*, 120:854–859, 1998.

[7] Y. Ben-Haim and U. Prells. Selective sensitivity in the frequency domain-i. theory. *Mechanical System and Signal Processing*, 7(6):461–475, 1993.

[8] Y. Ben-Haim. *Robust Reliability in the Mechanical Sciences*. Springer, Berlin, 1996.

[9] D. J. Ewins. *Modal Testing: Theory, Practice and Application*. Research Studies Press, Baldock, second edition, 2000.

[10] T. Lauwagie, H. Sol, and E. Dascotte. Damage identification in beams using inverse methods. In P. Sas and B. Van Hal, editors, *Proceedings of ISMA*, Leuven, Belgium, September 16-18, 2002. On CD-ROM.

[11] M. I. Friswell and J. E. Mottershead. *Finite Element Model Updating in Structural Dynamics*. Kluwer Academic Publishers, 1995.

[12] M. Link. Identification of structural parameters based on inverse modification theory. In *Proceedings of IMAC-XXII*, Dearborn, Michigan, USA, January 26-29, 2004. On CD-ROM.

[13] N. Roitman, C. Madluta, and L. A. C. M. Aragão Filho. Structural failure localization using direct updated methods. In *Proceedings of IMAC-XXII*, Dearborn, Michigan, USA, January 26-29, 2004. On CD-ROM.

[14] H. Sol, T. Lauwagie, and P. Guillaume. Identification of distributed material properties using measured modal data. In P. Sas and B. Van Hal, editors, *Proceedings of ISMA*, Leuven, Belgium, September 16-18, 2002. On CD-ROM.

[15] A. Esfandyari and O. Rezaifar. Damage assessment of structures using incomplete measured eigenvectors and eigenvalues. In *Proceedings of IMAC-XXIII*, Orlando, Florida, USA, January 31 - February 3, 2005. On CD-ROM.

[16] W. X. Ren and G. D. Roeck. Structural damage identification using modal data. part i: Simulation verification. *Journal of Engineering Mechanics*, 128:87–95, 2002.

[17] W. X. Ren and G. D. Roeck. Structural damage identification using modal data. part ii: Test verification. *Journal of Engineering Mechanics*, 128:96–104, 2002.

[18] F. Vestroni and D. Capecchi. Damage detection in beam structures based on frequency measurements. *Journal of Engineering Mechanics*, 126:761–768, 2000.

[19] S. Vanlanduit, E. Parloo, and P. Guillaume. A robust singular value decomposition to detect damage under changing operation conditions and structural uncertainties. In *Proceedings of IMAC-XXII*, Dearborn, Michigan, USA, January 26-29, 2004. On CD-ROM.

[20] V. Zabel and C. Bucher. Parametric system identification by means of the wavelet transformation. In H. Grundmann and G.I. Schuëller, editors, *Structural Dynamics - EURODYN 2002*, pages 1027–1032, Lisse, 2002. Swets & Zeitlinger.

[21] V. Zabel. A parametric system identification approach based on wavelet analysis. In *Proceedings of IMAC-XXII*, Dearborn, Michigan, USA, January 26-29, 2004. On CD-ROM.

[22] V. Zabel. A wavelet-based damage detection indicator for reinforced concrete structures. In *Proceedings of IMAC-XXIII*, Orlando, Florida, USA, January 31 - February 3, 2005. On CD-ROM.

[23] M. Brehm, V. Zabel, and K. Markwart. Applications of biorthogonal wavelets in system identification. In K. Majava P. Neittaanmäki, T. Rossi and O. Pironneau, editors, *Proceedings of the 4th European Congress on Computational Methods in Applied Sciences and Engineering*, Jyväskylä, July 24-28, 2004.

[24] M. Brehm, V. Zabel, and K. Markwart. Applications of wavelet packets in system identification. In *76. Jahrestagung der Gesellschaft für Angewandte Mathematik und Mechanik e. V. (GAMM)*, University of Luxembourg, March 28 - April 1, 2005.

[25] M. Brehm and C. Bucher. Wavelet packet system identification. In C. A. Mota Soares et.al, editor, *Proccedings of III European Conference on Computational Mechanics 2006 (ECCM 2006)*, Lisbon, Portugal, June 5-9, 2006. Springer, on CD-ROM.

[26] D. Bernal. Extracting physical parametrs of mechanical models from identified states-pace representations. *Journal of Engineering Mechanics, ASCE*, 128(1):7–14, 2002.

[27] D. Bernal and B. Gunes. Damage localization in output-only systems: A flexibility based approach. In *Proceedings of IMAC-XX*, pages 1185–1191, Los Angeles, California, USA, February 4-7, 2002. On CD-ROM.

[28] K. L. Napolitano and J. B. Kosmatka. Statistical damage detection of highly damped structures using frequency response. In *Proceedings of the SPIE Symposium on Smart Structures and Materials*, February 25-29, 1996.

[29] M. I. Friswell, J. E. Mottershead, and H. Ahmadian. Finite-element model updating using experimental test data: parametrization and regularization. *Phil. Trans. R. Soc. Lond. A*, 359:169–186, 2001.

[30] M. I. Friswell, J. E. T. Penny, and S. D. Garvey. Parameter subset selection in damage location. *Inverse Problems in Engineering*, 5(3):189–215, 1997.

[31] M. I. Friswell, J. E. T. Penny, and D. A. L. Wilson. Using vibration data and statistical measures to locate damage in structures. *Modal Analysis: The International Journal of Analytical and Experimental Modal Analysis*, 9(4):239–254, 1994.

[32] Y. Ben-Haim. Adaptive diagnosis of faults in elastic structures by static displacement measurement: The method of selective sensitivity. *Mechanical System and Signal Processing*, 6:85–96, 1992.

[33] U. Prells and Y. Ben-Haim. Selective sensitivity in the frequency domain-ii. applications. *Mechanical System and Signal Processing*, 7(6):551–574, 1993.

[34] S. Cogan, G. Lallement, F. Ayer, and Y. Ben-Haim. Updating linear elastic models with modal selective sensitivity. *Inverse Problem in Engineering*, 2:29–47, 1995.

[35] M. Oeljeklaus. *Das lineare Ausgangsgroessenverfahren mit rechnerish adaptiver Erregung im Frequenzbereich*. PhD thesis, University of Hannover, 1995.

[36] C.-P. Fritzen and D. Jennewein. Model-based detection of structural damage by means of vibration measurement data. In *European Conference on Composite Materials, ECCM-8*, pages 261–268, Naples, Italy, Juni 3-6, 1998.

[37] D. E. Kirk. *Optimal Control Theory - An Introduction*. Dover Publications, 2004.

[38] O. C. Zienkiewicz and R. L. Taylor. *The finite element method*, volume 2. Elsevier Butterworth-Heinemann, Amsterdam, 6th edition, 2005.

[39] J. Rodellar, A. H. Barbat, and J. M. Martin-Sanchez. Predictive control of structures. *Journal of Enginerring Mechanics*, ASCE, 113:797–812, 1987.

[40] T. T. Soong. *Active Structural Control: Theory and Practice*. Longman Scientific & Technical, Harlow, Essex, 1990.

[41] J. L. Beck and L. S. Katafygiotis. Updating models and their uncertainties. I: Bayesian statistical framework. *Journal of Engineering Mechanics*, ASCE, 124(4):455–461, 1998.

[42] K. V. Price, R. M. Storn, and J. A. Lampinen. *Differential Evolution : A Practical Approach To Global Optimization*. Springer Verlag, 2006.

[43] K. V. Yuen and L. S. Katafygiotis. Bayesian modal updating using complete input and incomplete response. *Journal of Engineering Mechanics*, ASCE, 128(3):340–350, 2002.

[44] C. Bucher and H.-A. Pham. On model updating of existing structures utilizing measured dynamic responses. *Structure and Infrastructure Engineering*, 1(2):135–143, 2005.

Appendix A

DE algorithm for optimization

We want to search for the optimal solution, $\widehat{\boldsymbol{a}}$, that minimize the function, $g(\boldsymbol{a})$, over a continuous space $\boldsymbol{a} = \{a_i\},\ a_i \in [a_{i,min}, a_{i,max}],\ i = 1 \ldots N_a$. Differential Evolution (DE) algorithm invented by Price and Storn [42] was utilized for this optimization problem and is described in the following.

For each generation G, a population of NP parameter vectors $\mathbf{a}_p,\ p = 1 \ldots NP$, is utilized. The initial population is generated as

$$(\mathbf{a}_p)_i = a_{i,min} + r \cdot (a_{i,max} - a_{i,min}) \tag{A.1}$$

where r is a uniformly distributed random real value in the range [0,1]. For each vector $\mathbf{a}_p,\ p = 1 \ldots NP$, a perturbed vector $\mathbf{v}$ is generated according to

$$\mathbf{v} = \mathbf{a}_{r_1} + F \cdot (\mathbf{a}_{r_2} - \mathbf{a}_{r_3}) \tag{A.2}$$

with $r_1, r_2, r_3 \in [1,NP]$, integer and mutually different, and $F > 0$. The integers r_1, r_2 and r_3 are also chosen to be different from the running index p. F is a real and constant factor $\in [0, 2]$ which controls the amplification of the differential variation $(\mathbf{a}_{r_2} - \mathbf{a}_{r_3})$.

Then crossover is introduced to increase the diversity of the parameter vectors. The element i-th of $\mathbf{v}$ are kept unchanged for $i = |n|_{N_a}, |n+1|_{N_a}, \ldots, |n+L-1|_{N_a}$; otherwise, they are substituted by $(\mathbf{a}_p)_i$. Here, n is randomly chosen integer from the interval $[1, N_a]$; L is drawn from the interval $[1, N_a]$, so that the probability $\Pr(L \geq \nu) = (Cr)^\nu,\ \nu > 0$ with Cr is taken from $[0, 1]$. The notation $|\cdot|_{N_a}$ denotes the modulo function with modulus N_a.

The new vector $\mathbf{v}$ is then compared to $\mathbf{a}_p$. If $\mathbf{v}$ yields,

$$g(\mathbf{v}) < g(\mathbf{a}_p) \tag{A.3}$$

then $\mathbf{v}$ becomes a member of the next generation $(G+1)$; otherwise, the old value $\mathbf{a}_p$ is retained. The illustration of this algorithm is depicted in Fig. A.1. Source codes of DE for different programming environments can be found in
$http://www.icsi.berkeley.edu/\sim storn/code.html\#basi$

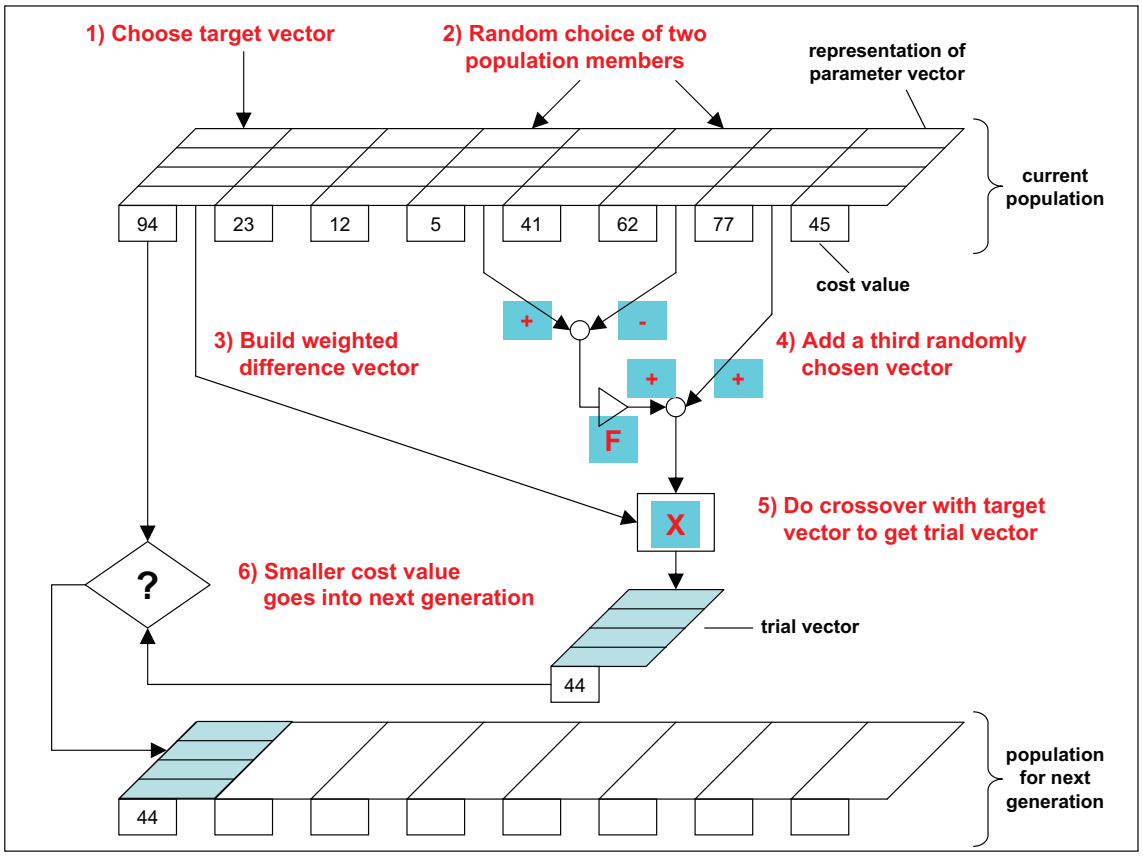

Figure A.1: Differential evolution: scheme DE/rand/1

For the numerical examples in this dissertation, the control parameter are $F = 0.5$ and $Cr = 0.8$, the population size is $NP{=}10 \times N_a$.

Appendix B

Derivation of the Hessian matrix

The elements of the Hessian matrix, $\mathbf{H}(\boldsymbol{a})$, of a function $g(\boldsymbol{a})$ are computed by

$$H_{ij} = \frac{\partial^2 g(\boldsymbol{a})}{\partial a_i \partial a_j} \tag{B.1}$$

For a general case, the vector of model parameters can be, $\boldsymbol{a} = \left\{\theta_1, \ldots, \theta_{N_p}, v_1, \ldots, v_{N_o}\right\}^T$. In this study, it is assumed that the variances of prediction error at all observed DOFs are equal to v. Thus, we have $\boldsymbol{a} = \left\{\theta_1, \ldots, \theta_{N_p}, v\right\}^T$, and

$$g(\boldsymbol{a}) = J(\boldsymbol{a}) - \ln \frac{1}{v^{N_o N_f N_m}} + const \tag{B.2}$$

where

$$J(\boldsymbol{a}) = \frac{1}{2}\left[\boldsymbol{a}^T \mathbf{C}^{-1} \boldsymbol{a} + \frac{1}{v^2} \sum_{f=1}^{N_f} \sum_{m=1}^{N_m} \left(\widehat{\mathbf{y}}_m(\omega_f) - \mathbf{y}(\theta)\right)^T \left(\widehat{\mathbf{y}}_m(\omega_f) - \mathbf{y}(\theta)\right)\right] \tag{B.3}$$

and

$$\begin{aligned} \mathbf{y}(\theta) &= \mathbf{G}\left[\mathbf{I} - \left(-\omega^2 \mathbf{M} + \mathbf{K}_0 + \sum_{k=1}^{N_p} \theta_k \mathbf{K}_k\right)^{-1} \sum_{k=1}^{N_p} \theta_k \mathbf{K}_k\right] \mathbf{x} = \\ &= \mathbf{G}\left[\mathbf{I} - \left(-\omega^2 \mathbf{M} + \mathbf{K}_0 + \Delta\mathbf{K}\right)^{-1} \Delta\mathbf{K}\right] \mathbf{x} = \mathbf{G}\left[\mathbf{I} - \mathbf{S}^{-1}\Delta\mathbf{K}\right] \mathbf{x} \end{aligned} \tag{B.4}$$

For convenience, let $\delta = \left(\widehat{\mathbf{y}}_m(\omega_f) - \mathbf{y}(\theta)\right)$, representing the vector of error between measured and model's displacements, and

$$g(\boldsymbol{a}) = g_1 + g_2 + g_3 \tag{B.5}$$

with

$$g_1 = \frac{1}{2}\boldsymbol{a}^T\mathbf{C}^{-1}\boldsymbol{a};\ g_2 = \frac{1}{2v^2}\sum_{f=1}^{N_f}\sum_{m=1}^{N_m}\delta^T\delta;\ g_3 = -\ln\frac{1}{v^{N_oN_fN_m}} + const \tag{B.6}$$

The Hessian matrix is now determined from

$$H_{ij} = \frac{\partial^2 g_1}{\partial a_i \partial a_j} + \frac{\partial^2 g_2}{\partial a_i \partial a_j} + \frac{\partial^2 g_3}{\partial a_i \partial a_j} \tag{B.7}$$

Firstly, we determine $\frac{\partial^2 g_1}{\partial a_i \partial a_j}$. Starting from

$$\frac{\partial g_1}{\partial a_i} = \frac{1}{2}\left(\frac{\partial \boldsymbol{a}}{\partial a_i}^T\mathbf{C}^{-1}\boldsymbol{a} + \boldsymbol{a}^T\mathbf{C}^{-1}\frac{\partial \boldsymbol{a}}{\partial a_i}\right) \tag{B.8}$$

we obtain

$$\frac{\partial^2 g_1}{\partial a_i \partial a_j} = \frac{1}{2}\left(\frac{\partial \boldsymbol{a}}{\partial a_i}^T\mathbf{C}^{-1}\frac{\partial \boldsymbol{a}}{\partial a_j} + \frac{\partial \boldsymbol{a}}{\partial a_j}^T\mathbf{C}^{-1}\frac{\partial \boldsymbol{a}}{\partial a_i}\right) = \frac{1}{2}\left(\mathbf{C}_{ij}^{-1} + \mathbf{C}_{ji}^{-1}\right) \tag{B.9}$$

Secondly, it can be easily seen that

$$\frac{\partial^2 g_3}{\partial \theta_k \partial \theta_l} = \frac{\partial^2 g_3}{\partial \theta_k \partial v} = \frac{\partial^2 g_3}{\partial v \partial \theta_l} = 0 \tag{B.10}$$

and

$$\frac{\partial^2 g_3}{\partial v \partial v} = -\frac{N_oN_fN_m}{v^2} \tag{B.11}$$

Finally, we are going to compute $\frac{\partial^2 g_2}{\partial a_i \partial a_j}$. We obtain the first derivatives as:

$$\frac{\partial g_2}{\partial \theta_k} = \frac{1}{v^2}\sum_{f=1}^{N_f}\sum_{m=1}^{N_m}\delta^T\frac{\partial \delta}{\partial \theta_k} \tag{B.12}$$

$$\frac{\partial g_2}{\partial v} = -\frac{1}{v^3}\sum_{f=1}^{N_f}\sum_{m=1}^{N_m}\delta^T\delta \tag{B.13}$$

The second derivatives therefore are obtained as:

$$\frac{\partial^2 g_2}{\partial \theta_k \partial \theta_l} = \frac{1}{v^2}\sum_{f=1}^{N_f}\sum_{m=1}^{N_m}\left(\frac{\partial \delta}{\partial \theta_l}^T\frac{\partial \delta}{\partial \theta_k} + \delta^T\frac{\partial^2 \delta}{\partial \theta_k \partial \theta_l}\right) \tag{B.14}$$

$$\frac{\partial^2 g_2}{\partial \theta_k \partial v} = \frac{\partial^2 g_2}{\partial v \partial \theta_k} = -\frac{2}{v^3}\sum_{f=1}^{N_f}\sum_{m=1}^{N_m}\delta^T\frac{\partial \delta}{\partial \theta_k} \tag{B.15}$$

$$\frac{\partial^2 g_2}{\partial v \partial v} = \frac{3}{v^4}\sum_{f=1}^{N_f}\sum_{m=1}^{N_m}\delta^T\delta \tag{B.16}$$

In these equation, the derivatives of the vector of displacement error with respect to the stiffness parameters are computed as

$$\frac{\partial \delta}{\partial \theta_k} = -\frac{\partial \mathbf{y}(\theta)}{\partial \theta_k} = \mathbf{G}\left(\frac{\partial \mathbf{S}^{-1}}{\partial \theta_k}\Delta\mathbf{K} + \mathbf{S}^{-1}\frac{\partial \Delta\mathbf{K}}{\partial \theta_k}\right)\mathbf{x} \tag{B.17}$$

Notice that

$$\frac{\partial \mathbf{S}^{-1}}{\partial \theta_k} = -\mathbf{S}^{-1}\frac{\partial \mathbf{S}}{\partial \theta_k}\mathbf{S}^{-1} = -\mathbf{S}^{-1}\frac{\partial \Delta\mathbf{K}}{\partial \theta_k}\mathbf{S}^{-1} = -\mathbf{S}^{-1}\mathbf{K}_k\mathbf{S}^{-1} \tag{B.18}$$

then we obtain

$$\frac{\partial \delta}{\partial \theta_k} = \mathbf{G}\left(-\mathbf{S}^{-1}\mathbf{K}_k\mathbf{S}^{-1}\Delta\mathbf{K} + \mathbf{S}^{-1}\mathbf{K}_k\right)\mathbf{x} \tag{B.19}$$

The second derivatives can be computed by differentiating this expression further (the notation $,l$ indicates a derivative with respect to θ_l

$$\frac{\partial^2 \delta}{\partial \theta_k \partial \theta_l} = \mathbf{G}\left(-\mathbf{S}_{,l}^{-1}\mathbf{K}_k\mathbf{S}^{-1}\Delta\mathbf{K} - \mathbf{S}^{-1}\mathbf{K}_k\mathbf{S}_{,l}^{-1}\Delta\mathbf{K} - \mathbf{S}^{-1}\mathbf{K}_k\mathbf{S}^{-1}\Delta\mathbf{K}_{,l} + \mathbf{S}_{,l}^{-1}\mathbf{K}_k\right)\mathbf{x} \tag{B.20}$$

Utilizing the previous results, this eventually leads to

$$\begin{aligned}\frac{\partial^2 \delta}{\partial \theta_k \partial \theta_l} = \mathbf{G}(&\mathbf{S}^{-1}\mathbf{K}_l\mathbf{S}^{-1}\mathbf{K}_k\mathbf{S}^{-1}\Delta\mathbf{K} + \mathbf{S}^{-1}\mathbf{K}_k\mathbf{S}^{-1}\mathbf{K}_l\mathbf{S}^{-1}\Delta\mathbf{K} - \\ &-\mathbf{S}^{-1}\mathbf{K}_k\mathbf{S}^{-1}\mathbf{K}_l\mathbf{S}^{-1}\mathbf{K}_l\mathbf{S}^{-1}\mathbf{K}_k)\mathbf{x}\end{aligned} \tag{B.21}$$

Appendix C

Mass model of the beam structure

The mass measurements of the structure components are given in the following table:

Original IPE80:	6.000 kg/m
Distributed mass added to Element 1 & 2:	1.616 kg/m
Distributed mass added to Element 3 & 4:	1.620 kg/m
Accelerometer No.1:	0.268 kg
Accelerometer No.2:	0.272 kg
Accelerometer No.3:	0.269 kg
Accelerometer No.4:	0.271 kg
Shakers No.1:	
- mass below force transducer:	0.421 kg
- mass above force transducer:	1.051 kg
- transducer:	0.010 kg
Shakers No.2:	
- mass below force transducer:	0.421 kg
- mass above force transducer:	1.044 kg
- transducer:	0.010 kg

Table C.1: Mass measurements for the experiment

The element's mass matrix is computed as:

$$\mathbf{m}_e = \mathbf{m}_a + \mathbf{m}_c \tag{C.1}$$

where $\mathbf{m}_a$ is the average element's mass matrix

$$\mathbf{m}_a = \frac{\rho A \times L}{420} \begin{bmatrix} 183 & & & sym \\ 11L & 2.5L^2 & & \\ 27 & 6.5L & 183 & \\ -6.5L & -1.5L^2 & -11L & 2.5L^2 \end{bmatrix} \tag{C.2}$$

and $\mathbf{m}_c$ is the contribution of a lump mass m to the element's mass model

$$\mathbf{m}_c = m \times \begin{bmatrix} N_1 \\ N_2 \\ N_3 \\ N_4 \end{bmatrix} [N_1, N_2, N_3, N_4] \tag{C.3}$$

with the shape functions given by

$$[N_1, N_2, N_3, N_4] = \left[1 - \frac{3x^2}{L^2} + \frac{2x^3}{L^3}, x - \frac{2x^2}{L} + \frac{x^3}{L^2}, \frac{3x^2}{L^2} - \frac{2x^3}{L^3}, -\frac{x^2}{L} + \frac{x^3}{L^2}\right] \tag{C.4}$$

Zusammenfassung

Einführung

Systemidentifikation wird oft als Werkzeug im Zusammenhang mit der Beurteilung von Schädigungen an Strukturen eingesetzt. Zu diesem Zweck erfolgt oftmals eine Abschätzung der Parameter eines vorgegebenen Strukturmodells mittels der in dynamischen Versuchen gemessenen Daten. Dies erfordert die Lösung eines inversen Problems. Es stellt sich dabei heraus, dass die mathematische Formulierung des zugrundeliegenden inversen Problems in der Regel zu sehr schlecht konditionierten Gleichungssystemen führt, insbesondere bei einer großen Anzahl von zu bestimmenden Parametern. Dies bedeutet, dass die Präzision der identifizierten Parameterwerte oft nicht ausreichend hoch ist, um die ursprünglich gestellte Frage nach einer Schädigungsentwicklung beantworten zu können.

Die Arbeit der Dissertation greift dieses Defizit in der Systemidentifikation auf und versucht, einen existierenden Lösungsansatz, nämlich "*Selective Sensitivity*" für die Strukturmechanik zugänglich zu machen.

Die Zielsetzung dieser Arbeit ist die Entwicklung eines experimentellen Verfahrens auf der Grundlage der selektiv sensitiven Anregung, das es erlaubt, die Systemeigenschaften in Substrukturen mit hoher Verlässlichkeit zu identifizieren. Die Arbeit besteht im wesentlichen aus folgenden Punkten:

- Bestimmung der selektiv sensitiven Anregungen mit Hilfe der vorhandenen Informationen über die Systemparameter.
- Ansatz zur effizienten Parameterabschätzung.
- Einführung in das Verfahren der Bayesschen Aktualisierung.
- Aspekte zur Realisierung des selektiv sensitiven Versuchs.
- Entwicklung eines Steuerungsalgorithmus zur Einstellung der adaptiven Anregungen.
- Experimentelle Überprüfung der Vorgehensweise durch Laboruntersuchungen.

Betrachtet werden nur ungedämpfte lineare Strukturen. Die Arbeit konzentriert sich auf die Identifikation der Steifigkeiten, während die Massen als mit ausreichender Genauigkeit bekannt vorausgesetzt werden.

Systemidentifikation

Unter dem Begriff Systemidentifikation verbirgt sich ein sehr breit gefächertes Forschungsfeld. Oftmals steht die Detektion oder Lokalisierung von Schäden im Vordergrund. In aktuellen Forschungen werden zwei Ansätze verfolgt. Der erste Ansatz basiert auf der Identifikation mit Hilfe experimentell ermittelter modaler Parameter, während der zweite Ansatz die direkt gemessenen Zeitreihen oder Frequenz-Antwort-Funktionen (Frequency Response Functions) verwendet.

Es stellt sich dabei heraus, dass eine qualitative und quantitative Schadensdetektion meist nur mit Hilfe eines mathematischen Modells möglich ist. Die benötigten Parameterwerte werden dann aus gemessenen Werten geschlossen. Dies erfordert die Lösung eines inversen Problems. Oftmals sind inverse Probleme schlecht konditioniert.

Die schlechte Konditionierung des inversen Problems kann am einfachsten verbessert werden, indem die Anzahl der gleichzeitig zu identifizierenden Parameterwerte möglichst klein gehalten wird.

Selektive Sensitivität und adaptive Anregung

Der selektiv sensitive Ansatz vermag es, die Anzahl der gleichzeitig zu bestimmenden Parameterwerte durch eine geeignete Auswahl der Anregung signifikant zu reduzieren. Die Anregungsvektoren werden so festgelegt, dass die dynamischen Antworten des Rechenmodells jeweils nur noch von wenigen ausgewählten Steifigkeitsparametern abhängen. Dabei ist es notwendig, dass die Sensitivität der Reaktionsgrößen im Frequenzbereich bzgl. der unerwüschten Parameter verschwindet. Darüber hinaus soll ein alternative Konzept, die sogenannt schwache selektive Sensitivität ("*Weak Selective Sensitivity*") verfolgt werden.

In der vorliegenden Arbeit werden die Grundlagen des Verfahren der selektiven Sensitivität mit verschiedenen Beispielen aufgezeigt. Es stellt sich dabei heraus, dass die selektiv sensitiven Anregungen nur noch Spannung in den ausgewählten Elementen (Substrukturen) bewirken, in denen Steifigkeiten identifiziert werden sollen.

Allerdings müssten dafür die Parameterwerte schon bekannt sein, um solche adaptiven

Anregungen zu bestimmen, was nicht praktikabel ist. Auch die Schwierigkeiten bei der Realisierung dieser speziellen Anregungen erschweren den Einsatz der selektiven Sensitivität in der Praxis.

Quasistatischer Ansatz

Eine neuer Ansatz, nämlich "*Quasi-Static Approach*" zur Bestimmung der selektiv sensitiven Anregungen ohne Vorkennisse der Parameterwerte wird vorgestellt. Damit erhält man bei Anregung unterhalb der ersten Eigenfrequenz eine nahezu perfekt selektive Sensitivität. Der Ansatz ist für statisch bestimmte Systeme geeignet. Zwar wird die Fähigkeit des Ansatzes an Simulationen demonstriert, jedoch soll der Ansatz anhand von Experimenten verifiziert werden.

Da es im Allgemeinen nicht möglich sein wird, die gewünschte Sensitivität a-priori zu erreichen, muss eine adaptive Strategie implementiert werden.

Iteratives experimentelles Verfahren

Auf dem Konzept der vorbestimmten Steuerung ("*Predictive Control*") wird ein experimentell iteratives Verfahren hergeleitet. Die Strategie ist, in jedem iterativen Experimentschritt die Anregung so zu steuern, dass der Unterschied zwischen der selektiv sensitiven Verschiebung und der sogenannten vorbestimmten Verschiebungsantwort minimiert wird.

Die Vorgehensweise beinhaltet drei Phasen:

- Bestimmung der selektiv sensitiven Anregungs- und Verschiebungsvektoren bzgl. der ausgewählten Parameter mittels der vorhandenen Informationen
- Dynamische Belastung der Versuchsstruktur und Messung der benötigen Werte
- Parameteraktualisierung

Dieser Verlauf wird weiter durchgeführt, bis die gemessenen Verschiebungsgrößen und die Anworten des Rechenmodells übereinstimmen.

Ausgehend von der Eigenschaft der selektiv sensitiven Verschiebung wird zunächst die Steuerungskraft in Form der zu identifizierten Parameter dargestellt. Damit wird die vorbestimmte Verschiebungsantwort als eine Funktion von den im Versuch gemessenen Größen und den erwünschten Parametern formuliert. Die Parameterwerte können dann direkt durch Optimierung der Verschiebungsfehler bestimmt werden. Die Voraussetzung für die beschriebene

Vorgehensweise ist die Existenz eines (nahezu) selektiv sensitiven Anregungsvektors. Anschließend wird in das Verfahren die Bayesschen Aktualisierung eingeführt, damit optimale (wahrscheinlichste) Werte der Steifigkeitsparameter und ihr Unsicherheiten systematisch abgeschätzt werden können. Es sei darin angenommen, dass die vorbestimmte Verschiebungsfehler einer statistischen mittelwertfreien Nomalverteilung folgt.

Anhand mehrerer simulierter Beispiele wird demonstriert, dass die Steifigkeitsparameterwerte mit verhältnismäßig hoher Genauigkeit abgeschätzt werden können, auch unter Verwendung von Störanteilen in den simulierten Daten. Außerdem können die erforderten Anregungen effizient adaptiert werden.

Versuchsrealisierung

Die Realisierung der selektiv sensitiven Anregungen ist oftmals mit einem erheblichen versuchstechnischen Mehraufwand verbunden. Eine sorgfältige Planung mit Hilfe von Computersimulationen als "*Virtual Testing*" kann große Vorteile hinsichtlich der Effizienz und der Kosten des Versuchs bringen. Die folgenden Aspekte werden in der Planung betrachtet:

- Parameterauswahl und Versuchsreihenfolge
- Anregungs- und Messpunkte
- Belastungsfrequenz

Das Versuchssystem besteht aus folgenden Bestandteilen:

- Erregungsmechanismus
- Signalerfassungssystem
- Analysator
- Steuerpult

Ein entscheidender Punkt zur Realisierung der speziellen Anregungen ist es, die Präzision der selektiv sensitiven Belastungsfunktion zu gewährleisten. Zu diesem Zweck wird ein automatischer Steuerungsalgorithmus basierend auf der Grundlage der vorbestimmten Steuerung vorgeschlagen. Der Algorithmus ist für harmonische Anregungen geeignet.

Die Vorgehensweise wird anhand eines Laborexperiments verifiziert. Die experimentelle Anordnung wird in einer einfachen, aber prinzipiell funktionsfähigen Variante mit vorhandenen Material und Geräten realisiert. Die Versuchsstruktur ist somit ein Stahlträger, der mit 4-Balkenelementen modelliert und von zwei Shakern belastet wird. Die Biegesteifigkeiten

der Elemente werden für verschiedene Veränderungen der Steifigkeit des Balkens identifiziert. Diese Variante zeigt die grundsätzliche Eignung der geplanten Vorgehensweise. Die Steuerung des Versuchsaufbaus wird mit LabView realisiert.

Es wird gezeigt, dass mit dieser Vorgehenweise verhältnismäßig kleine lokale Änderungen der Steifigkeit der Balkenstruktur identifiziert werden können.

Schlußfolgerungen

In dieser Arbeit wird ein experimentelles Verfahren auf der Grundlage der selektiven Sensitivität zu dynamischer Systemidentifikation vorgestellt. Zwei Probleme bei der Verwendung des selektiv senitiven Ansatzes konnten im Rahmen dieser Arbeit gelöst werden. Das Verfahren kann die Steifigkeitsparameterwerte eines Finite-Element-Modells einer ungedämpften Struktur mit verhältnismäßig hoher Genauigkeit abschätzen. Ein Laborversuch beweist die Realisierbarkeit des entwickelten Verfahrens zur Schädigungsdetektion und Schädigungslokalisierung in der Strukturmechanik.

Die Anwendbarkeit des Vorgehens hängt jedoch größtenteils von experimenteller Kapazität ab. Es wurde auch festgestellt, dass ein solcher Versuch mit einem erheblichen versuchstechnischen Mehraufwand und zeitraubender Arbeit verbunden ist.

Das vorgestellte Verfahren basiert auf einem mathematischen Modell ohne Dämpfung. Daher ist die Anwendung auf gedämpfte Strukturen eingeschränkt. Eine weitere Entwicklung der Vorgehenweise ist erforderlich. Außdem sind Untersuchungen an komplexen Strukturen notwendig. Beispielsweise soll es möglich werden, die Steifigkeit eines lokalen Bereiches einer Platte unabhängig von der Steifigkeit der restlichen Platte zu bestimmen. Die Kraftsteuerung in einem komplexen Anregungssystem stellt auch eine notwendige Aufgabe für weitere Forschungsaktivitäten dar.